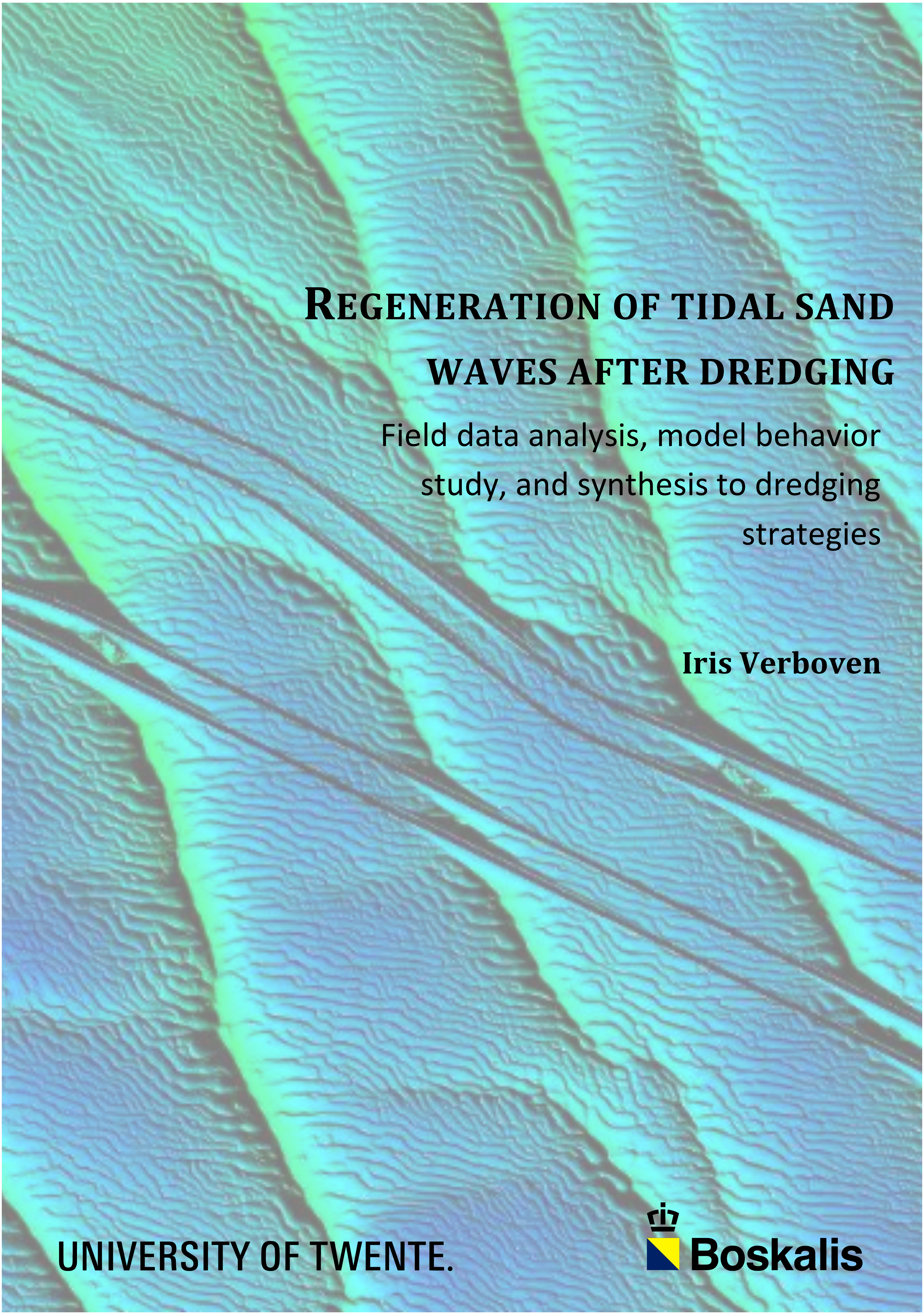

REGENERATION OF TIDAL SAND WAVES AFTER DREDGING

Field data analysis, model behavior study, and synthesis to dredging strategies

Iris Verboven

UNIVERSITY OF TWENTE.

Boskalis

REGENERATION OF TIDAL SAND WAVES AFTER DREDGING

Field data analysis, model simulations, and synthesis to dredging strategies

By

IRIS VERBOVEN

To obtain the degree of Master of Science

at the University of Twente,

to be defended publicly at the on December 1st, 2017 at 11:00 AM

Project duration:	May 17th - December 1st 2017	
Thesis committee:	Prof. dr. S.J.M.H. Hulscher	University of Twente
	Dr. ir. B.W. Borsje	University of Twente
	Ir. F.C.R. Melman	Boskalis
	Ir. R.J. de Koning	Boskalis

Student number: 1721135

Student contact: iris.verboven@xs4all.nl

UNIVERSITY OF TWENTE.

PREFACE

Before you lies the final result of my Master thesis into obtaining my master's degree in Water Engineering and Management at the University of Twente. It has been quite the journey from obtaining my bachelor's degree in the United States, moving to Enschede to continue my education at the University of Twente and finally to Boskalis where I got the opportunity to perform this research at Hydronamic, the engineering department of Boskalis.

The combination of scientific research and challenges that arise in dredging and offshore industry caused by sand waves is what initially interested me in this subject. During my research I discovered

Of course, I would not have been able to come to this point without the help of my supervisors and support of family and friends. I wish to thank Bas Borsje for giving me the opportunity to work with this subject and for guiding me through this final assignment of my master's degree.

When I arrived at Boskalis, Rick de Koning and Frank Melman really helped me with the transition. So thank you, Rick, for the interesting discussions, your commitment, and checking in with me every once in a while. I have to thank Frank for his fresh points of view and for reminding me that there are times to be serious and times to laugh.

My gratitude also goes to Prof. Hulscher, for her critical reviews, refreshing insights and her enthousiasm for sand waves.

I also want to thank Wietse van Gerwen for taking the time to help me with the numerical model.

Thank you, Jason for teaching me that anything worthwhile is hard to achieve and for always supporting me. Lastly, I want to thank my parents, who were there for me from the beginning to the end of this journey and for shaping me to the person I am today.

Iris Verboven
Papendrecht, November 2017

SUMMARY

The study into the regeneration of tidal sand waves after dredging becomes more and more important as offshore infrastructure becomes more demanding. In order to gain insight in the modeling of the regeneration of sand waves, this study is split up in two parts. The first part assesses the performance of a numerical model to predict the regeneration behavior of tidal sand waves after dredging. The second part focuses on the practical application of different dredging strategies, as well as whether the regeneration behavior of sand waves can be modeled and predicted for practical applications by using this numerical model.

Sand extraction sites on the Kwinte Bank in the Belgian North Sea are used as study sites in this research. Two transects that represent a dredged, and a undredged cross-section are determined and analyzed in order to gain insight in the wave height, wavelength, growth rates, and migration rates of the sand waves in the study site. The depth along both transects varied between 6.8 m to 22.8 m during those 11 $years$, and the wave heights and wavelengths showed a range of 23 $cm - 3.89\ m$ and $75 - 327\ m$ respectively. The growth and migration rates are determined linearly between two timesteps on the dredged and the undredged transect. The wave heigths of the dredged transect showed a positive trend and correspond to the initial stages of sand wave growth, whereas the wave heights of the undredged transect did not vary much and suggest that the sand waves have reached their equilibrium height. Migration of the sand waves in this area is oriented in Northwest direction with a magnitude of $9.8 - 17.8\ m/yr$. Furthermore, the sediment grain size, and the tidal current velocity amplitude are found from literature and the field data to use as input in the model. These values are set at 0.65 m/s for the tidal current velocity amplitude, and 0.35 mm for the sediment grain size. With these environmental input parameters, as well as the water depth that resulted from the data analysis a sensitivity analysis is performed for the wavelength of the fastest growing mode. This sensitivity analysis showed that the wavelengths that were found for the different combinations of input parameters fell within the range of wavelengths that are found in the field.

The wavelength of the sand wave that is visible in the field is considered the wavelength of the fastest growing mode. These wavelengths are found for the dredged and the undredged transect and have values of 178 m and 155 m respectively. Furthermore, the effect of different initial beds on the sand wave dynamics in the model is studied by applying three different bed profiles. The first initial bed is a small amplitude sine function that represents the dredged bed, the second is a schematized initial bed with a sine function that represents an undredged bed, and the third implemented initial bed is an idealized cross-section from the field data. The results of the long-term bed developments showed that the original and the schematized initial beds gave good results on the sand wave dynamics. However the equilibrium wave height of the sand waves in the model are generally overestimated. The idealized initial beds showed to be sensitive to the forcing of the system due to several wavelengths that are present on the transect. However, the development of idealized bed showed similar behavior to the field data. Furthermore, the timescale of regeneration of sand waves after dredging showed to depend on the environmental influences and the depth and ranged from approximately 35 $years$ to approximately 140 $years$. The model showed to generally underestimates the migration rates for all implemented initial seabeds.

In the design of offshore infrastructure, sand waves should be a point of attention because these dynamic seabed features can make the execution of a project more challenging and can interact

with structures that are placed on the seabed. A better understanding of the behavior of tidal sand waves after dredging can help identify specific challenges and find the best fitting solutions.

Two locations are selected based on the presence of sand waves and the presence of offshore projects. The locations that are used are Hollandse Kust (Zuid) Wind Farm, and Borssele Wind Farm. Three dredging strategies are applied at these locations namely: Peak Removal, Cut & Fill, and total sand wave Removal. In order to perform a behavior study, the input parameters (water depth, grain size diameter, and tidal current velocity amplitude) are varied.

The strategies that result in a flattened bed, Total sand wave Removal and Cut & Fill showed to have the lowest growth rates. Whereas 1/3 Peak Removal showed the highest growth rate, followed by 2/3 Peak Removal and full Peak Removal. Furthermore, the growth rates of the dredged sand waves can be linked to a 'base' growth curve for that location. The trend of the growth rates of the sand waves after dredging seemed to agree with the growth rates of the 'base' growth rates. Therefore, this may be used as an estimation of the growth rates in the design of dredging strategies for projects.

LIST OF PARAMETERS

H_0	Water depth
U_0	Depth average flow velocity
D_{50}	Mean sediment grain size
ρ_s	Sediment density
α_{bs}	Bed slope correction factor
C	Chézy coefficient
U_{S0}	Amplitude of horizontal tidal velocity (represents residual current)
U_{S2}	Tidal current velocity amplitude
FGM/ L_{FGM}	Fastest growing mode/ Wavelength of the fastest growing mode

TABLE OF CONTENTS

1. INTRODUCTION

Shallow sandy seas like the North Sea are covered in a variety of bed forms. These bed forms can reach heights ranging from centimeters for ripples, to hundreds of meters for tidal sand banks, and wavelengths (distance between two successive crests) of centimeters to kilometers. Large-scale bed forms are static and do not migrate, whereas smaller bed forms tend to be mobile. The sand wave crests are often almost orthogonal to the direction of the tidal current, and these sand waves usually do not appear alone but in patches, forming a sand wave field (Besio et al., 2008b). Furthermore, the migration of these sand waves is determined by the magnitude of the net current velocity and the dominant direction of the current (Tonnon, 2007).

Nowadays, there are many different kinds of human interventions that influence the dynamics of these bed forms. Sand mining, pipelines, cables, wind farms and shipping routes are examples of some of the human interventions that occur in the North Sea. Sand waves have shown to be the biggest threat to these human interventions due to their dimensions and behavior (Figure 1).

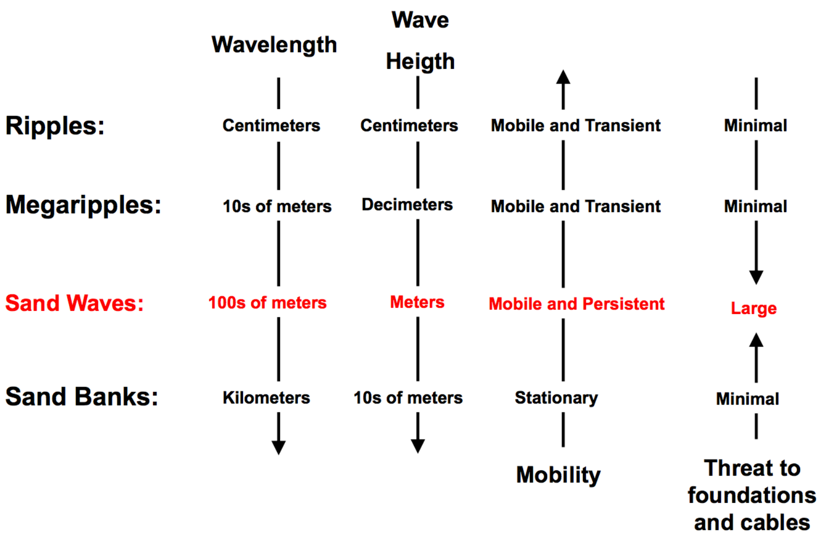

FIGURE 1 MORPHODYNAMIC SEABED FEATURES THE NORTH SEA (BORSSELE WIND FARM ZONE) AND SOME TYPICAL CHARACTERISTICS (HASSELAAR ET AL., 2015).

This dynamic behavior, and the growth of sand waves, makes it important to understand these bed features. For example, the depth of shipping routes can decrease due to the growth and migration of sand waves, and in order to keep these shipping routes functional they have to be dredged (Knaapen and Hulscher, 2002). Furthermore, sand wave migration can cause free spans in pipelines and can impact the integrity of the pipeline (Morelissen et al., 2003). Wind farms can also be affected by changes in sand wave fields in multiple ways. The scouring around foundations can cause instabilities, and cables have to be buried in the sand at a certain depth to make sure they will not get damaged (Hasselaar et al., 2015). A better knowledge about sand wave dynamics, especially the time-scale of formation, can improve the design and reduce the costs of offshore activities.

The formation of bed forms is caused by the interaction between the seabed and the tidal current (Hulscher, 1996). The time scales of the hydrodynamic processes and morphological processes have different magnitudes; a fast time scale t for the hydrodynamics, and a slow time τ for the seabed evolution (Roos and Hulscher, 2003). Hulscher (1996) explained the formation of sand waves with a vertical flow structure over small perturbations on the sea floor. The flow is accelerated on the stoss side of the perturbation due to decreasing water depths, whereas on the lee side, the increasing water depth causes the flow to slow down. An oscillating current causes this process to occur in both directions, which results in a net transport of sediment towards the crest. Borsje et al. (2013) stated that the balance between the net transport towards the crest, and the opposing factor, gravity, determine the preferred wavelength (see Figure 2). The wavelength of the sand wave that is visible on the seabed is also known as the wavelength of the fastest growing mode. As the sand wave grows, the wave height is defined as the vertical distance between crest and two adjacent troughs (Van Santen, 2009). *Németh et al.* (2006) investigated the non-linear behavior of sand wave development. Tracking the wave height through time results in a growth curve that results in the equilibrium height of the sand wave.

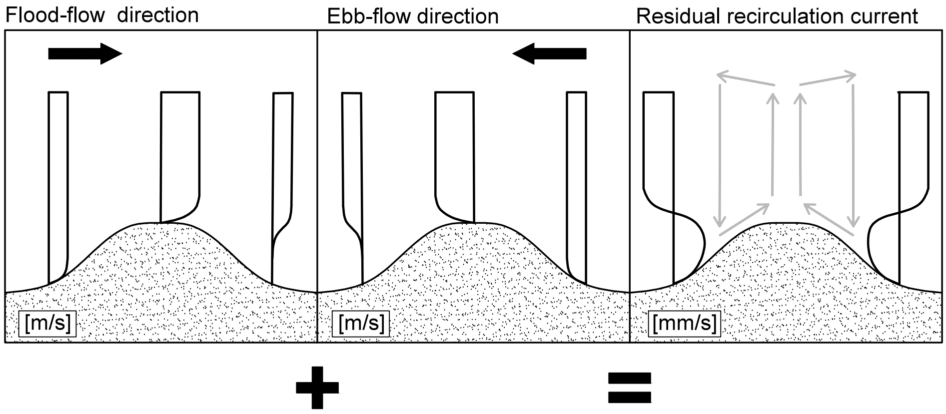

FIGURE 2 FORMATION OF SAND WAVES. THE FLOW PROFILES OF THE TIDES AND THE NET RECIRCULATION CURRENT (UNITS OF FLOW VELOCITY IN BOTTOM LEFT CORNER) (ADAPTED AFTER TONNON ET AL., 2007).

In an effort to accurately model sand wave dynamics, several models have been created to predict sand wave evolution. A distinction has been made in the literature review by *Verboven* (2017) between three kinds of models: linear, non-linear, and complex numerical. Linear models are limited to calculating the initial growth of sand waves due to non-linear components that become more dominant as the sand wave grows, whereas non-linear models can model equilibrium conditions as well. Furthermore, the literature review showed that a non-linear model has an advantage over a complex numerical model, because it allows for faster computations. However, complex-numerical models allow the modeling of sand wave field interactions, whereas non-linear models do not. Another noteworthy difference is mentioned by *Van Gerwen,* (2016): the stability model takes decades to reach the equilibrium height, whereas it takes centuries in the complex numerical model.

The first part of this thesis focuses on a study area located in the Belgian North Sea, and the numerical model Delft3d. The wavelength, wave height, migration rate, and regeneration time from the model are compared to the values from the field data in order to assess the time-scale of the regeneration of sand waves after dredging, and what the predictability of the model is for this part of the sand wave development. The second part of this thesis focuses on the synthesis between the model and practical applications for engineering purposes.

1.1 RESEARCH APPROACH

1.1.1. GOALS OF THIS RESEARCH

The first aim is to assess the performance of a numerical model to predict the regeneration behavior of tidal sand waves after dredging, and the second aim is to assess the applicability of this model for engineering requests.

Research questions

Research question 1:

What are the most influencing processes of a numerical model in order to predict the regeneration of tidal sand waves after dredging?

a. *What are the environmental conditions (flow velocity amplitudes, water depths, and grain sizes) and the dynamics from the sand wave field (wavelength, wave height, migration rate, and growth rate) of the study site in the North Sea?*
b. *What are the dynamics (wavelength, wave height, migration rate, and regeneration time) of the sand wave field when modeled in Delft3D, and what are the most influencing parameter settings?*
c. *How do the wavelengths, wave heights, migration rates, and growth rates from the model (RQ1.b) compare to the field data from the study site (RQ1.a)?*

Research question 2:

What insights does the model give towards the prediction of regeneration of tidal sand waves?

a. *What insights does the model provideon the prediction of sand wave characteristics (wavelengths, wave height and migration rates) and about the time scale of the regeneration of tidal sand waves after dredging?*
b. *What insights does the model provide about the usability for the design of offshore infrastructure in the North Sea?*

1.1.2. MATERIALS

Koen Degrendele of the Federal Public Service of Belgium, and Vera van Lancker of the Royal Belgian Institute of Natural Sciences have made the data that is used in this research available.

A Delft3D morphological model for the simulation of sand wave growth that is developed by *Borsje et al.* (2013), and *Van Gerwen* (2016) is used to conduct the numerical evaluation of the regeneration of sand waves after dredging.

1.1.3. METHODOLOGY

In order to answer the research questions, the study is divided in four parts:

- Literature review and research proposal
- System description: Extraction sites in the Belgian North Sea
- Data analysis
- Numerical modeling

Literature review and research proposal

A literature review and research proposal have been written in preparation for this thesis. The information and insights about sand waves, and Delft3D gained in these reports are further used in this study.

System description: Extraction sites in the Belgian North Sea

This section provides the necessary background information about the extraction sites in the Belgian North Sea. The hydrological conditions, and extraction dates, as well as other extraction sites in the area are studied here.

Data analysis

The goal of the data analysis is to answer the first research question. The wavelength, wave height, migration rate, and regeneration time are found in this section.

Numerical modeling

The first part of the numerical modeling uses site characteristics that are found in the data analysis, and the background information of the study site, in order to model the regeneration of sand waves after dredging. The second part of the modeling applied different dredging strategies at several locations in order to model the regeneration of sand waves after dredging for 5 $years$ after dredging.

1.2 OUTLINE

A literature study and research proposal preceded this Master's thesis, where sand wave dynamics, human interventions in the North Sea, and different models that are used to model sand waves, are discussed. Furthermore, the data from the study site on the Belgian Continental Shelf was studied, as well as the Delft3D model (Verboven, 2017). Chapter 2 gives a description of the study site where the field data has been collected. Chapter 3 contains the wave heights, wavelengths, depths, migration rates, and growth rates extracted from the study site data by performing data analysis that is described in that section as well. Furthermore, Chapter 4 is about the numerical modeling, and a sensitivity analysis on the short term calculations. This is followed by Chapter 5 where different initial beds are implemented in the model, and the wave heights, wavelengths, depths, migration rates, and growth rates are found and compared. The comparison of the model with the field data is described in Chapter 6. A synthesis of the model and engineering practice is formed in Chapter 7. Chapter 8 describes the discussions for previous chapters. Finally, Chapter 9 elaborates on the conclusions, limitations, and recommendations drawn from this study.

2. STUDY SITE

The data set and the study site are thoroughly discussed in this chapter in order to get an understanding of where it is located, what dredging activities occurred in that area, and how the monitoring of these sites happened.

2.1 DATA SET

From the literature review by *Verboven* (2017) it was found that data was scarce about (re-) generation of sand waves. However, a dataset is made available of two former sand extraction points in the Belgian Continental Shelf on the Kwintebank, off the coast near Ostend (see Figure 3). At these locations, the last sand extractions were performed February 15th, 2003 at KBMA, and October 1st, 2010 at KBMB. The reason that these sand extractions were stopped was that the, the geology, and ecology of the seabed were not taken into account. Therefore, when the depth at those locations had increased more than 5 m below the reference bed level, the extractions were stalled (Roche et al., 2011). After the extractions had stopped, these locations continued to be monitored in order to see how they would respond. The surveys of these areas were part of two monitoring plans for the Belgian North Sea, created by FPS Economy, for the periods between 2000 – 2010 and 2011 – 2014. A complete map of extraction, and monitoring sites in the Belgian North Sea can be found in the Appendix.

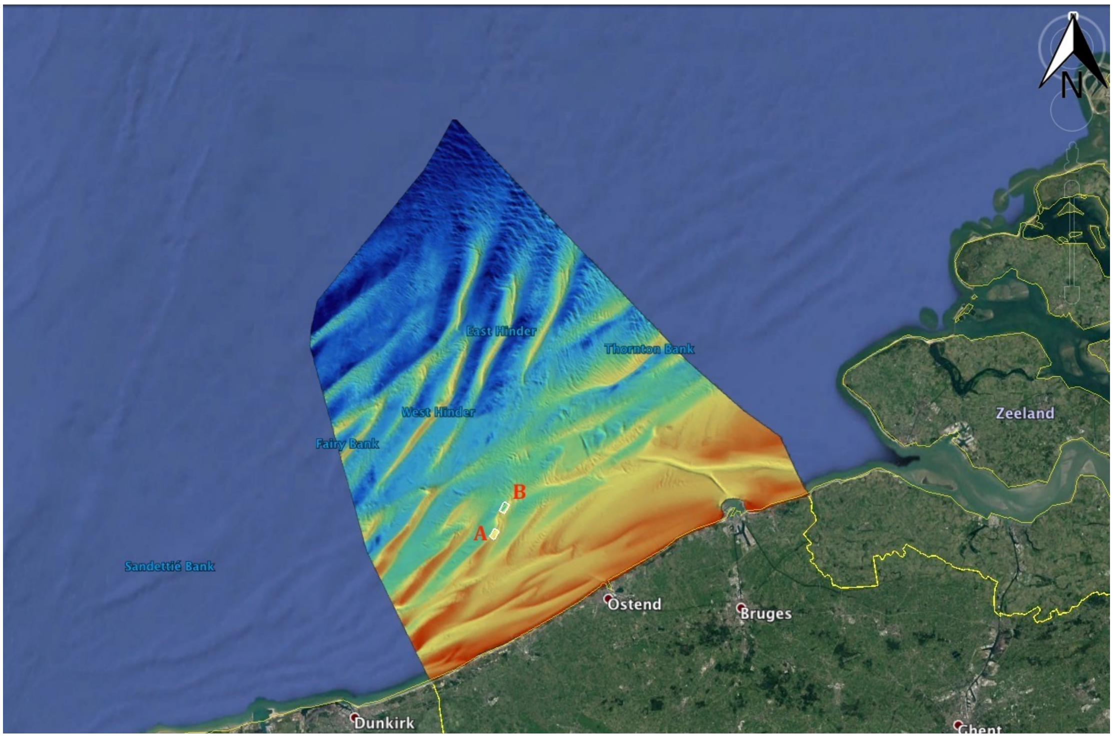

FIGURE 3 LOCATIONS A AND B OF THE FIELD MEASUREMENTS (WHITE AREAS) IN THE BELGIAN CONTINENTAL SHELF, (GOOGLE EARTH, AND DIENST CONTINENTAL PLAT & VLAAMSE HYDROGRAFIE, 2017).

Figure 4 shows the bathymetry for the two extraction sites. On the North side of the map, a darker area can be seen, which corresponds to the edge of the sand bank where these extraction sites are situated on. In the center of both maps, some sort of channel can be recognized; this is caused by the sand extractions.

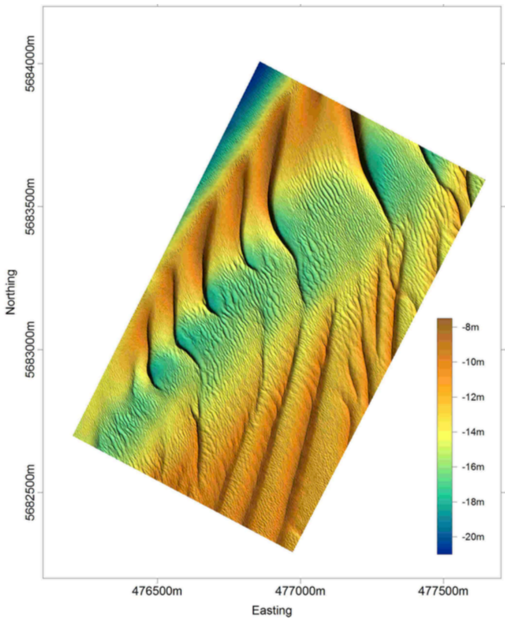

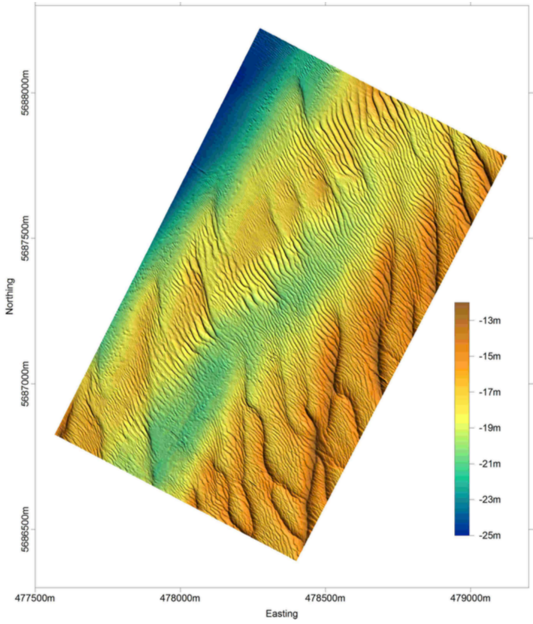

FIGURE 4A. MONITORING AREA KBMA. FIGURE 4B. MONITORING AREA KBMB. BOTH WITH TERRAIN RESOLUTION OF $1m$ BY $1m$ (ROCHE AND DEGRENDELE, 2011).

Figure 5 shows the evolution of the extracted volume from 2003 till 2010 for both monitoring locations. At KBMA, the volume of sand extractions decreased a lot until the site was eventually closed, however Figure 5a shows that some violations occurred in 2008. For KBMB, the volume of extractions was also decreasing until it was closed, and there were no problems with violations there. Until the closure of the extraction sites, it was found that there is very good correlation between extracted volume and depth increase. After the closure of the sites they showed to be stable; no significant erosion or accretion (Roche et al., 2011).

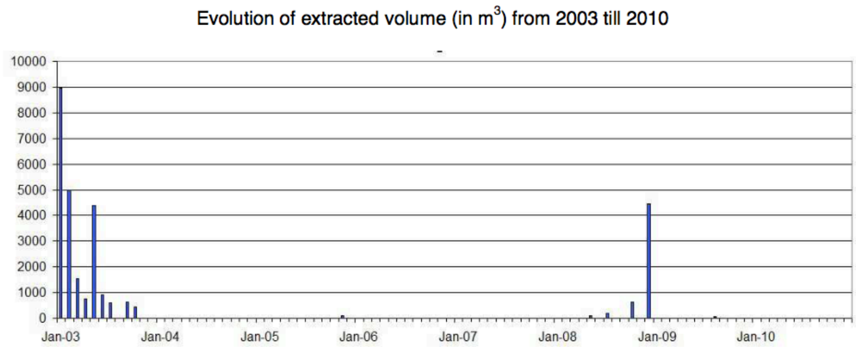

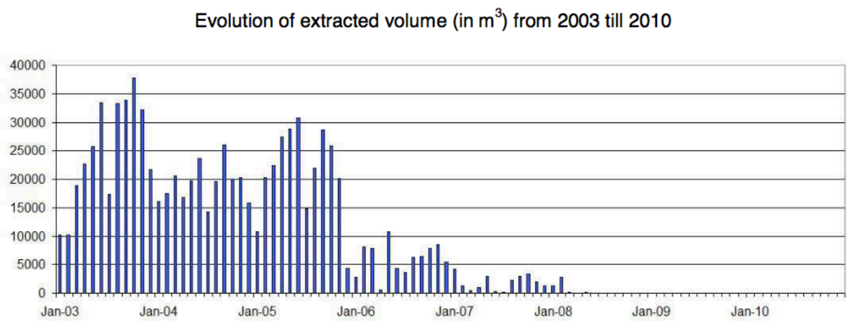

FIGURE 5A. EXTRACTED VOLUME FOR KBMA. FIGURE 5B. EXTRACTED VOLUME FOR KBMB (ROCHE ET AL., 2011).

The conclusions of the monitoring for the second period from 2010 – 2014 were similar as the conclusions drawn from the previous period (2000 – 2010). The bathymetry and sediments of the areas remain stable, however a slightly negative trend since 2011 is visible (see Figure 41 in Appendix) (Degrendele et al., 2014). Currently surveys are still performed at the monitoring locations, and the effects on the seabed, ecology, and environment of past dredging is being studied (Roche et al., 2016). Figure 42 in the Appendix shows the surveys that have been performed after 2014.

The monitoring was performed with an EM1002 multibeam on the R/V Belgica until the summer of 2008. After that they upgraded to an EM3002D multibeam system. During measurements in 2009, it was found that there was a systematic difference of 0.25 m between the measurements with the EM3002D and the EM1002 systems. It was also concluded that the source of this error was an error in the installation parameters of these systems, therefore a shift of 0.25 m is introduced for all monitoring calculations performed by the EM1002. Furthermore, an extra 0.10 m has to be corrected for a systematic error in the used draught that also affected the calculations of the EM1002. Thus, all values are recalculated to the EM3002D level (Roche et al., 2011). The surveys, and their corresponding corrections can be found in Table 17 the Appendix.

There were a total of 30 measurements taken for location A, and 29 measurements for location B. For location A, most of these measurements have taken place between 2000 and 2009, after that period the surveys were done once a year until 2014. However, the measurements that have taken place at location B were more evenly distributed between 2003 and 2014.

2.2 CHARACTERISTICS OF THE STUDY AREA

To be able to fully understand the behavior of the sand waves in the study areas, the characteristics of the Belgian North Sea are looked at. Table 1 shows the three parameters that are taken into consideration in the numerical model, for several locations on the Belgian Continental Shelf (Figure 6). Furthermore, Table 1B shows that there is a significant variety in depth, ranging between 5 m and 25m. Furthermore, the flow velocity that is used for the tidal current velocity amplitude is the depth average flow velocity derived from the mean velocity of the spring-neap cycle. The lowest depth average flow velocity found in the area is 0.1 m/s, and the highest flow velocity is 0.9 m/s. For the sediment grain size diameter the range falls between 0.18 mm and 0.40 mm, which corresponds to medium sands.

Location	$H0$ (m)	U_0 (m/s)	D_{50} (mm)
Kwintebank	23.8	0.52	0.35
Nieuwpoortbank	10.0	0.49	0.24
Trapegeer	6.3	0.47	0.21
Thorntonbank	21.5	0.46	0.33
Wandelaar	11.8	0.59	0.30
Westhinder	21.5	0.70	0.34
Akkaert NE	16.3	0.64	0.32
Akkaert N	24.1	0.62	0.31

Source	$H0$ (m)	U_0 (m/s)	D_{50} (mm)
Degrendele et al., 2010	5 - 25	Max 1 m/s at surface	0.18 - 0.40
Bellec et al., 2010	8 - 22	Max 1 m/s at surface	0.20-0.40
Garel, 2010	5 - 20/25	0.15-0.7	0.25 - 0.80
Van den Eynde et al., 2010	5 - 25	0.1 - 0.9	0.18 - 0.40

TABLE 1A PARAMETERS FOR LOCATIONS IN THE AREA (CHERLET ET AL., 2007). TABLE 1B PARAMETERS FOR LOCATIONS OF THE BELGIAN NORTH SEA USED BY OTHER SOURCES.

Where $H0$ is the mean depth at that location, U_0 is the depth average velocity, and D_{50} is the mean sediment grain size.

Several values for these parameters have been selected for the sensitivity analysis for the fastest growing mode in Delft3D. The depth range is determined by the results from the data analysis. The range of flow velocity of this parameter is determined from previous studies by *Cherlet et al.* (2007), and *Degrendele et al*. (2010). Furthermore, the range of the sediment grain size has been selected, by using the information provided by *Cherlet et al.* (2007), *Verfaillie et al*. (2006), and *Degrendele et al*. (2010) by looking at the exact location of the extraction site on the Kwintebank. *Cherlet et al.* (2007), and *Verfaillie et al*. (2006) focused on several locations in the Belgian North Sea, whereas *Degrendele et al*. (2010) thoroughly studied the Kwintebank area.

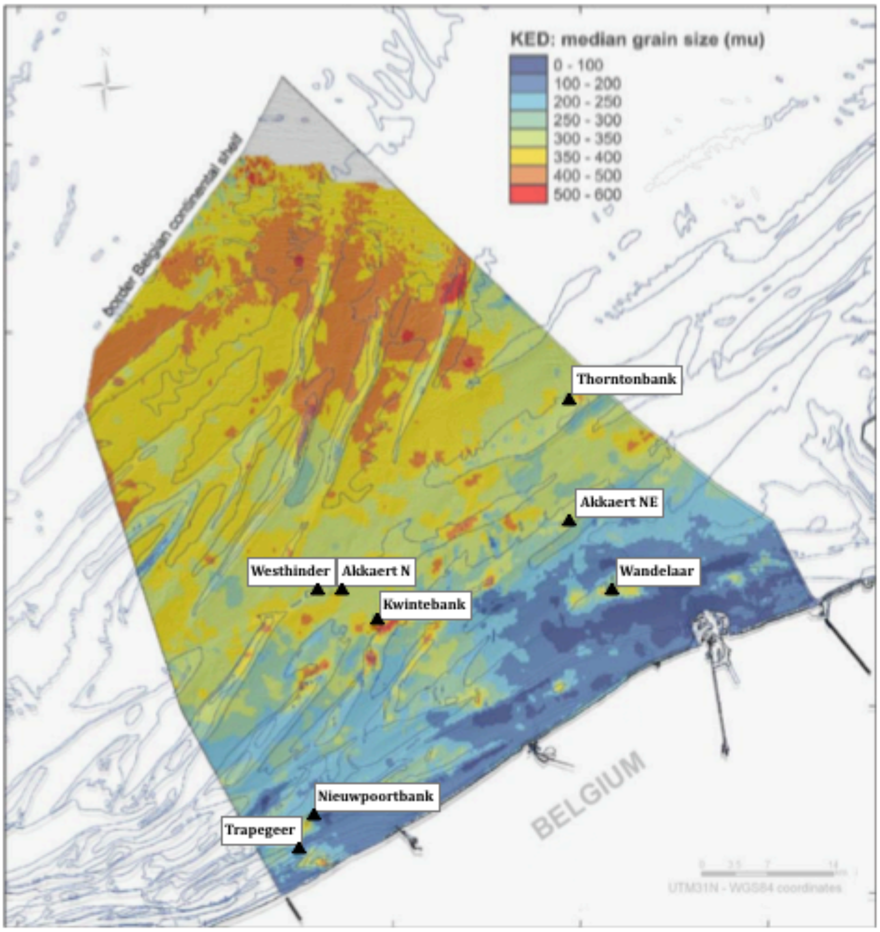

FIGURE 6 GRAIN SIZE DISTRIBUTION ON THE BELGIAN CONTINENTAL SHELF (ADAPTED AFTER VERFAILLIE ET AL., 2006 AND CHERLET ET AL., 2007)

3. DATA ANALYSIS

This chapter will analyze the data set that is used in order to gain a better understanding of the behavior of the seabed in the Belgian North Sea. The methods that are used for the data analysis that are performed are discussed. These methods are implemented for the two study sites that are discussed in the previous section and the sand wave characteristics (the wave height, sand wavelength, growth rate, and migration rates) at these locations are obtained. Moreover, the methods and results of this data analysis are discussed. In Chapter 6, the model results that are obtained in this research are compared to the results from the field data.

3.1 METHOD OF DATA ANALYSIS

The provided data has a resolution of approximately 1 m by 1 m and it is formatted as XYZ point data. Matlab and ArcMap are used to perform the data analysis of the provided measurements. To get a visual description of the bathymetry, the data is loaded in ArcMap and formatted as a raster in order to plot the depth at each grid point. In order to obtain the sand wave characteristics (wave height, wavelength, migration rate, and growth rates), three transects are analyzed at KBMA. The orientation of these transects is preferably parallel to the direction of the migration so that the sand wave development can be analyzed most accurately. After studying the characteristics of the study site in the previous section, it is determined not to analyze location B due to the many sand extractions that occurred during the time of the measurements.

The transects that are chosen at location A, have different orientations and locations in the wave field as can be seen in Figure 7 (as well as the names that have been given to the transects). The behavior within the dredged area is of great interest, therefore the first transect is located within, and parallel to the dredged channel (Dredged transect). On the North-West side of the Dredged transect , transect 2 is located, and its orientation is along the dredged channel in the undredged part of the study area (Undredged transect). A third transect was chosen on the Southeast side of the dredged area, this transect is parallel to the Dredged transect and is also located in an un-dredged part of the area (Parallel transect). The two transects located in undredged areas can be compared with the transect in the dredged channel and possible differences and similarities in their behavior can be found. Furthermore, it might be possible to find out whether the dredged channel has an effect on the un-dredged area, and what that effect could be. It has to be noted that the focus of this research is on the Undredged and the Dredged transects and the Parallel transect serves merely as a check. The depth along these transects was interpolated and exported from ArcMap with corresponding x- and y-coordinates in order to be able to analyze them in Matlab.

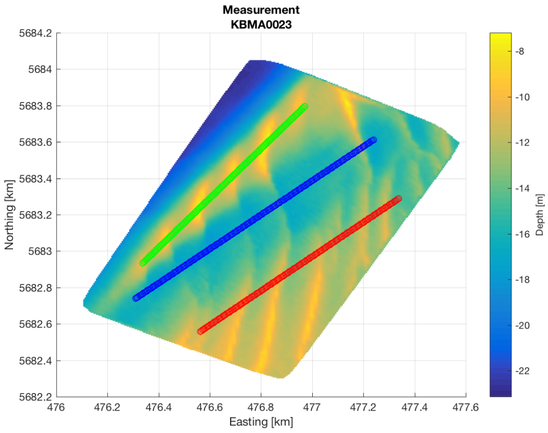

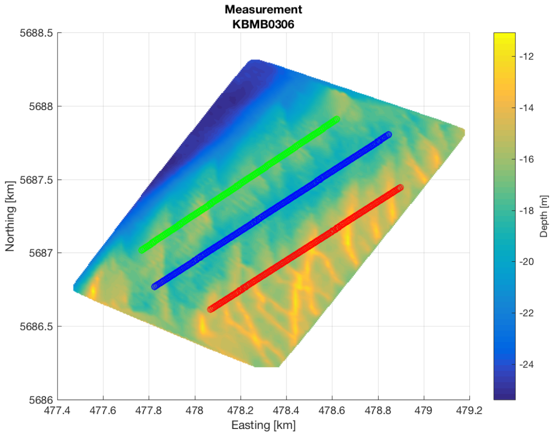

FIGURE 7A. SEABED AT LOCATION A, AT SEPTEMBER 28TH , 2000. FIGURE 7B. SEABED AT LOCATION B, AT MARCH 4TH, 2003.

NAMES OF TRANSECTS WHERE: GREEN IS UN-DREDGED TRANSECT, BLUE IS DREDGED TRANSECT, RED IS PARALLEL TRANSECT

The xyz-data is plotted on a grid that is created in Matlab, and this grid has a resolution of 5 m by 5 m in the x- and y- direction. The resolution of the grid is varied and plotted to find the optimal resolution that should be used, where the run time and accuracy were taken into account. The differences between a 1 m by 1 m grid and a 5 m by 5 m grid are plotted and are shown in Figure 43 in the Appendix. The figures show that the maximum difference that occurred was 0.21 m, however the average difference for that measurement along the cross section is 0.7 cm. The grid size of the original measurements is approximately 1 m by 1 m, however after comparing the results of the two grids, and the substantially longer run time needed for a smaller grid size, the decision was made to use a grid of 5 m by 5 m. The coordinates of the location of the points on the transects from ArcMap are interpolated in order to represent the coordinates, and corresponding depth, on the grid that is created in Matlab. The bottom profile is linearly interpolated so that the depth along the profile can be found for evenly spaced points.

A 1D-Fourier analysis is performed on the cross sections, and shows the distribution of the frequency spectrum, from which the dominant wavelengths are found. This is done in order to be able to filter out smaller and larger bed forms that are present in this measurement area. A low- and high-pass filter are applied in Butterworth filtering for wavelengths between 50 m and 1000 m respectively. The limits of these filters respond to the wavelengths of sand waves, however the lower limit is taken slightly smaller in order to be able to see how the smaller bed forms are situated on the sand waves (Van Santen et al., 2011). The magnitude of response of the Butterworth filters are shown in Figure 45 in the Appendix. The low-pass filter causes the smaller bed forms to be filtered out, whereas the high-pass filter will take care of the large bed forms like sand banks that can make the area look like it is lying under an angle.

After the Fourier analysis, the cross sections can be plotted and their behavior is analyzed. In order to study the behavior, the wave height, wavelength, growth rate, and migration rate is found. The wave height is defined as the vertical distance between crest and two adjacent troughs, whereas the wavelength is the distance between two successive troughs (see Figure 8). Therefore, in order to find the wave characteristics, the crests and troughs are found, as well as their locations. Sand wave migration causes some new sand waves to enter the domain, therefore a selection of crests and troughs is analyzed and these can be seen in Figure 9.

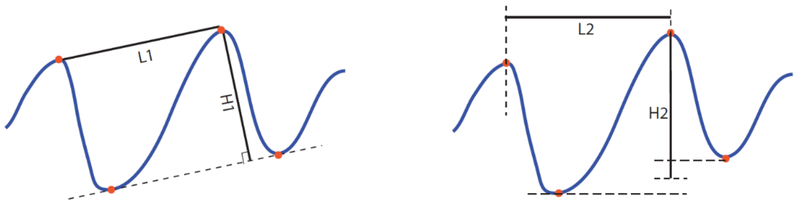

FIGURE 8 DEFINITIONS OF SAND WAVELENGTH AND HEIGHT, THE WAVE HEIGHT AND WAVELENGTH OF THE RIGHT FIGURE ARE ADOPTED HERE (VAN SANTEN, 2009)

Furthermore, the dashed triangle in Figure 9 shows the tracked crests and troughs, and the application of the method explained in Figure 8 to the field data. This method results in wave heights of 3 sand waves for the dredged and undredged transect, and only 1 wave height for the undredged transect.

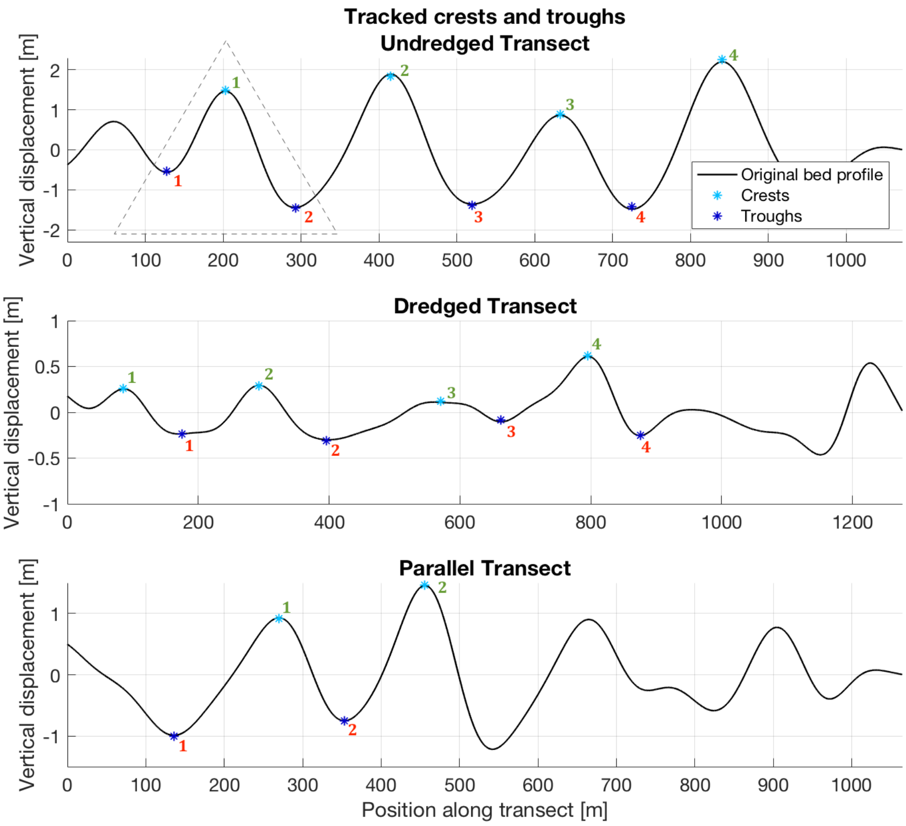

FIGURE 9 INITIAL CROSS-SECTIONS OF THE TRANSECTS WITH THE ANALYZED CRESTS AND TROUGHS. THE DASHED TRIANGLE INDICATES AN EXAMPLES OF COMBINATIONS OF CREST AND TROUGHS TO DETERMINE THE WAVE HEIGHTS AND WAVELENGTHS.

In order to obtain the growth rate, the wave height is plotted linearly between two measurements in time. During some years there were more measurements taken than other years, and the growth rates for those years are calculated as a weighted average of the individual measurements of that year. Migration rates are approximately linear through time, however they decrease slightly during the sand wave evolution (Németh and Hulscher, 2007). Therefore the migration rates are determined linearly in this research.

3.2 Results of data analysis

The data analysis is performed for the measurements that occurred after the last sand extractions in order to minimize the effect that these can have on the results. The top figure in Figure 10 shows the effect of the filters on the frequencies of the sand waves (where T_0 is March

4th, 2003 the first measurement after the sand extractions stopped), whereas the bottom figure shows the effect of the filters on the profile of the dredged cross section. It can be seen that the cross section is located on an angle with the horizontal axis, this could be caused by different dredging depths or sand is extracted at different times for different locations, and this angle shows up as the longer wavelengths in the single-sided amplitude spectrum. Furthermore, the effect of the sand extractions can be seen in Figure 10 because the sand waves on this cross section do not show a regular pattern like in an undisturbed transect (Figure 11).

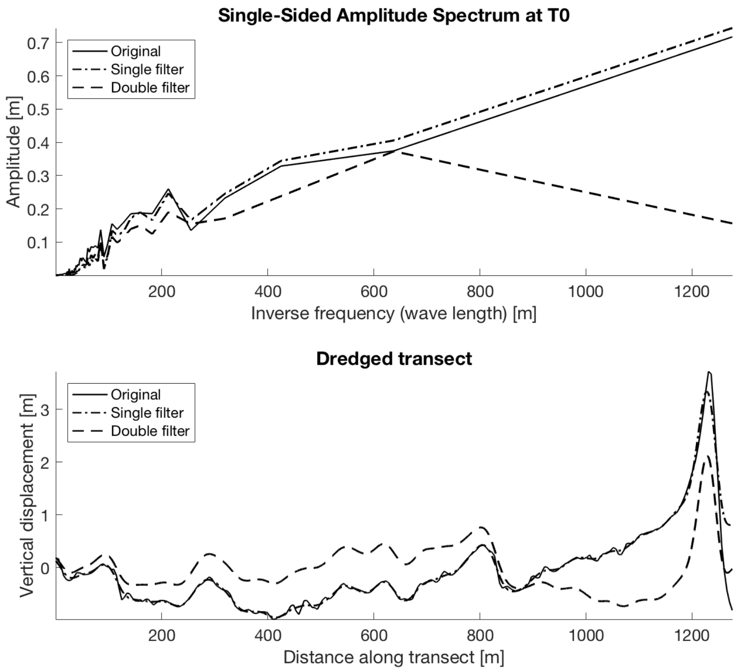

FIGURE 10 FOURIER ANALYSIS ON DREDGED TRANSECT OF KBMA IN THE TOP FIGURE, AND THE EFFECT OF THE BUTTERWORTH FILTERS ON THE TRANSECT IN THE BOTTOM FIGURE

The same Butterworth filters are applied for this transect as for the dredged transect and the results are shown in Figure 11. It can be seen that the undredged transect follows a more regular pattern and wavelengths of approximately 200 m are the most dominant.

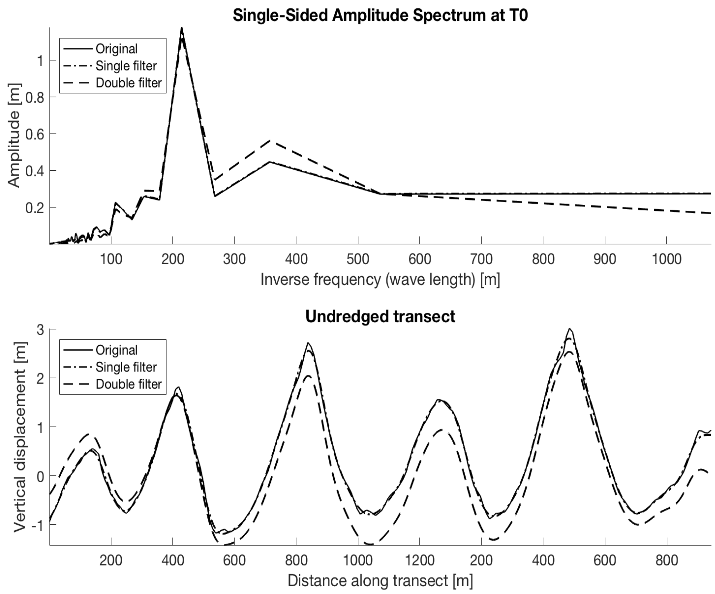

FIGURE 11 FOURIER ANALYSIS ON UNDREDGED TRANSECT OF KBMA IN THE TOP FIGURE, AND THE EFFECT OF THE BUTTERWORTH FILTERS ON THE TRANSECT IN THE BOTTOM FIGURE

The sand wave development along the cross sections from March 4th, 2003 through March 11th, 2014 is shown in Figure 12. It can be seen that the behavior of the un-dredged, and the parallel transect are more sinusoidal from the beginning than the behavior of the dredged transect. However, it can be seen that the dredged transect does regain that sinusoidal shape over time as the crests grow higher, and the troughs become deeper. A first impression of the bed development of the three transects shows that the wave heights of the undredged transect increase for some sand waves and decrease for others. The dredged transect shows general sand wave growth however this growth is not consistent through time. However, the wave heights of the parallel transect seem to decrease through time. The next sections elaborate on these first impressions of the bed development.

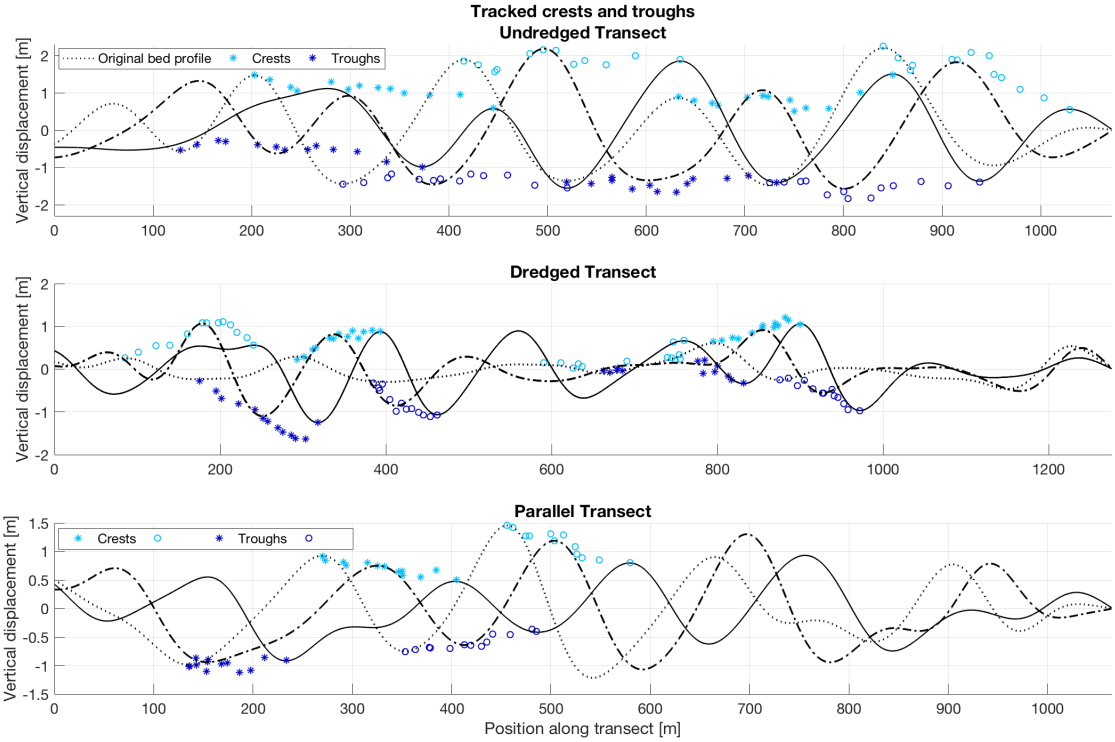

FIGURE 12 SEABED DEVELOPMENT BETWEEN 2003 AND 2014 FOR THE UN-DREDGED TRANSECT (GREEN), DREDGED TRANSECT (BLUE), AND PARALLEL TRANSECT (RED). CRESTS AND TROUGHS ARE PLOTTED FOR APPROXIMATELY EACH YEAR FOR CLARITY (FIGURE 49 IN THE APPENDIX) SHOWS ALL MEASUREMENTS FOR THE CRESTS AND TROUGHS.

Figure 13 shows the range of wave heights that are found for each year, thus the minimum and maximum value of the wave heights in a year indicate the range. Note that the measurements from the data set are not evenly spaced in time, therefore the time steps do not represent exactly one year between one and another. Furthermore, the range of wave heights includes all analyzed sand waves of a cross section in that year, so if more measurements are taken during that period, the wave heights recorded for those times are included as well. Figure 13A shows the wave heights of the dredged cross section. This cross section represents a dredged seabed, therefore it corresponds to the initial stage of sand wave formation. The trend of wave heights in Figure 13A, shows a positive trend that could translate to the general growth curve of sand waves. Furthermore, in Figure 13B it can be seen that the wave heights of the undredged transect do not show a clear trend of increase or decrease. The trend of the parallel transect shows a decrease in wave heights, however this transect is supposedly positioned in an undisturbed area. A possible explanation for this decrease in wave heights is that the dredged area may feed on sediment from undredged surrounding areas.

The range of wave heights of the dredged cross section is between 23.0 cm, up to 2.28 m. The maximum wave height that is found for the un-dredged and the parallel cross section are 3.47 m, and 2.28 m high respectively. The minimum wave height in the un-dredged cross section was 1.76 m, and 1.22 m for the parallel cross section.

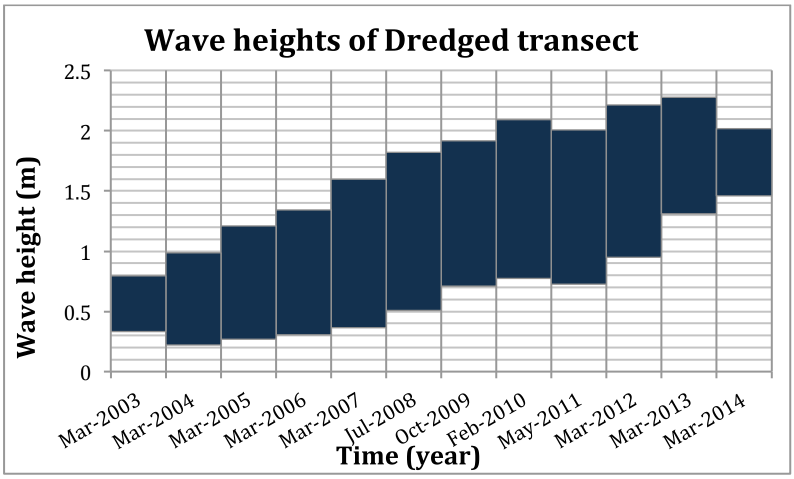

FIGURE 13A WAVE HEIGHTS FOR THE DREDGED TRANSECT (MEASUREMENTS ARE NOT EVENLY SPACED, THEREFORE THE TIME STEPS DO NOT REPRESENT EXACTLY ONE YEAR BETWEEN ONE AND ANOTHER).

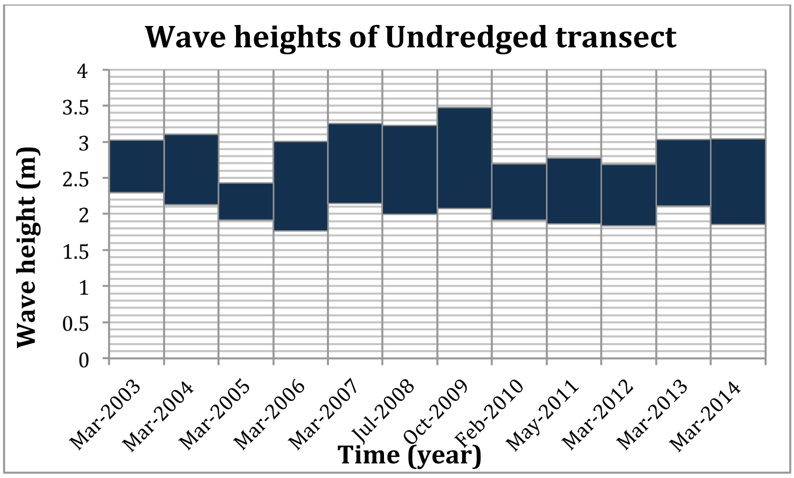

FIGURE 13B WAVE HEIGHTS FOR THE UNDREDGED TRANSECT

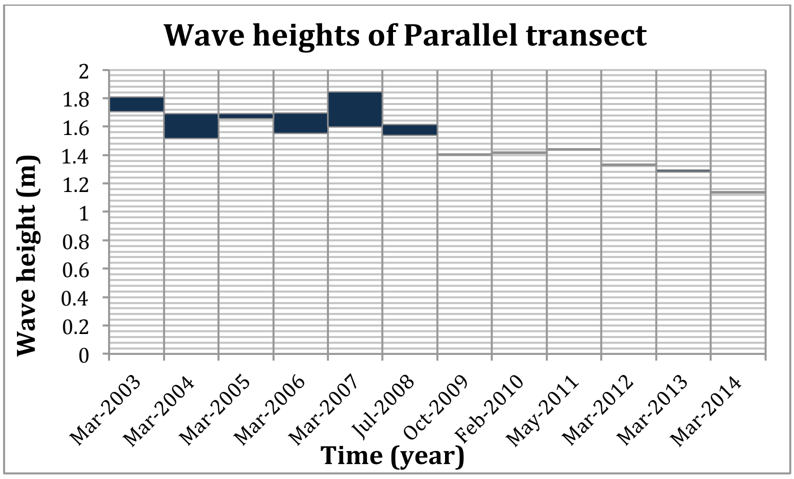

FIGURE 13C WAVE HEIGHTS FOR THE DREDGED TRANSECT

The wavelengths for the dredged transect range between 79.0 m and 290.7 m, which is a similar range as for the parallel transect that has a range of 75.2 m to 291.0 m. The wavelengths for the un-dredged transect are significantly longer and fall within a range of $147.3\ m$ to $327.2\ m$. Chapter A.3 in the Appendix shows the results for KBMB.

The sand wavelengths that are found for each cross section are plotted over time in Figure 14 in order to get a better understanding of their behavior and to possibly relate it to the findings from plotting the sand wave height over time.

Figure 14 shows all the different sand wave wavelengths that are found along the transects for each measurement. Due to changes in bathymetry during these periods, there can be a different number of data points at different measurement times. This is especially clear for the dredged transect, where the number of measured sand wave wavelengths varies between 8 and 4. It can be seen that the wavelengths of the undredged transect are divergent towards the last measurements taken, whereas they do not vary much in the first years of the measurements. The opposite can be seen for the dredged transect; the wavelengths of this transect seem to vary less towards the end of the measurements. Furthermore, the wavelengths found for the parallel transect increase slightly during the first couple of years, but they do not vary much until the last measurement.

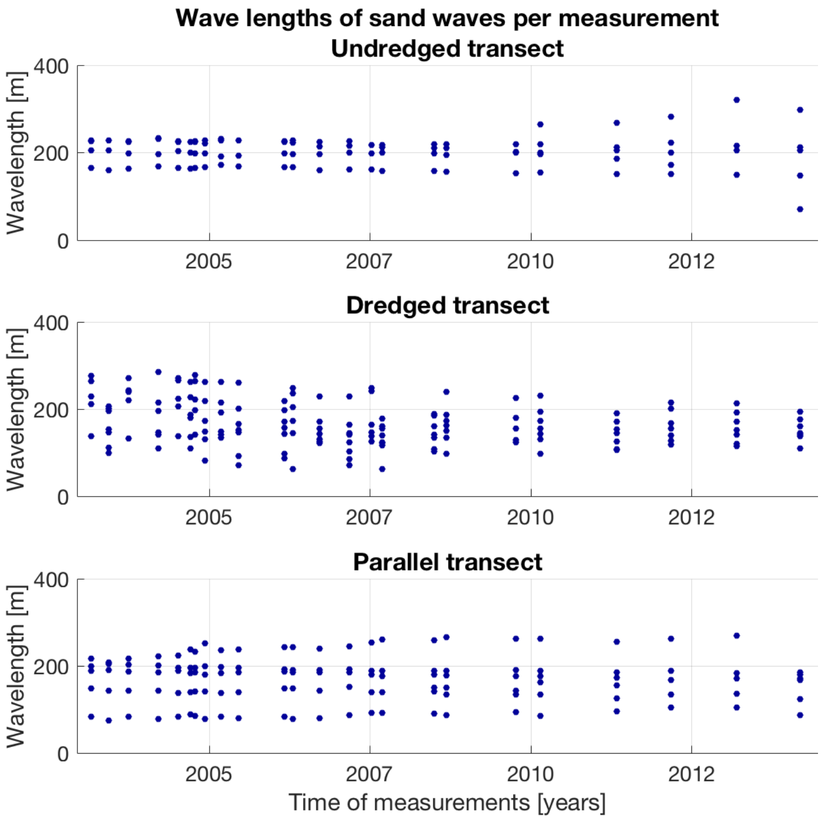

FIGURE 14 SAND WAVE WAVELENGTH PLOTTED OVER TIME

Figure 15A, B, and C show the results of the growth rates for the analyzed sand waves. Figure 50 in the Appendix shows the growth rates for each measurement individually where high growth rates (i.e. $144\ cm/yr$) or low growth rates (i.e. $-355\ cm/yr$) that occurred for only a short period of time (in this example 25 $days$) can be seen. These values are not representative of the growth rate during the whole year; therefore the (weighted) average value gives a better insight into the growth rate for those years. These high or low growth rates may be caused by for example, extreme weather events or illegal sand extractions.

In Figure 15A the growth rates for the dredged transect are shown and it can be seen that they range from $-26\ cm/yr$ to $38\ cm/yr$. Furthermore it can be seen that there are positive growth rates in every year except 2010, this may be caused by illegal sand extractions that happened between 2008 and 2009, and in 2010 at KBMA. A greater effect of this may be seen in Figure 15B for the undredged transect, where the negative growth rates in 2009 stand out compared to the growth rates of other years. The ranges of the growth rates for the undredged transect are generally smaller than the ranges of the dredged transect and they range from $-78\ cm/yr$ to $54\ cm/yr$.

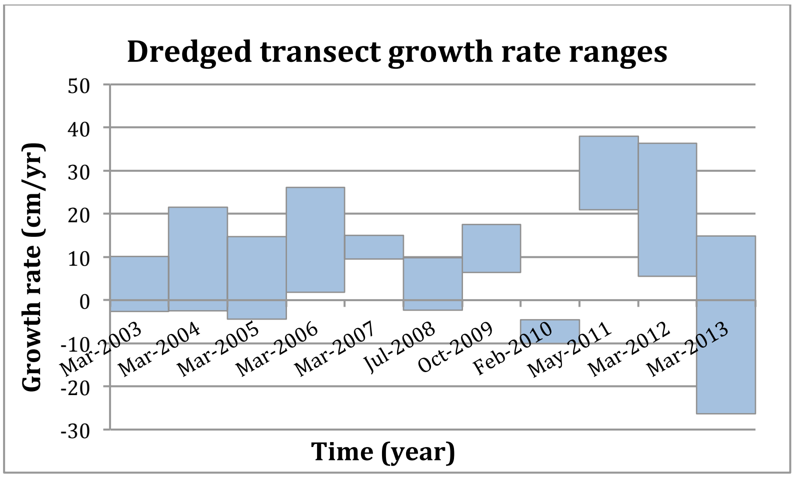

FIGURE 15A GROWTH RATE RANGES OF DREDGED TRANSECT (MEASUREMENTS ARE NOT EVENLY SPACED, THEREFORE THE TIME STEPS DO NOT REPRESENT EXACTLY ONE YEAR BETWEEN ONE AND ANOTHER).

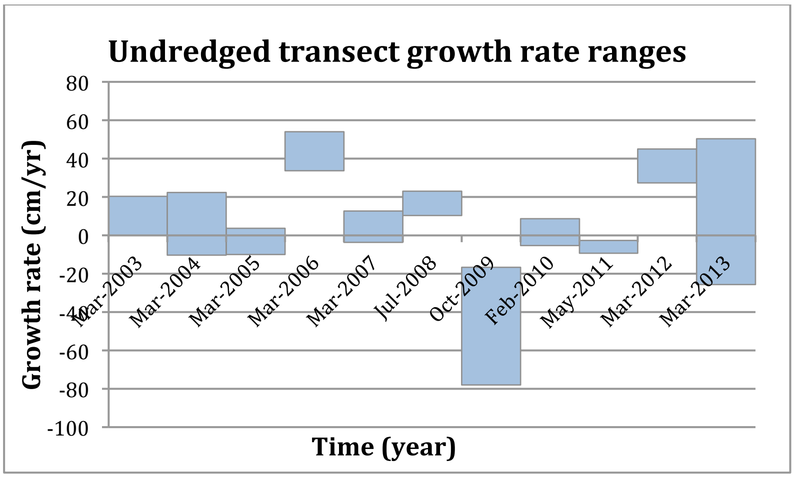

FIGURE 15B GROWTH RATE RANGES OF UNDREDGED TRANSECT

The growth rates of the parallel transect are generally negative, and this could be caused by the dredged area in the study site that takes away sediment from the surrounding undredged areas (in this case the parallel transect). The range of growth rates for this transect falls between $15\ cm/yr$ and $6\ cm/yr$.

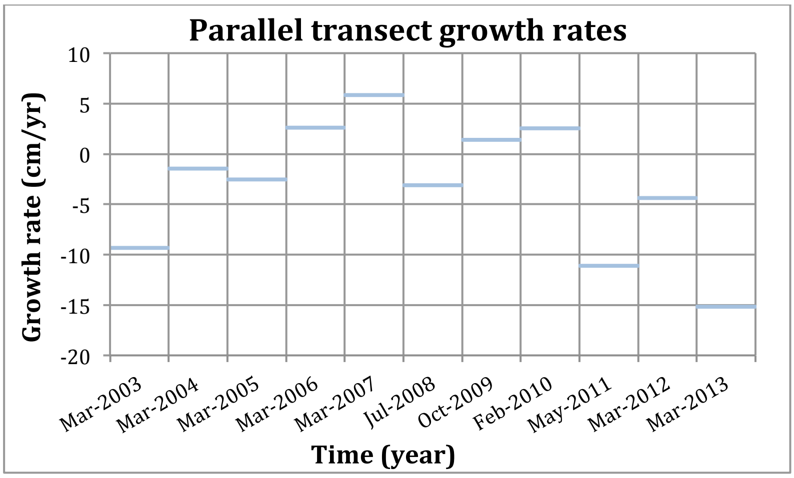

FIGURE 15C GROWTH RATE RANGES OF PARALLEL TRANSECT

It can be seen in Table 2 that the migration rates of the crests of the undredged transect are slightly lower than the migration rates of the troughs. Whereas the migration rates of the dredged transect show opposite behavior. It is remarkable that the rates of the parallel transect are significantly lower than from the undredged transect even though both are located in supposedly undisturbed areas.

	Migration (m/yr)	
	Crests	*Troughs*
Un-dredged (green)	16.8	17.7
Dredged (blue)	13.5	12.4
Parallel (red)	11.2	9.8

TABLE 2 AVERAGE MIGRATION RATES

3.3 RECAP OF FINDINGS FROM DATA ANALYSIS

The wave heights of the dredged area show a positive growth curve, even though the growth rates found are not all positive. This positive trend could correspond to the initial stage of sand wave growth. Furthermore, the wave heights of the undredged transect did not show a clear positive or negative trend; these wave heights showed not much variation through time. This could indicate that these sand waves have approximated their equilibrium height. The results of the wave heights of the parallel transect may imply that the illegal sand extractions that took place between 2008 and 2009, and once more in 2010 may have happened on, or near this transect. Furthermore, a decrease in wave heights could be caused by the dredged area that draws sediment from surrounding areas.

Wavelengths in the study area ranged from 75 m to 327 m including all three transects. The wavelength of the sand waves present on the dredged transect showed to vary more in the beginning, whereas towards the end there was less variation and four clear sand waves are present. The undredged transect showed four clear sand waves on the transect at all times, and migration of sand wave in and out of the transect could be seen as well.

The migration rates of the sand waves in the study area showed a range of 9.8 m/yr to 17.8 m/yr. The lower migration rates resulted from the dredged transect where an extra trough that formed during the time of the measurements.

4. NUMERICAL MODEL: DELFT3D

This chapter describes the way that Delft3D is set-up, and what input parameters are used in the model. Furthermore, a sensitivity analysis on the fastest growing mode is performed in order to see the effect of different input parameters on the wavelength of sand waves. The outcomes of the sensitivity analysis are used for the selection of input parameters for later parts of this research. Furthermore, the results of the short-term calculations of the model serve as an input parameter for the long-term calculations.

4.1 MODEL DESCRIPTION

Delft3D is a process-based numerical model developed by Deltares for two- and three-dimensional modeling of rivers, coastal areas, and estuarine environments (Lesser et al., 2004). *Borsje et al.* (2013) gives a detailed description of the Delft3D-FLOW model; the system of equations consists of the horizontal momentum equations, a continuity equation, a turbulence closure model, a sediment transport equation and a sediment continuity equation. Furthermore, the vertical momentum equation is reduced to the hydrostatic pressure relation as vertical accelerations are assumed to be small compared to gravitational acceleration (Borsje et al., 2013). The model exploration by *van Gerwen* (2016b) stated that, due to long computation times for three-dimensional calculations, the model is run in the two-dimensional vertical (2DV). This could only hold under the assumption that Coriolis effects can be neglected (as shown by *Hulscher*, 1996). Furthermore they stated that wind effects are neglected by imposing a no-stress condition at the surface boundary, and in order to reduce computation time, a morphological acceleration factor is added to the model. This factor is multiplied by bed level change computations after a hydrodynamic time step (Van Gerwen, 2016).

Previous model results show that the growth of the sand waves is highly influenced by the choice of the sediment transport formula that is used (Choy, 2015). *Borsje et al.* (2014) uses a transport formulation by *van Rijn* (1993), which included bed load, suspended load, and sediment transport due to surface waves, whereas Choy et al. (2015) also tested the transport formulation from both *Engelund and Hansen* (1967), and *van Rijn* (2007). The implementation of Engelund and Hansen (1967), results in extremely high sand waves in a very shore time. This effect can be suppressed by increasing the bed slope effect, but it is not eliminated over time. The formula by *Van Rijn* (1993) has proven to predict sediment transport reasonably well in various environments. Van Rijn (2007), is an improved version of Van Rijn (1993) concerning the sediment transport under wave action (Choy, 2015).

Van Gerwen et al. (2016) developed Matlab scripts in order to implement adjustments to the Delft3D model. These scripts depend mainly on an MDF-file and files that describe the corresponding process parameters (Van Gerwen, 2016). The model output will also be handled with Matlab scripts.

4.1.1 DELFT3D MODEL SET-UP

The settings for the model are based on the model settings by *van Gerwen* (2016). For a more detailed description, we refer to *Borsje et al.* (2014). The numerical model finds the wavelength of the fastest growing mode in the short-term calculations. This wavelength of the fastest growing mode is the wavelength that is visible in the sand wave field, and serves as an input parameter for the long-term bed development calculations of the model.

Grid

The grid for the vertical plane is chosen as the commonly used σ-grid, which results in a constant number of layers over the whole model domain. In this case, the vertical resolution is set to 60 σ-layers that have an increasing resolution towards the bed. The distribution of these calculation layers is non-uniform, which allows for higher resolutions near the bottom topography (*van Gerwen* (2016) from *Deltares,* 2014a). The horizontal grid has 558 calculation points over a total distance of 50 kilometers. The middle of the domain has a higher grid resolution of 2 meters, whereas the boundary has a resolution of 1500 meters. The grid can be extended for the modeling of migration. The GRD-file of the model contains the grid information, and this is created using Matlab with the *gridgeneration.m* file that is part of the model (Van Gerwen, 2016).

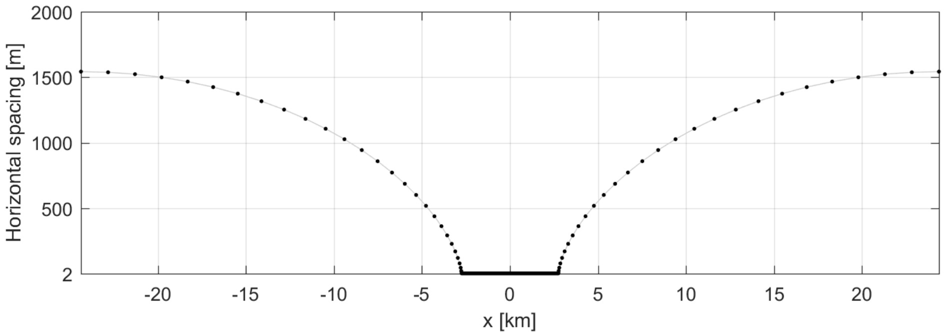

FIGURE 16 HORIZONTAL GRID SET-UP

Initial bed profile

The model has a sinusoidal initial bed profile, and a wavelength equal to the fastest growing mode (L_{FGM}) will be used. In the center, the sand waves have an amplitude of 1% of the mean water depth (0.25 m) for the initial profile. The *envelope.m* file is used to create a gradual transition from the flat bed to the sand wave field. For the long-term calculations, the migration of the seabed has to be taken into account; therefore the 2 m grid resolution is extended into the direction of the migration (van Gerwen, 2016).

Choy (2015) and *Van Gerwen* (2016) investigated the effect of a random initial bed. It was found that the seabed reorganized itself to find the fastest growing mode before sand waves start growing. The simulation time is shortened by implementing a sinusoidal initial bed with a wavelength of the fastest growing mode.

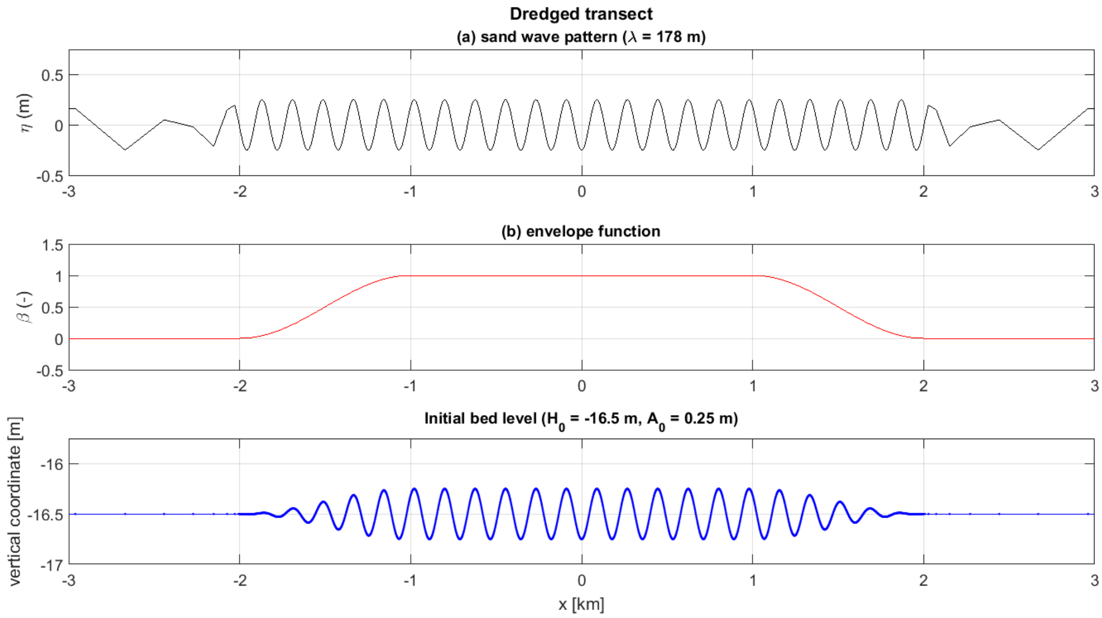

FIGURE 17 EXAMPLE OF INITIAL BED LEVEL IMPLEMENTED IN THE MODEL

Morphodynamics
Delft3D has a default transport formulation, which is adapted after *Van Rijn et al*. (2001). In the SED-file, the median grain diameter can be defined, as well as the sediment density and the thickness of the bed layer. Furthermore, the MOR-file includes the defined bed slope correction factor, and morphological scale-factor.

The MORFAC value is used to optimize the relationship between the results and the computation time. The deposition and erosion fluxes are multiplied with a factor 2000 during each time step, to speed up the geomorphological changes. The result is that one tidal period corresponds to $12\ hours * 2000 \approx 2.7\ years$ of geomorphological changes. Smaller MORFAC values showed quantitatively the same results but required longer simulation times (van Gerwen, 2016).

Hydrodynamics
The tide is forced at the boundary, with one boundary on the East side of the domain, and another on the West side. Riemann boundary conditions are applied, allowing for flow trough the boundary with minimal reflection. The tidal components are expressed in a tidal amplitude and phase. Furthermore, the hydrodynamic time step is set to 12 seconds. The four strongest tidal components in the North Sea are the semidiurnal lunar tide (M_2), the semidiurnal solar tide (S_2), the diurnal luni-solar declinational tide (K_1) and the diurnal lunar declinational tide (O_1). Where the M_2-tide has the greatest impact (Velema, 2010). However, the S_2-tide is used in the model because the velocity is symmetrical in time, and the frequency is almost identical. This symmetry makes it easier to calculate the tide-average velocity values. The values that are used for the tidal current velocity amplitude are the depth average velocities that are found in the area. Furthermore a tidal asymmetry is implemented to simulate sand wave migration. This tidal asymmetry is implemented by introducing a residual S_0 tidal velocity.

1.2.1 METHODOLOGY OF SHORT TERM FASTEST GROWING MODE CALCULATIONS

The grain size is varied in order to analyze its effects on the results of the model, the values that have been studied are shown in Table 4. This range is determined by the use of *Verfaillie et al.* (2006), and *Cherlet et al.* (2007) for the Kwintebank area. Furthermore, the sediment density (for sand), the bed slope correction factor, and the Chézy coefficient are shown in Table 3. The bed slope factor corresponds to an angle of repose of sand of 19°. Brière et al. (2010) and Ruddick & Lacroix (2006) stated that the asymmetric tidal flow (Amplitude of horizontal S_0 tidal velocity in Table 3) in the North Sea typically falls between 0.01 m/s and 0.1 m/s.

	Value	Units	Parameter
Sediment density	2650	kg/m^3	ρ_s
Bed slope correction factor	3	[-]	α_{bs}
Chézy coefficient	75	$m^{1/2}/s$	C
Amplitude of horizontal S_0 tidal velocity	0.05	m/s	U_{S0}

TABLE 3 VALUES USED IN DELFT3D FOR HYDRODYNAMIC PARAMETERS

The parameters shown in Table 4 are used for a sensitivity analysis in order to establish whether these ranges comply with the wavelengths found in the field, and what their impact is on the wavelength of the fastest growing mode. The depth is varied for different values that are found in the study site from the data analysis, and are shown in Table 4. The selected values for the minimum, mean, and maximum depths come from the three transects that are analyzed. For the maximum and the minimum, the absolute minimum and maximum values that are found on the transects are used. Whereas the mean is firstly calculated from the spatial depth distribution along each transect. This gives a mean value for each transect of each time step. In order to end up with the value that is used, the time average of these values is taken.

	Depth (m)	Tidal current velocity amplitude (m/s)		Grain size diameter (mm)
Maximum	22.8	0.70	Westhinder	0.20
Mean	14.1	0.52	Kwintebank	0.35
Minimum	6.8	0.46	Thorntonbank	0.50

TABLE 4 RANGES OF VARIABLES FOR THE STUDY SITE THAT ARE USED IN DELFT3D, WHERE THE DEPTH VALUES COME FROM THE DATA ANALYSIS, AND THE TIDAL AMPLITUDES AND GRAIN SIZE DIAMETERS FROM *CHERLET ET AL.* (2007).

A table with the different runs that are performed is shown in the table Table 5. Case I through VI represent the sensitivity analysis, and case VII uses all mean values. . It is important to note that each minimum or maximum value that is included in this sensitivity analysis is combined with average values that are found in the area. Therefore it is expected that the results do not show the absolute minimum or maximum that are found in the data analysis. In the case that the wavelengths that are found are not representative of all wavelengths that occur in the area, an additional set of combinations of parameters is created. To extend the wavelengths found by the sensitivity analysis and to show that the model is capable of modeling all wavelengths that occur in the area.

Case	Depth	Tidal amplitude	Grain size diameter
I	Max	Mean	Mean
II	Min	Mean	Mean
III	Mean	Max	Mean
IV	Mean	Min	Mean
V	Mean	Mean	Max
VI	Mean	Mean	Min
VII	Mean	Mean	Mean

TABLE 5 COMBINATIONS OF PARAMETERS

In order to simulate the long-term sand wave growth, the fastest growing modes for the dredged, and the undredged transects have to be determined. For those short-term calculations, the sediment grain size is set to 0.30 mm, the tidal current velocity amplitude (S_2) is 0.65 m/s, the asymmetric tide (A_0) has a value of 0.05 m/s, and the water depth is 16.5 m and 13.8 m for the dredged, and the undredged transect respectively. These values come from a combination of the data analysis, and the different papers that are presented that performed studies in the area. Furthermore, it has to be noted that the water depths that are used for these simulations are the average depths of the transects of the first measurement after the last sand extraction.

4.2 RESULTS SENSITIVITY ANALYSIS OF FASTEST GROWING MODES

The fastest growing mode (L_{FGM}) is determined in similar fashion as is done in *Borsje et al.* (2013). A spin-up time of one tidal cycle is used, and a second tidal cycle is used to determine the bed evolution. This fastest growing mode will be used to run the model for long-term bed changes. Whenever the input conditions changes, the fastest growing mode will be recalculated, therefore the long-term bed changes will also be affected. For practical applications, the results of this sensitivity analysis can be used to determine which parameters can have a bigger impact on the fastest growing mode, and the sand wave development. When determining how accurate certain parameters have to be for a simulation of sand waves at a specific location, these results can provide some insight.

Figure 18 shows the results of the sensitivity analysis on the fastest growing mode by varying environmental parameters. It can be seen that the wavelengths that are found for all cases fall within the wavelength range that is found in the field by the performed data analysis. It can be seen that the ranges of fastest growing modes that are found fall in the lower part of the range of wavelengths that are found in the field. The growth curves of the fastest growing mode for each case are shown in Figure 54 in the Appendix

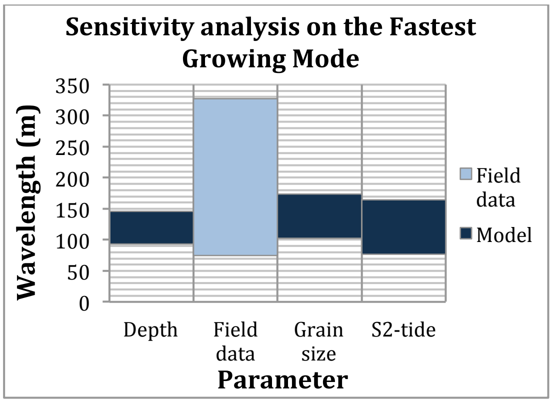

FIGURE 18 SENSITIVITY ANALYSIS OF GRAIN SIZE DIAMETER (D50), TIDAL CONSTITUENT (US2), AND WATER DEPTH (H0) ON THE FASTEST GROWING MODE.

Table 6 shows the deviation of the mean value for each of the parameter and Table 7 shows the effect on the wavelength of the fastest growing mode caused by the parameter change, compared to the wavelength of the fastest growing mode when all parameters are set to their mean values. It can be seen that the tidal velocity has the greatest impact on the fastest growing mode. Whereas the grain size diameter shows that an increase in diameter results in a slightly smaller wavelength, and a decrease in diameter results in a significantly larger wavelength. The change in depth shows a moderate effect on the change in wavelength.

	Depth	Tidal current velocity amplitude	Grain size diameter (mm)
Maximum	+62%	+35%	+43%
Mean	14.1 m	0.52 m/s	0.35
Minimum	-52%	-12%	-43%

TABLE 6 RELATIVE CHANGE OF INPUT PARAMETER FOR THE SENSITIVITY ANALYSIS

	Depth	Tidal current velocity amplitude	Grain size diameter (mm)
Maximum	+26%	+41%	-12%
Mean FGM	116 m	116 m	116 m
Minimum	-20%	-34%	+50%

TABLE 7 EFFECT OF PARAMETERS ON THE WAVELENGTHS OF THE FASTEST GROWING MODE

Figure 18 shows that the range of wavelengths found in the field is significantly greater than the fastest growing modes that are found by the model. In order to expand this range, another set of parameters is created where the maximum values are used instead of the mean values (see Table 8). The exception to this is the grain size diameter; the value for this parameter is set to the minimum size. It has to be noted that for each set, one parameter is changed to the mean value that is specified previously.

Name of parameter set:	Depth (m)	Tidal current velocity amplitude (m/s)	Grain size diameter (mm)	Wavelength FGM (m)
Maximum	22.8	0.70	0.20	605
D_{50}	22.8	0.70	0.35	227
S_2	22.8	0.56	0.20	223
Depth	14.1	0.70	0.20	322

TABLE 8 ADDITIONAL PARAMETER SETS IMPLEMENTED IN THE MODEL IN ORDER TO STUDY THE SENSITIVITY OF THE FASTEST GROWING MODE, AND THE RESULTS OF THE FASTEST GROWING MODE

The results of the wavelengths for the additional parameter sets are shown in Figure 19, as well as the field results and the initial model results that are based on the mean values of the input parameters. It can be seen that the combination that uses the maximum flow velocity, maximum depth, and minimum grain size diameter results in the greatest wavelength. For the other combinations one parameter is changed to the mean value, and it can be seen that this results in smaller wavelengths, however they are greater than the wavelengths shown in Figure 18.

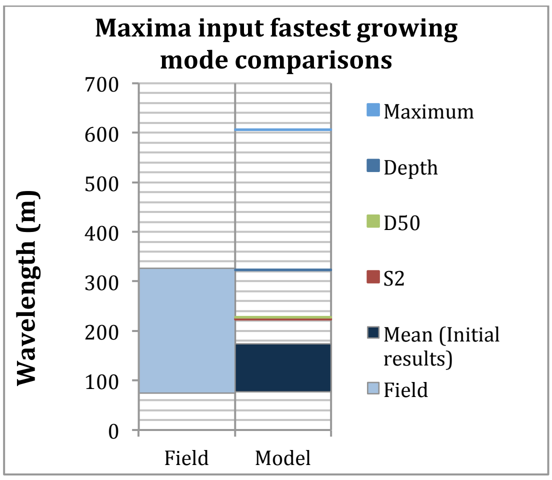

FIGURE 19 RESULTS OF THE WAVELENGTHS OF THE FASTEST GROWING MODE, COMPARED TO THE FIELD DATA AND THE INITIAL MODEL ('MEAN') RESULTS.

The wavelengths of the fastest growing mode for the dredged case, and the undredged case that are found by these short term calculations, are used as input for the long-term calculations. The wavelengths that are found for each case are 178 m, and 155 m respectively. These ranges fall within the wavelengths that are found for the study area in the data analysis, therefore it is assumed that they are representative of these two transects.

5. SIMULATION AND ASSESSMENT OF DIFFERENT INITIAL BEDS

In this section, the methodology of the long-term calculations that are performed is described. A model behavior study is performed that originated from the idea that the implemented initial bed in this Delft3D model is a perfect sine function with the wavelength of the fastest growing mode, however in reality this is not the case. As mentioned in the Introduction *Choy* (2015), and *van Gerwen* (2016) already looked into implementing a random initial bed into the model, therefore a random initial bed is not implemented in this research. Three different initial beds are implemented here, that transition from the perfect sine function to an idealized cross section from the data analysis. Wave heights, wavelengths, growth rates and migration rates of each case are obtained and compared to each other in order to assess their performance. These results are used in the next chapter as well, in order to compare them to the sand wave characteristics found in the data analysis.

5.1 METHODOLOGY OF LONG-TERM RUNS

In the data analysis, three different transects are analysed; the undredged, dredged and parallel transect. The results indicated that there may be interaction between dredged, and undredged areas, and this could explain the behavior of the parallel transect where the wave heights decreased through time. As stated previously, the focus is on the undredged and the dredged transect, therefore only the dredged and the undredged transect are used for the following parts of this research. The initial beds that are implemented are sorted into three categories that are shown in in Figure 20 and they are explained in the following section.

Category 1: Original small amplitude sine function
It is mentioned before that the formation of bed forms is caused by the interaction between the seabed and the tidal current, and *Hulscher* (1996) explained the formation of sand waves with a vertical flow structure over small perturbations on the sea floor. Therefore, the first category is adapted after *Borsje et al.* (2014), and *van Gerwen* (2016), where the initial bed corresponds to a dredged surface with only small perturbations. This is represented in the model by using a sine shape with small amplitudes. In this category, two model runs are performed that use the original small amplitude sine function as shown in Figure 17. The fastest growing modes that are found in the short-term calculations for the average depth at T_0 (the time that the extractions have stopped), of the dredged-, and the undredged transect are used. Table 9 shows the input parameters that are used to find the wavelength of the fastest growing mode, and for the long-term calculations.

Category 2: Schematized initial bed
In order to make the transition from the perfect sine function to the cross section found in the data analysis, an extra category is added. A schematized sine function is applied as an initial bed for the undredged transect only. This initial bed is not used for the dredged transect because it seems an unrealistic representation of the dredged seabed. Two runs are completed with this initial bed where the first run uses the wavelength of the fastest growing mode that is found from the short term calculations, and the second run uses a wavelength that is found by the data analysis in the field at T_0. Since this measured wavelength is different from the wavelength of the fastest growing mode, a fundamental error is made where the input parameters do not match with the wavelength that is forced onto the initial bed. Therefore, it is expected that wavelengths that differ slightly from the fastest growing mode are still grow, however they grow slower than

the fastest growing mode. For the amplitude of the sine function, the average wave height that is found in the field at T_0 is used.

Category 3: Idealized seabed

The seabed profile at the first measurement after the extractions stopped is extracted from the dataset, and used in this category. In order to fill the domain, a sine function complements the idealized bed on either side so the idealized bed is located in the center of the domain. For the first case that uses this idealized initial bed, the wavelength of the fastest growing mode is used for the sine function. However, the wavelength of the fastest growing mode that is found for the parameter set (that is assumed to represent the study area), does not comply with the wavelengths that are found on the idealized cross sections. This causes the same fundamental error in the model as for the schematized initial bed with the measured wavelength. Therefore, another parameter set is found by trial and error that approximates one of the wavelengths found in the cross section as close as possible. Both the dredged and the undredged transect are used in this category, and as explained before, two sets of wavelengths are used for the complementary sine function. The sine function uses a wave height that is found in the field (from the data analysis), and two different wavelengths; the wavelength of the fastest growing mode, and a wavelength that approximates the wavelengths found in the field. Figure 20 shows the initial beds that are used, and Table 10 shows the long-term runs that are performed. Furthermore, Table 10B shows the parameter sets that correspond to the wavelengths found on the undredged and dredged transect.

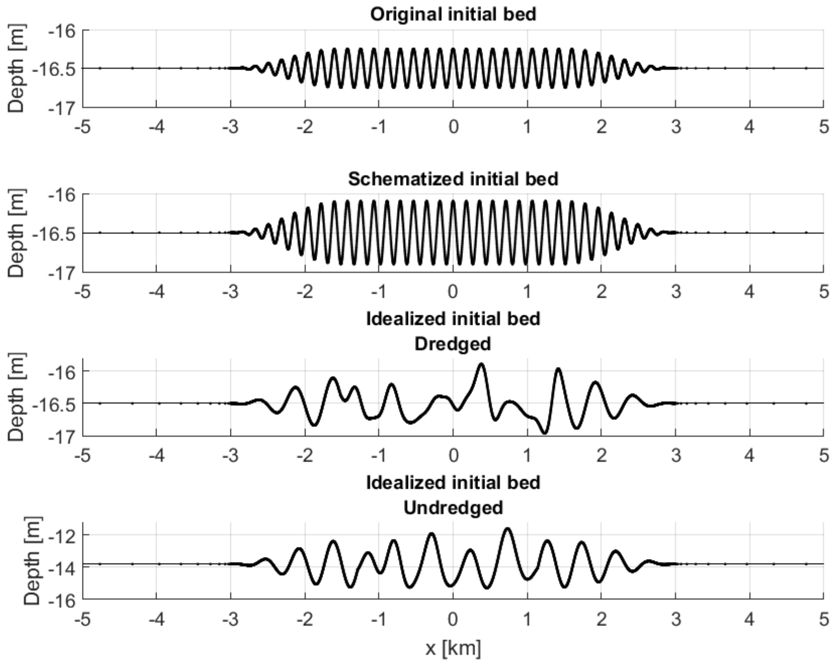

FIGURE 20 DIFFERENT INITIAL BEDS WHERE THE ORIGINAL INITIAL BED REPRESENTS A DREDGED SEABED, THE SCHEMATIZED INITIAL BED REPRESENTS AN UNDREDGED SEABED, AND THE IDEALIZED INITIAL BEDS ARE EXTRACTED FROM THE FIELD DATA

The tidal asymmetry results in migration for the long-term runs. Furthermore, The rest of the model settings can be found in Table 9, and the long-term runs are summed up in Table 10. Where the wave height is defined as the vertical distance between a crest and two adjacent troughs. The amplitude that is applied to the sine function in the initial beds is the distance from the mean bed level to the peak, and is implemented as half the wave height.

FGM (m)		H_0 (m)		U_{S2} (m/s)	A_0 (m/s)	D_{50} (mm)
Dredged	Undredged	Dredged	Undredged			
178	155	16.5	13.8	0.65	0.05	0.30

TABLE 9 PARAMETER SETTINGS FOR LONG-TERM CALCULATIONS CASE I THROUGH CASE VI

Run Name	Transect	Description	Wave height (m)	Wavelength (m)
Case I	Dredged	Original initial bed	0.50	178
Case II	Undredged	Original initial bed	0.50	155
Case III	Undredged	Schematized bed	2.87	206
Case IV	Undredged	Schematized bed	2.87	155
Case V	Dredged	Idealized bed	0.80	178
Case VI	Undredged	Idealized bed	2.87	155
Case VII	Dredged	Idealized bed	0.80	257
Case VIII	Undredged	Idealized bed	2.87	233

TABLE 10A LONG-TERM RUNS THAT ARE PERFORMED

The wavelengths that are found in the field at T_0 on the dredged transect are 137 m, 229 m, 264 m, 212 m and 276 m. The wavelength of the fastest growing mode that is used for the previous cases is 178 m, therefore the wavelength that is selected for the second case that uses the idealized transect is closer to the longer wavelengths. By varying the grain size diameter and the tidal current velocity amplitude, a wavelength of 257 m is found. The depth is kept the same because this value came from the data analysis whereas the grain size diameter and tidal current velocity amplitude are selected by studying literature.

For the undredged transect, the same method is used to find a parameter set that corresponds to a wavelength closer to wavelengths found in the field. The wavelengths present on the transect at the time that the idealized cross section is extracted are 165 m, 228 m, 205 m and 227 m, and the wavelength that is used for Case VIII is 233 m.

Run Name	Transect	H_0 (m)	U_{S2} (m/s)	D_{50} (mm)	Wave height (m)	Wavelength (m)
Case VII	Dredged	16.5	0.62	0.20	0.80	257
Case VIII	Undredged	13.8	0.63	0.20	2.87	233

TABLE 10B PARAMETER SETS FOR CASE VII AND CASE VIII FOR THE IDEALIZED BEDS

5.2 RESULTS OF LONG-TERM BED DEVELOPMENT FOR DIFFERENT INITIAL BEDS

The results of the long-term bed development are split up into two parts; the original and schematized initial beds, and the idealized initial beds.

5.2.1 ORIGINAL AND SCHEMATIZED INITIAL BED RESULTS

In the previous sections, the long-term bed development is simulated in time for various initial beds and the results are presented here. Figure 21 gives an overview of the sand wave developments for the first four cases. As was mentioned before, the dredged transect translates to the original small amplitude sine function(category 1) to represent a dredged bed. The undredged transect is used for the original initial bed in order to be simulate a situation if dredging had occurred at that depth. Furthermore, for cases III and IV, the schematized initial bed is applied to represent the undredged transect with a wave height that is found in the field, and a different wavelengths for each case. The fastest growing mode, and a measured wavelength from the field data are used to study similarities and differences.

It can be seen from Figure 21 that in all four cases, the troughs reach their equilibrium depths before the crests do. Furthermore, the wavelengths that resulted from the model are the same wavelengths that are used as an initial condition in the model. The model is run for 225 years, and it has to be noted that an equilibrium wave height is reached (as can be seen in Figure 22). The equilibrium wave height for Case I is $5.3\ m$, and for Case II it is $4.3\ m$. Moreover, the equilibrium wave heights for Case III and Case IV are $4.8\ m$, and $4.3\ m$ respectively. This shows that for a situation where an undredged and a dredged situation are modeled, the resulting equilibrium height is the same. However, the time to reach equilibrium height is larger for the dredged bed than for the undredged bed.

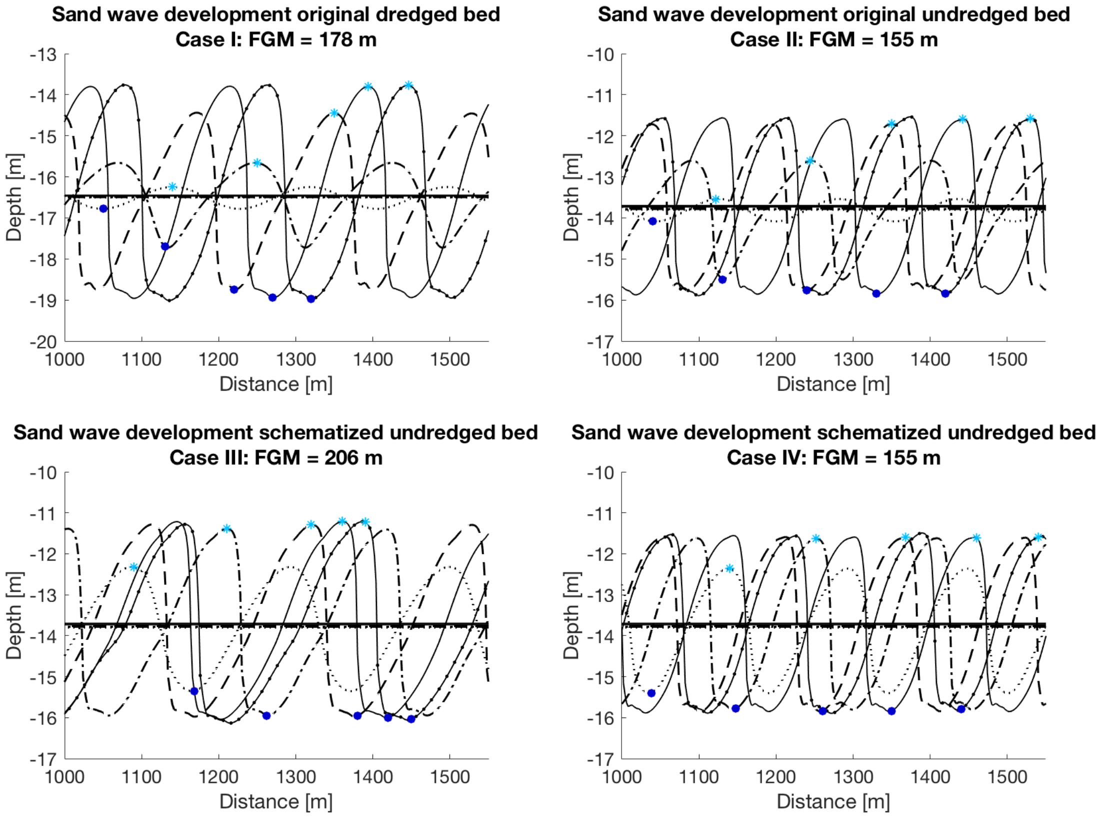

FIGURE 21 SAND WAVE DEVELOPMENT. (WHERE THE DREDGED TRANSECT IS REPRESENTED BY CASE I (TOP LEFT), AND THE UNDREDGED TRANSECT IS REPRESENTED BY CASES II (TOP RIGHT), III (BOTTOM LEFT), AND IV (BOTTOM RIGHT).)

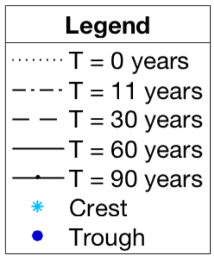

Figure 22 shows the sand wave growth curves for those four cases for approximately 150 $years$. It can be seen that the growth curves of the dredged (Case I, and Case II), and the undredged beds (Case III, and Case IV) have different trends, however these trends can be related to the general growths curve of sand waves. The dredged cases show wave heights starting at a small amplitude, whereas the undredged cases start further along the growth curve. Case I reaches a higher equilibrium wave height, and it takes longer to reach that equilibrium height (see **Error! Reference source not found.**). Case II, and Case IV use the same input parameters except Case IV simulates an undredged situation whereas Case II simulates a dredged situation, however the equilibrium height that they reach is the same as expected.

Case III uses the same input parameters as Case IV, however its wavelength is taken from the data analysis. The wavelength that is used is not the same as the wavelength of the fastest growing mode, however the model still shows sand wave growth in this case. Since the parameters that are used for this case, do not match with the wavelength that is forced onto the system, the results of this case are not taken into account for the rest of this research. This case is merely run in order to see whether the model can handle wavelengths that are different from the fastest growing mode.

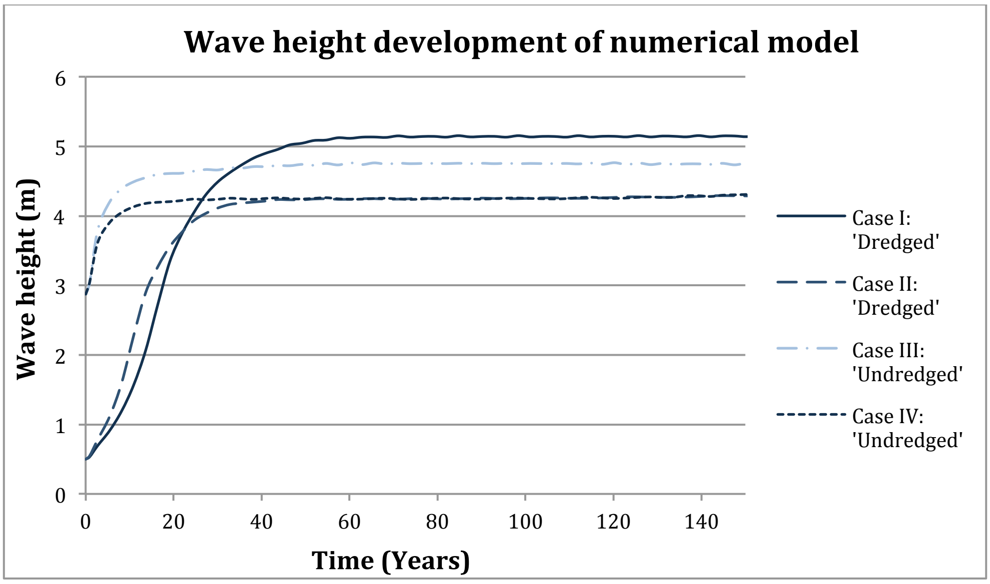

FIGURE 22 SAND WAVE GROWTH CURVES (NOTE THAT CASE III HAS A SHADED COLOR TO EMPHASIZE THAT THE FOCUS IS ON CASE I, II AND IV)

The growth and migration rates for all four cases are shown in Figure 23. The growth rates are linearly approximated for each time step (2.7 years due to the chosen MORFAC). The peaks in Figure 23 correspond to the steepest section of the wave height development (Figure 22). Case I and Case II both represent a dredged situation, and it can be seen that Case II reaches its highest growth rate before Case I, and Case II reaches a higher growth rate than Case I. The growth rates of the undredged Case III and Case IV confirm that these sand waves are positioned further on the growth curve. Figure 23 shows that the growth rates immediately peak after the first timestep, and the results of Case II can be compared to Case IV. The growth rates of Case II imply that the initial sand wave height that is implemented is greater than the wave height that correspond to the highest growth rate for this case. Furthermore, the time scale of the regeneration of sand waves is approximately 45 *years* for Case I and 35 *years* for Case II, which corresponds to a regeneration time of decades that is found in literature (Knaapen and Hulscher, 2002).

Figure 23 is limited to 60 *years* to clearly show the growth rates during those years, after 60 *years* the behavior of the growth rate curves shows similar results as for the last 10 *years* in the figure. Furthermore, the small ripples that are visible in Figure 22 after the wave height has reached its equilibrium correspond to the negative values and small peaks (ripples) of the growth rates that show up in Figure 23. These 'ripples' are caused by the combination of the MORFAC and the moment of the tide at the moment that the model writes the output.

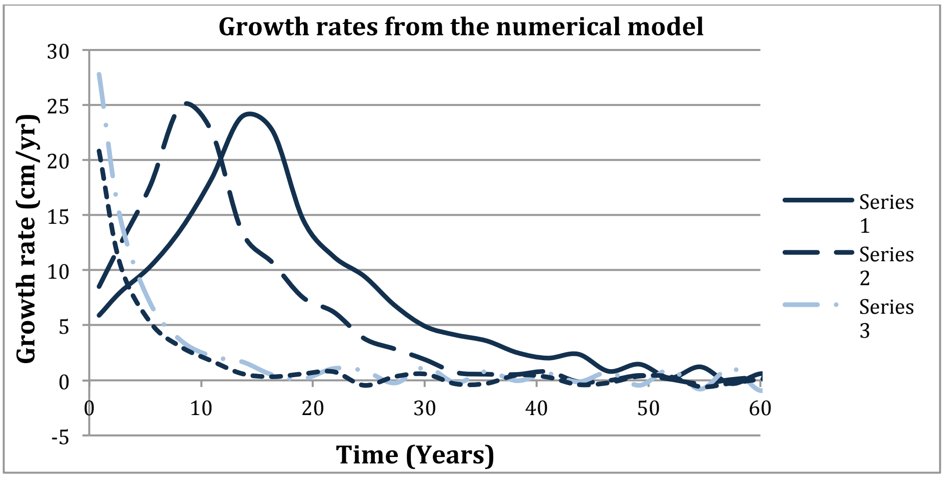

FIGURE 23 GROWTH RATES OF CASE I THROUGH CASE IV FOR EACH YEAR (CASE III HAS A SHADED COLOR TO EMPHASIZE THAT THE FOCUS IS ON CASE I, II AND IV)

The migration rates of Case I through Case IV are presented in Table 11. It can be seen that the crest generally migrate faster than the troughs, and migration of the troughs of the undredged cases is slightly higher than the migration of the troughs of Case I and Case II. The same assumption is made in the evaluation of these migration rates as was done for the field data; migration rates of sand waves are approximately linear. Therefore only one value is presented for the migration rates through the years.

Migration	Crest (m/yr)	Trough (m/yr)
Case I	3.9	3.1
Case II	4.4	3.1
Case III	4.4	3.8
Case IV	4.2	4.0

TABLE 11 MIGRATION RATES OF THE MODEL FOR CASE I THROUGH CASE IV

5.2.2 IDEALIZED INITIAL BED RESULTS

In order to analyze the bed development of the idealized initial beds, the same crests and troughs are analyzed as for the field data. The wave heights, growth rates, and migration rates are studied in this section and the cases that use the wavelength of the fastest growing mode for the complimentary sine function, and the cases that use a wavelength found in the field are compared. For the wave heights of the sand waves in the idealized transects, the same method is used as for the field data (Chapter 3.1).

Figure 24 shows the bed development for Case V through Case VIII after the first time step (approximately 2.7 *years*). The dredged Case V (top left) represents the idealized bed with the wavelength of the fastest growing mode on the sides, whereas Case VII (bottom left) uses a wavelength that is representative of the idealized section on the sides and uses a parameter set that corresponds to that wavelength. The same combinations are made for the undredged transect where Case VI (top right) uses the wavelength of the fastest growing mode, and Case VIII (bottom right) uses a wavelength that represents the idealized section to fill the domain.

Furthermore, the crests and troughs that are tracked are marked and the wave height is determined by using the same method as in previous sections. It can be seen that after that first time step of 2.7 years, some small differences between the crests and troughs of Case V and Case VII, and Case VI and Case VIII are already visible.

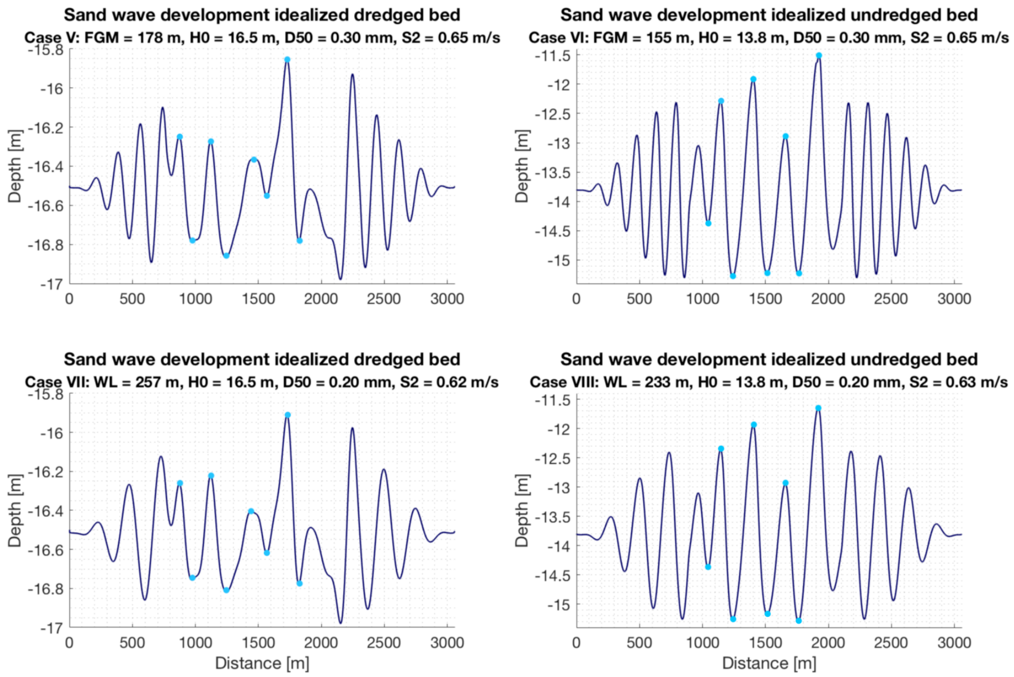

FIGURE 24 SAND WAVE DEVELOPMENT FOR CASE V THROUGH CASE VIII (DOTS IDENTIFY THE TROUGHS AND PEAKS THAT ARE ANALYZED).

Figure 25 shows the seabed development after approximately 25 years for the dredged and undredged transects and for the two corresponding cases. In previous research it was found that the implementation of random initial bed caused the seabed to reorganize itself until it represents the wavelength of the fastest growing mode before it starts growing. For Case V and Case VI a similar behavior seems to occur; the forcing of the system does not correspond to the wavelengths in the idealized cross section that is implemented. Therefore the system is instable and starts to reorganize until it represents the fastest growing mode that corresponds to the input parameters. The wavelength of the fastest growing mode that is found in a previous section is on the shorter side of the ranges of wavelengths that are found for this transect and this could explain why the instable bed forms shorter wavelengths.

The results of the wave heights, growth rates, and migration rates of Case V and Case VI are presented in the Appendix in order to focus on Case VII and Case VIII for the rest of this section.

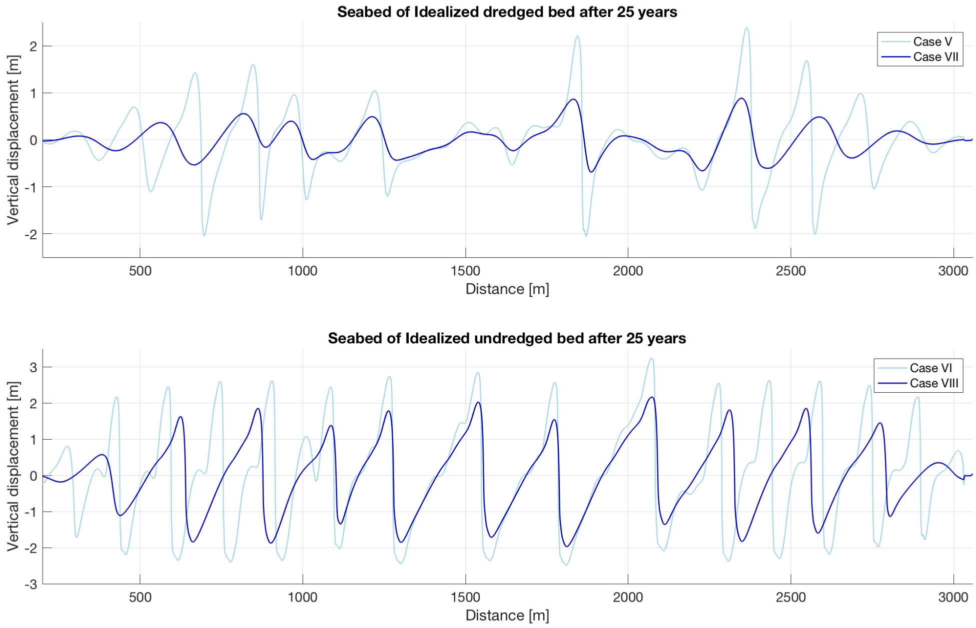

FIGURE 25 SEABED DEVELOPMENT FOR IDEALIZED TRANSECTS

The growth curves and the growth rates of the dredged and undredged transect are shown in Figure 26 for approximately 55 *years*. The beginning of the growth curve can be recognized for Case VII, whereas Case VIII shows the part of the growth curve where the sand wave is approximating its equilibrium height.

Moreover, the growth rates of both transects are lower than the growth rates that are found for the other initial beds (original and schematized) that are used. This can be explained by the adjusted parameters that are used for this case. The sediment grain size is smaller for both transect than it was previously and even though the tidal current velocity has decreased a little as well, the smaller sediment grain size results in more suspended sediment. According to *Borsje et al*. (2014) suspended sediment has proven to limit the sand wave growth. Furthermore, the idealized initial beds consist of different wavelengths and the parameter set corresponds to one specific wavelength. It was shown that wavelengths that differ slightly from the wavelength of the fastest growing mode still grow, however with a lower growth rate and this also may explain the lower growth rates of the sand waves in the domain.

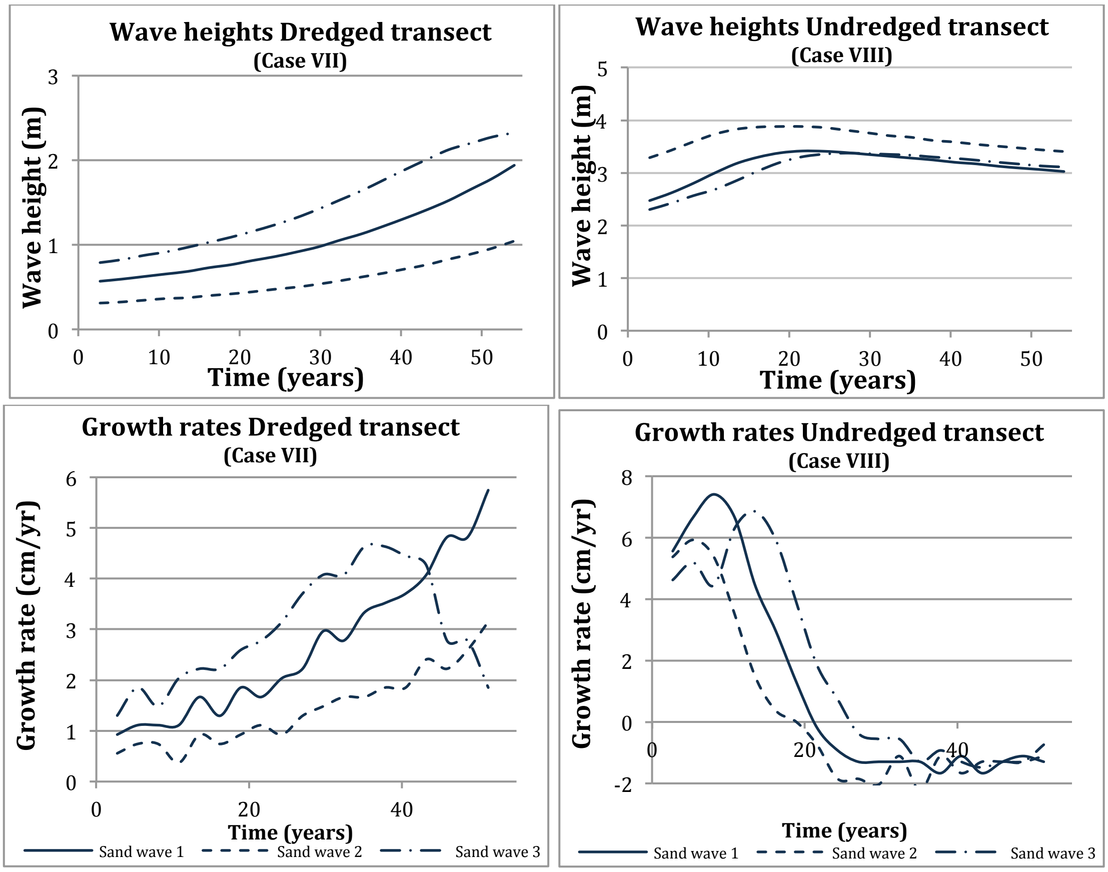

FIGURE 26TOP: WAVE HEIGHTS FOR CASE VII AND CASE VIII FOR THREE ANALYZED SAND WAVES

ERROR! REFERENCE SOURCE NOT FOUND.**BOTTOM: RESULTS OF THE GROWTH RATES FOR CASE VII AND CASE VIII.**

The migration rates of the crests and troughs are approximated linearly and presented in Table 12. It can be seen that for all four cases, the crests migrate faster than the troughs. Furthermore, it can be seen that the migration rates of Case V and Case VII are very similar. The migration rates of the troughs from Case VI and Case VIII differ with 0.7 m/yr, however the crest migration rates are very similar.

Migration	Crest (m/yr)	Trough (m/yr)
Case VII	3.8	2.8
Case VIII	4.6	3.8

TABLE 12 MIGRATION RATES OF CRESTS AND TROUGHS CASE V THROUGH CASE VIII

An idealized transect that is extracted from field data consists of multiple wavelengths and this automatically causes difficulties when trying to determine a parameter set that represents the whole idealized section of the domain.

The results for the idealized cross sections showed the differences between the case with the wavelength of the fastest growing mode and the case with an adjusted parameter set that corresponded to a wavelength that corresponded to the idealized of the domain. It is found that Case V and Case VII, with the wavelength of the fastest growing mode, showed instability as the seabed is reorganizing to find the wavelength that corresponds to the applied forcing. Therefore Case VI and Case VIII are used in the next chapter where the model results are compared to the field data.

6. COMPARISON OF MODEL RESULTS WITH FIELD DATA

This chapter compares the wavelength, wave height and migration rate from the model, with the values that are found from the field data in order to assess the performance of the model.

6.1 RESULTS COMPARISON OF MODEL RESULTS WITH FIELD DATA

The focus of the comparison of the model with the field data is on the first 11 *years*, since the available data ranges from 2003 until 2014. Furthermore, Case I (original initial bed), and Case VII (idealized initial bed) are compared to the dredged transect from the field data. Whereas the undredged transect from the field data is compared to Case IV (schematized initial bed), and Case VIII (idealized initial bed).

The seabed development for the dredged situation and undredged situation are plotted in Figure 27 and Figure 28 respectively. For both situations it can be seen that the bed development in de model is cleaner, and more predictable than the real bed developments. Furthermore, the instability in Case V and Case VI can already be seen after 11 *years*. It has to be noted that only the idealized section of the domain is plotted in order to compare it to the field data, therefore the complimenting sine function is left out for the model.

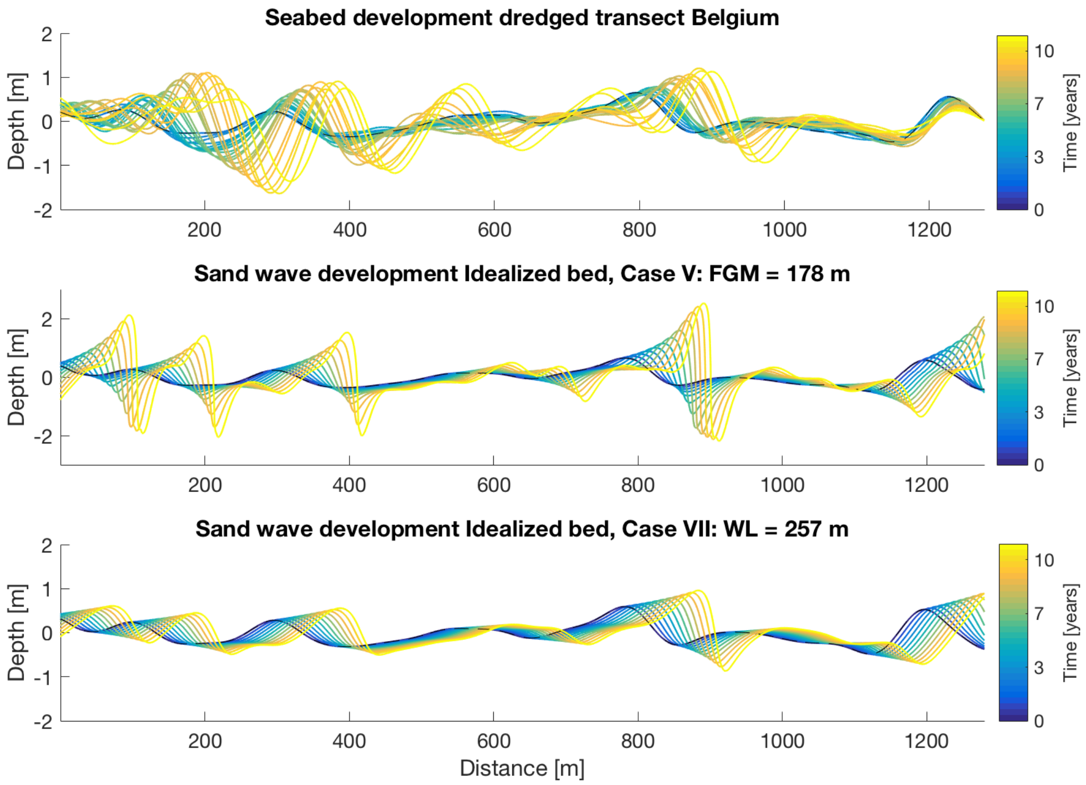

FIGURE 27 SEABED DEVELOPMENT COMPARISON OF DREDGED TRANSECT (NOTE THE SCALE OF THE Y-AXIS)

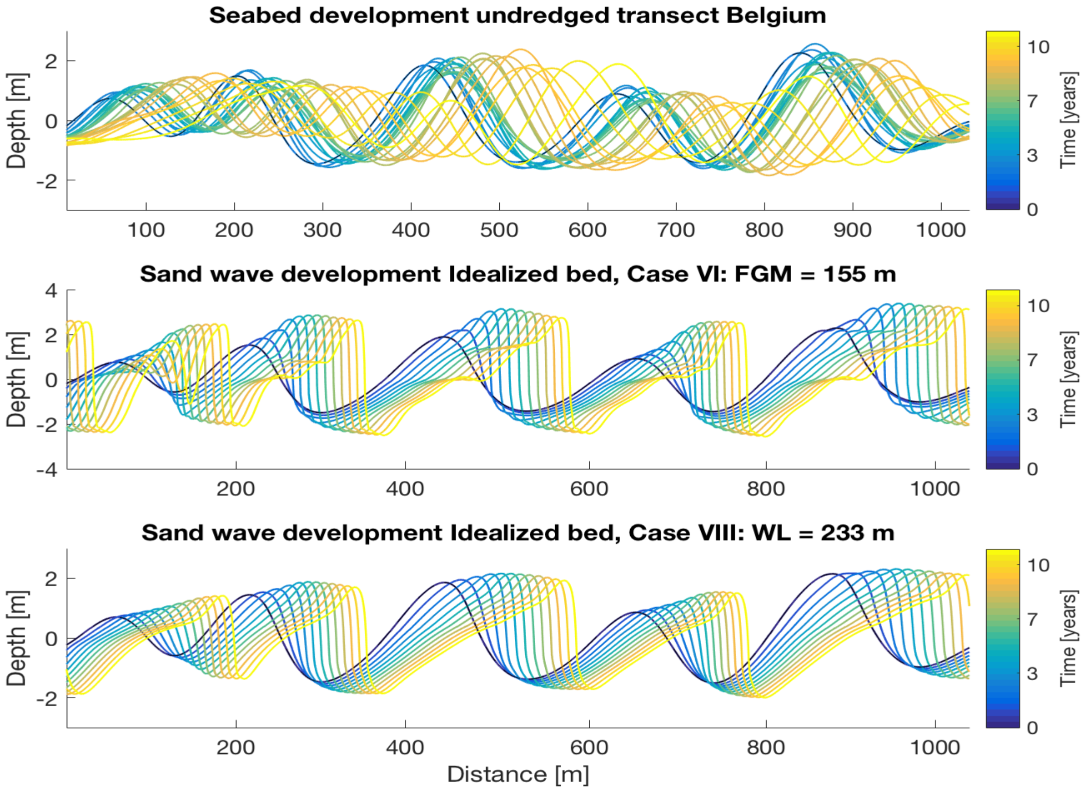

FIGURE 28 SEABED DEVELOPMENT COMPARISON OF UNDREDGED TRANSECT (NOTE THE SCALE OF THE Y-AXIS)

All the wave heights that are found for the field data and the models are shown in Figure 29. The vertical limits are set to be equal in order to make it easier to compare the model results with the field data. It can be seen that Case I seems to follow the trend of the wave heights from the field data better than the idealized transect. Furthermore, the wave heights of the field data seem to comply with the wave heights from Case I and thus with the initial stage of the general growth curve (refer to Figure 22 for the full growth curve of Case I). For the undredged case it seems like Case VIII follow shows a trend that complies with the field data better than Case IV (refer to Figure 22 for the full growth curve of Case IV). Both adjusted parameter sets used a smaller grain size than the initial sediment grain size. According to *Damen et al.* (submitted) larger grain sized result in higher wave heights, which can be seen for both the dredged and undredged transects in this research as well.

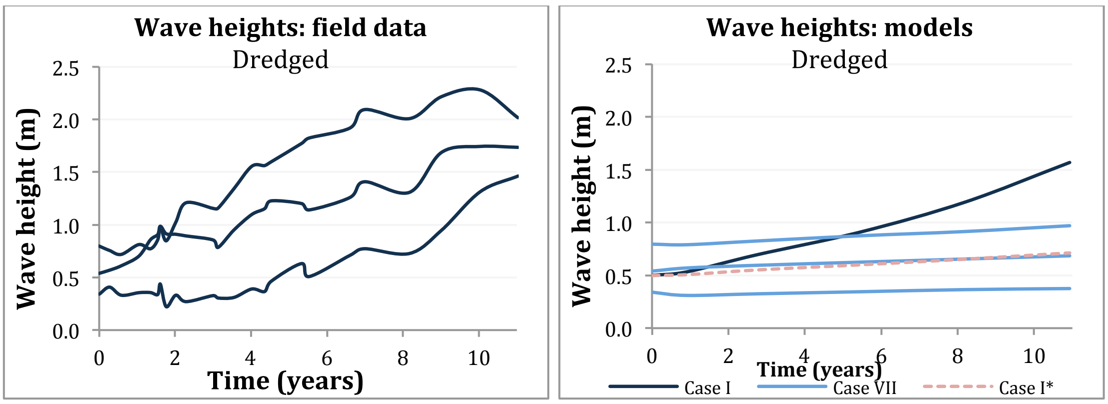

FIGURE 29A WAVE HEIGHT COMPARISON OF FIELD DATA WITH MODEL RESULTS: DREDGED

(CASE I: ORIGINAL, CASE V: IDEALIZED, CASE VII: IDEALIZED)

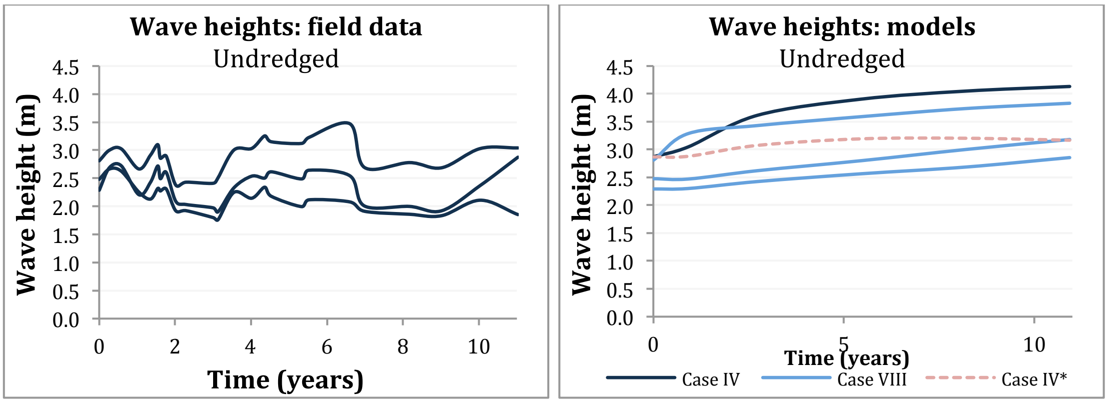

FIGURE 29B WAVE HEIGHT COMPARISON OF FIELD DATA WITH MODEL RESULTS: UNDREDGED

(CASE IV: SCHEMATIZED, CASE VI: IDEALIZED, CASE VIII: IDEALIZED)

After comparing the model results with the field data for the dredged transect, it could be argued that the original initial bed results in the closest approximation to the field data. However, the adjusted parameter set (Case VII) showed to be more representative of the wavelengths on the idealized transect than the parameter set that is used initially (Case I and V). This may mean that the growth curve for Case I that is presented in Figure 29A is not fully representative of the dredged transect in the study site either. Therefore another Case I* is run with the original initial bed, but with the adjusted parameter set that is used for Case VII (CaseVIII for Case IV*). The result is shown in Figure 29A and it can be seen that this growth curve falls within the range of wave heights of the idealized transect.

The undredged transect is represented by the results of the schematized initial bed and the idealized initial bed. For this undredged case the idealized initial bed seems to be a better fit, however the difference with the schematized bed is small for one of the sand waves.

The results of this comparison between the field data and the model results show that the input parameters have a great influence on whether the growth curve is similar to the field data. All parameter sets that are used in this study consist of parameters with values that are assumed to be representative of the study area. In the exploration of the study site a range of sediment grain size and tidal current velocities are found, as well as a varying depth. Thus, this shows the importance of accurate input data when the model performance is compared to a study site.

The migration rates for the dredged and undredged situations can be seen in Table 13, where it seems that the migration rates of the model are significantly underestimated compared to the field data.

Dredged	Crest (m/yr)	Trough (m/yr)
Case I	3.9	3.1
Case VII	3.8	2.8
Field	13.5	12.4

Undredged	Crest (m/yr)	Trough (m/yr)
Case IV	4.2	4.0
Case VIII	4.6	3.8
Field	16.8	17.7

TABLE 13 COMPARISON OF MIGRATION RATES

7. SYNTHESIS OF DREDGING STRATEGIES AND MODEL PREDICTIONS

7.1 INTRODUCTION TO APPLICATION OF DREDGING STRATEGIES

As is mentioned in the Introduction, the growth and migration of sand waves should be a point of attention in the design of offshore infrastructure. In reality, the process of a project from beginning to end can sometimes take several years. Therefore it can be helpful to know how much the bathymetry of a seabed changes in 1 till 5 *years* after a dredging strategy has been applied. This section is dedicated to the synthesis of the model and practical applications in field, with a focus on those first couple of years. An example of cables that cross a sand wave field is shown in Figure 30. This example shows one way that the model can contribute to engineering practices, and it is also included in the analysis of the results of the modeling of the dredging strategies.

In the case of routing cables through a sand wave field, the current standard is to determine the non-mobile seabed reference level. This is the lowest seabed level that is undisturbed by processes that affect the seabed level, including the growth, and migration of sand waves. Figure 31 shows how this non-mobile seabed reference level is currently determined for engineering practices. Relative to this non-mobile seabed reference level, and the thickness of the cover that is required to protect the cables, the cable is placed at a certain depth below this level. To minimize dredging costs, routing the cables trough the troughs of the sand waves in the sand wave field is preferred. Occasionally the cable has to cross a sand wave in order to reach its destination, and the preferred angle to do this is perpendicular to the propagation direction of the sand wave due to trenching tool limitations. The method that is currently used to cross the sand waves is complete removal of the sand wave to reach the determined non-mobile seabed reference level. Some of the current route design criteria are summed up here. The shortest distance of the route is preferred while taking into account the non-mobile seabed reference level, the burial depth of the cable, avoid sand waves if possible, and preferably cross sand waves perpendicularly. However, the characteristics and the behavior of the sand wave field are currently not considered in the design.

FIGURE 30 EXAMPLE OF CABLES CROSSING A SAND WAVE FIELD.

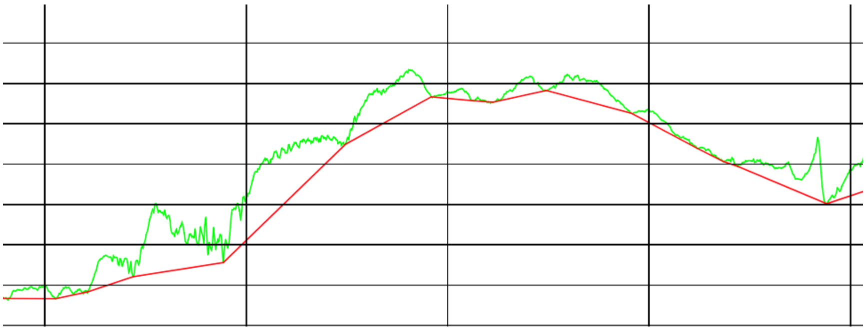

FIGURE 31 EXAMPLE OF DETERMINATION OF NON-MOBILE SEABED REFERENCE WHERE THE GREEN LINE REPRESENTS THE BATHYMETRY OF THE SEABED, AND THE RED LINE REPRESENTS THE NON-MOBILE SEABED REFERENCE LEVEL.

In previous sections this model has been validated and the accuracy of its predictions is compared with field data in a specific area. For the design of dredging practices this model might be a tool to simulate the behavior of sand waves after dredging in areas of interest. Therefore three different dredging strategies are implemented in the model to assess the growth rates of the sand waves after dredging. These dredging strategies are applied for three situations based on two locations in the North Sea. A behavior study is performed in order to cover a wider variety of locations, and to form a synthesis of how this model can be used to determine the effect of three dredging. The aim of this study is to gain insight in the behavior of the sand waves after different dredging strategies are applied and how these insights can be used in dredging practices, for example the routing of cables through a sand wave field.

7.2 DREDGING STRATEGIES

There are several dredging methods that can be applied. Three of those methods are studied and discussed in order to form a synthesis between the predictive capabilities of the sand wave model and usefulness in engineering practice. Figure 32 shows the schematized dredging strategies that are used.

Peak removal

With peak removal the depth of the channel or area is increased to its required depth by cutting of the peaks of the sand wave field. The troughs and sand wavelengths are relatively undisturbed; therefore this method does not have an impact that is as great as some other strategies on the sand wave field. This method is implemented for three different cut-off levels; full peak removal, 2/3 of peak removal, and 1/3 peak removal. Furthermore, it is assumed that with this method, the result is that the original sand wave height recovers relatively fast compared to the other dredging strategies.

Cut & fill

Instead of removing the sediment that is collected from the peak removal from the system, this can also be used to fill the troughs to create a more evenly distributed seabed. This technique causes a bigger disturbance to the system because the sand wave field is flattened out. It is assumed that the resulting water depth is approximately the mean water depth before the dredging is carried out. It is predicted that this method causes a longer regeneration time due to the disturbed system that has to find a balance first, and the fastest growing mode, before the sand wave field will grow again.

Total Removal

The strategy of complete removal increases the water depth to the depths of the troughs of the sand wave field. This method is similar to the cut and fill method because the result is an evenly distributed seabed. However, since the depth is increased to the depths of the troughs, the sand wave growth rate, and the fastest growing mode can be affected. This method should not be confused with one of the peak removal strategies where the complete peak is cut off, for this strategy the complete sand wave (trough to crest) is removed (see Figure 32).

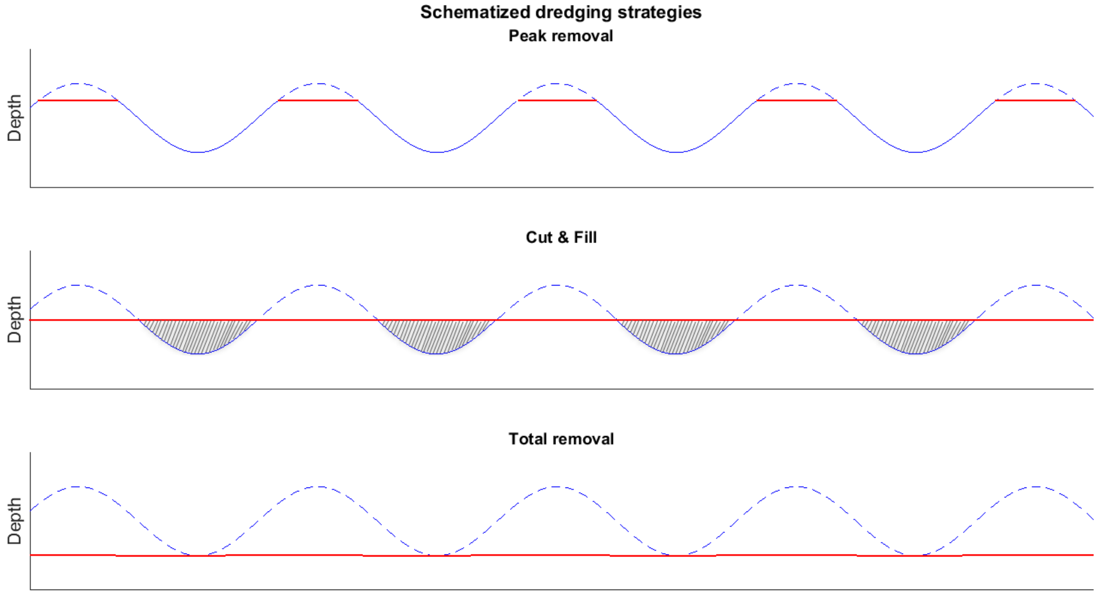

FIGURE 32 SCHEMATIZED DREDGING STRATEGIES WHERE THE SOLID (BLUE LINE REPRESENTS THE ORIGINAL SEABED, THE SOLID (RED) LINE REPRESENTS THE NEW SEABED LEVEL, THE DASHED (BLUE) LINE REPRESENTS THE REMOVED PART OF THE SAND WAVE AND THE HATCHED AREAS ARE THE FILLED UP TROUGHS OF THE SAND WAVES.

7.3 LOCATIONS AND PARAMETERS FOR THE NORTH SEA

For practical applications it is valuable to know what the seabed looks like after dredging has been performed in a location. In order to get an idea of the growth rates of sand waves in the North Sea, a behavior study of the model is performed. This is done for two specific locations in the North Sea, as well as other parameter sets that represent a hypothetical location in the North Sea. The two locations of existing project are selected and shown as the dark blue areas in Figure 33 and Table 14.

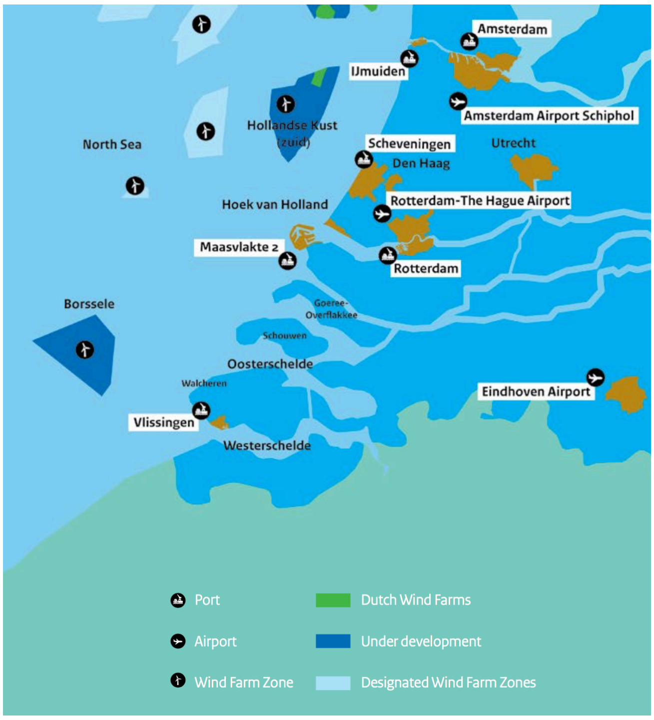

FIGURE 33 LOCATIONS OF WIND FARMS BORSSELE, AND HOLLANDSE KUST ZUID (ADAPTED AFTER NETHERLANDS ENTERPRISE AGENCY, 2017)

7.4 METHODOLOGY OF IMPLEMENTING DREDGING STRATEGIES FOR DIFFERENT LOCATIONS AND PARAMETER SETS

For the behavior study, the same parameters (H_0, D_{50} and U_{S2}) are used for this sensitivity analysis as were used for the short-term (FGM) calculations. In Chapter 4 through 6 the model is validated for the Belgian North Sea, and compared with field measurements. The values of the water depth, and sediment grain size that are found for the two locations complied with values found in literature for sand waves to occur in those areas (i.e. *Borsje et al.,* 2009). Furthermore, the reports that were provided with information on the locations of the wind farms stated that sand waves are present. Therefore it is assumed that this model can be used for other parts of the North Sea where sand waves occur as well. This behavior study is done in combination with the three dredging strategies that are explained in a previous section. Table 14 shows the variables parameters that are varied, as well as the values that are used.

In this study, the dredging method that removes the peaks of the sand waves causes the water depth at the locations of the peaks to be equal to the mean water depth from before the dredging. The cut & fill method redistributes the sediment from the crests into the troughs, which results in the same mean water depth as before the dredging practice. The wave heights that are used in the behavior study are 3.9 m and 2.3 m for Borssele Wind Farm (Hasselaar et al., 2015) and Hollandse Kust Zuid Wind Farm Zone (Deltares, 2016) respectively; these wave heights are the average wave heights found in the area. However the sand wave heights at Borssele range from 1.9 m to 5.9 m, and Hollandse Kust Zuid ranges from 1.3 m to 3.6 m.

A third virtual location is introduced by using the same values for the parameters as are used for Borssele Wind Farm, however the depth is increased to 37.5 m. In the report about Borssele Wind Farm it is stated that the depths range up to 40 meters in that area. Furthermore, in practice there can be projects located in deeper areas than 30 meters, therefore this location is added to the behavior study. Furthermore, for the behavior study, the sediment grain size diameter is varied to 0.30 mm for both locations, because it is found in literature (for example Table 1) that this is a grain size commonly found in the North Sea. The tidal constituent is varied for both locations to from their initial value to U_S2=0.65 m/. These values are determined from values that are from literature (i.e. Borsje et al. (2009) and tidal flow maps from Dienst der Hydrografie.

Location	H_0 (m)	D_{50} (mm)	U_{S2} (m/s)	Wave height (m)
Borssele Wind Farm	27.5	0.35	0.75	3.9
Borssele Wind Farm -10m	37.5	0.35	0.75	3.9
Hollandse Kust Zuid Wind Farm	21.5	0.25	0.55	2.3

TABLE 14 CASES FOR THE DREDGING STRATEGY SENSITIVITY ANALYSIS

In order to model the dredging methods and predict the regeneration of the sand wave field, the fastest growing mode is found for these new variables and corresponding dredging strategy. Moreover, the Morfac is changed 2000 to 200 in order to simulate the results approximately every 100 $days$. The strategies that are applied at each location are shown in Table 15.

Strategy:	Total Removal	Cut & Fill	Full Peak Removal	2/3 Peak Removal	1/3 Peak Removal
Borssele Wind Farm	X	X	X	X	X
Borssele Wind Farm -10m		X	X	X	X
Hollandse Kust Zuid Wind Farm	X	X	X		

TABLE 15 STRATEGIES APPLIED AT EACH LOCATION

7.5 RESULTS OF THE IMPLEMENTED DREDGING STRATEGIES

7.5.1 RESULTS OF DREDGING STRATEGIES

The fastest growing modes for each location are found and shown in Table 16. It turned out that the fastest growing modes that are found for Borssele Wind Farm, and Borssele -10m fell within the range that is found in the field (130 $m - 430$ m). However, for Hollandse Kust Zuid this was not the case, the values of wavelengths at that location varied between 287 m and 832 m. Since the results of the fastest growing modes for that location did not match the values in the field, the strategy where the peak of the sand wave is cut off is only applied for the full peak removal. This shifts the focus of the peak removal strategies to Borssele, and Borssele -10m. For the case of Borssele -10m, the complete sand wave removal strategy is not simulated since this situation uses all the same parameters as the normal Borssele case, however the depth is already set to 10 meters deeper. The fastest growing modes for the different values of grain size diameter, and tidal constituent are shown in Table 21 in the Appendix. Furthermore, the peak growth rates for all the cases are presented in Table 22.

Location	Wavelength Fastest Growing Mode (FGM)	Wavelengths found in field (m)
Borssele	305 m	[130-430]
Borssele -10m	392 m	[130-430]
Hollandse Kust Zuid	161 m	[287-832]

TABLE 16 RESULTS OF THE FASTEST GROWING MODES (EXTENDED TABLE 21 WITH VALUES FOR ALL SCENARIOS IN APPENDIX)

The initial beds that are used to implement the different dredging strategies are shown in Figure 34 (for the location based on Borssele Wind Farm). It can be seen that for the 'Removal' strategy, the seabed is lowered to what is assumed to be the trough level of the original seabed (this bed uses the same initial bathymetry as the original seabed, except it is placed at a greater depth). Furthermore, this figure shows that the wavelengths that are used for each strategy are the same, and the different heights at which the sand wave is cut off.

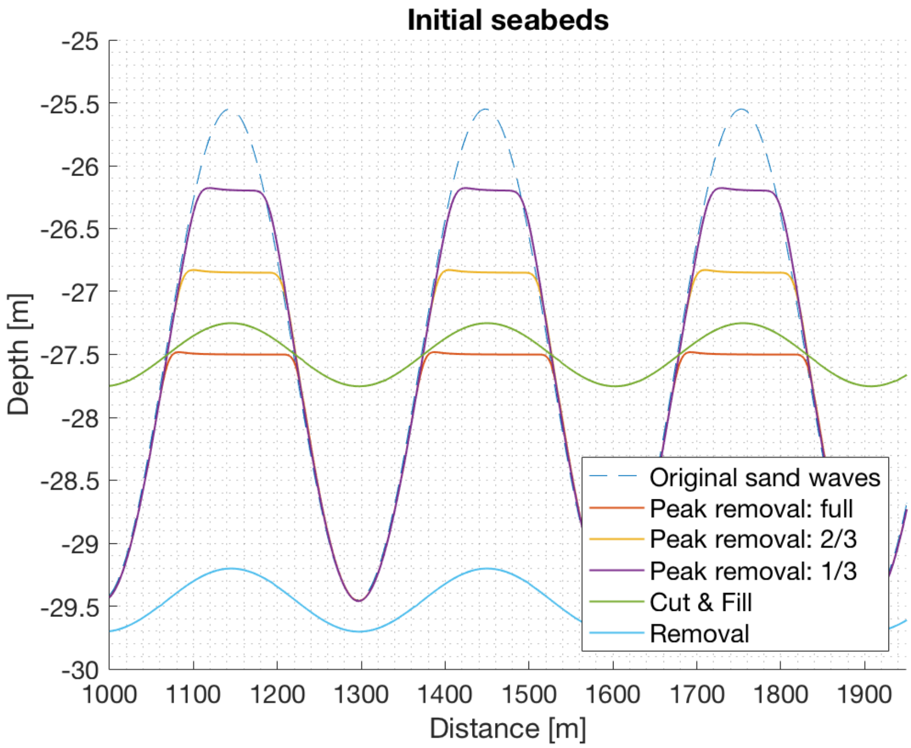

FIGURE 34 INITIAL SEABEDS FOR THE DREDGING STRATEGIES THAT ARE APPLIED TO MODEL THE SEABED DEVELOPMENT AT A LOCATION BASED ON BORSSELE WIND FARM

A general idea of the sand wave development per strategy for Hollandse Kust Zuid is shown in Figure 35, where the bed development is plotted after 1 year, 3 years, and 5 years (note the depth difference between Cut & Fill and Total Removal). The wave height development related to Hollandse Kust Zuid is presented in Figure 37C.

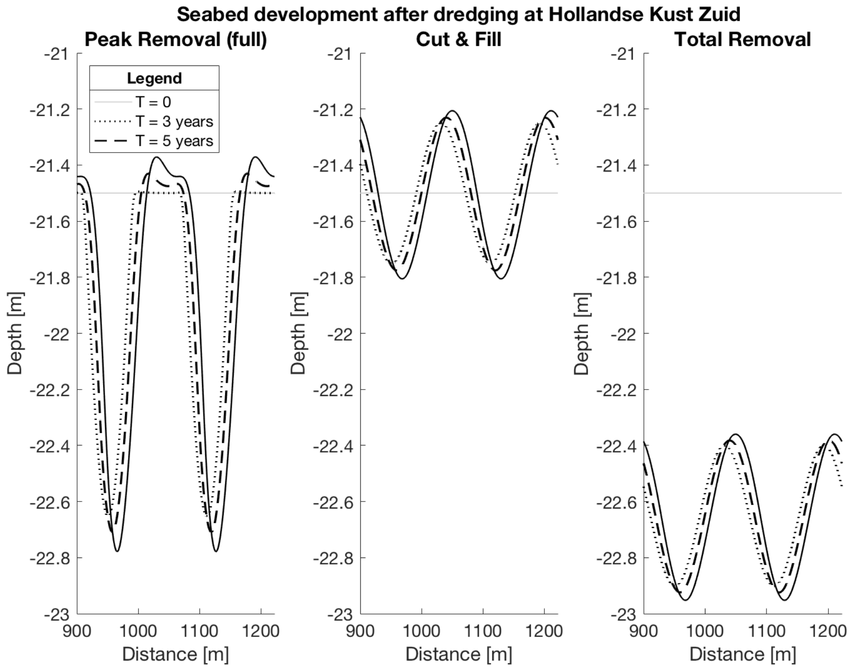

FIGURE 35 DIFFERENT DREDGING STRATEGIES APPLIED AT HOLLANDSE KUST ZUID (NOTE THE DIFFERENT DEPTHS ON THE AXIS FOR THE DIFFERENT METHODS)

The differences between the different peak removal heights for Borssele are shown in Figure 36 (Cut & Fill and Total Removal are also applied for this location). It can be seen that the shape of the crest that is cut off starts to look more like a peak again after 5 years of the bed development. Furthermore it can be seen that the growth rates for 1/3 of the peak removal are clearly higher than the growth rates of 2/3 Peak Removal and full Peak Removal. The wave height development related to Borssele (and Borssele -10m) is shown in Figure 37.

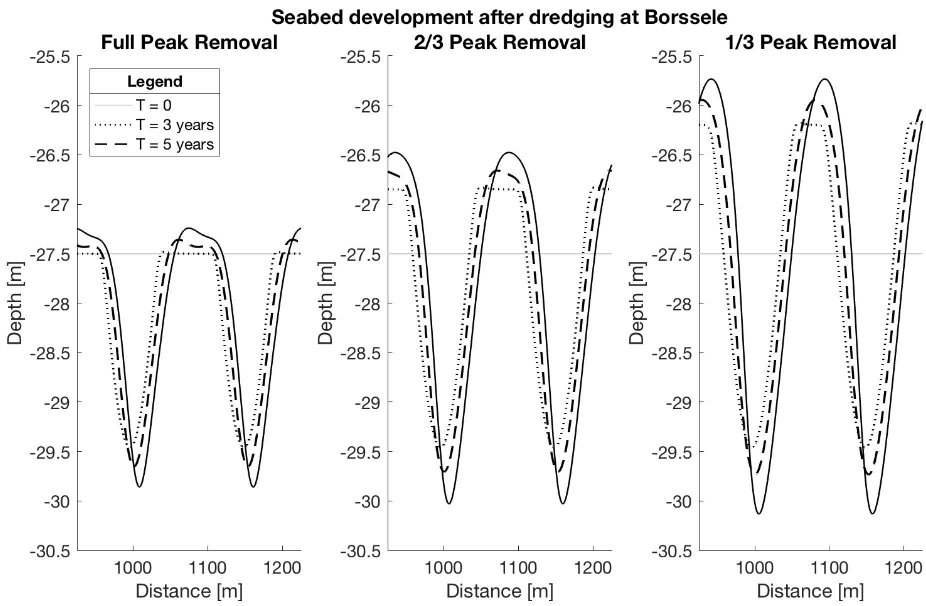

FIGURE 36 SAND WAVE DEVELOPMENT FOR THE PEAK REMOVAL STRATEGIES AT BORSSELE

Wave heights:
Figure 37 shows the wave height development for 5 $years$, and it can be seen that the wave heights of the Cut & Fill, and Total Removal strategies grow significantly slower than the wave heights of the different Peak Removal strategies. Furthermore, the different cut-off heights can be recognized as well as the differences between the resulting wave heights after 5 $years$.

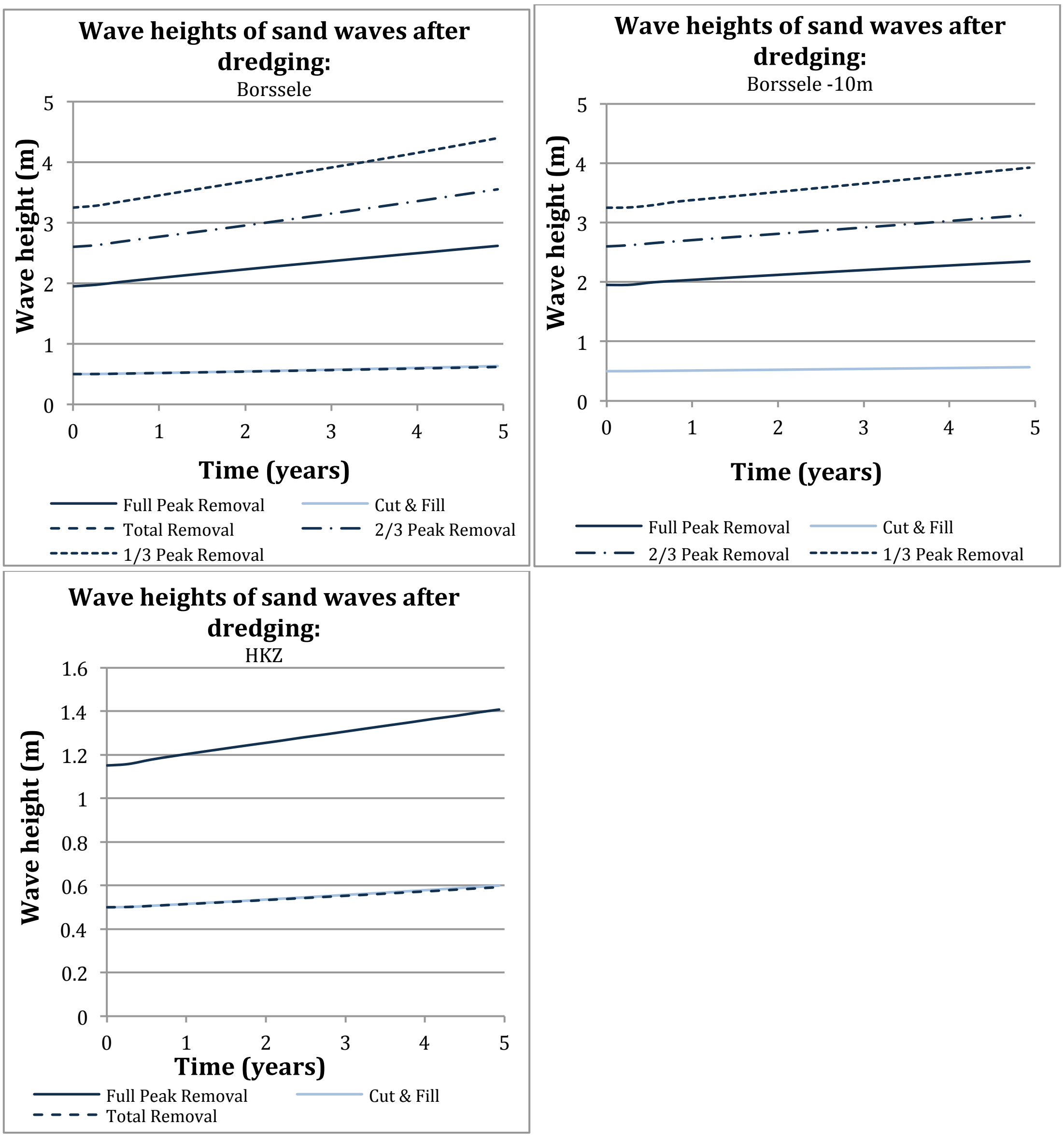

FIGURE 37 WAVE HEIGHTS OF SAND WAVES AFTER DREDGING

A. BORSSELE B. BORSSELE -10 M C. HOLLANDSE KUST ZUID

Growth rates:

The growth rates for the different dredging strategies, and different locations are determined by the wave height difference between each time step (see Figure 38). Moreover, the difference between the growth rates for Cut & Fill, and total Removal are very small, and their initial beds have the same profile, therefore they are grouped together in the figures where the growth rates are presented. The behavior study that included different values for the tidal velocity amplitude, and the grain size diameter is applied for the Cut & Fill, Total Removal, and full Peak Removal strategies. It can be seen that the first model output shows significantly lower growth rates for all cases. These growth rates are caused by the initiation of the system; the increase in sediment transport between the first and the second output is greater than the increase between time steps after the first one. However, full Peak Removal showed significantly higher transport rates at the sharp edge where the peak is cut off. This effect decreases in the following time steps.

It can be seen in Figure 38A that the growth rates follow a clear trend for Borssele, whereas the growth rates of Hollandse Kust Zuid have some extreme values. Generally, the lower limit of the growth rate range corresponds to the Total Removal strategy, whereas the upper limit corresponds to the Cut & Fill strategy (different parameter sets are included in the range). The minimum limit for Borssele comes from the Total Removal strategy in combination with a variation of the grain size diameter from 0.35 mm to 0.30 mm. The tidal amplitude velocity amplitude is set to 0.75 m/s, and in combination with a decrease in grain size this results in an increase in suspended sediment that limits sand wave growth. Furthermore, the upper limit of the growth rates at Borssele corresponds to the initial parameter set and showed to have the greatest bedload transport.

For Hollandse Kust Zuid, the lower limit is set by the case where the tidal current velocity amplitude is set to 0.65 m/s (initially 0.55 m/s) and Total Removal is applied, whereas the upper limit corresponds to the case where the grain size diameter is varied from 0.25 mm to 0.30 mm and Cut & Fill is applied. The cause of the extreme values for the growth rates of Hollandse Kust Zuid are investigated but no clear explanation has been found.

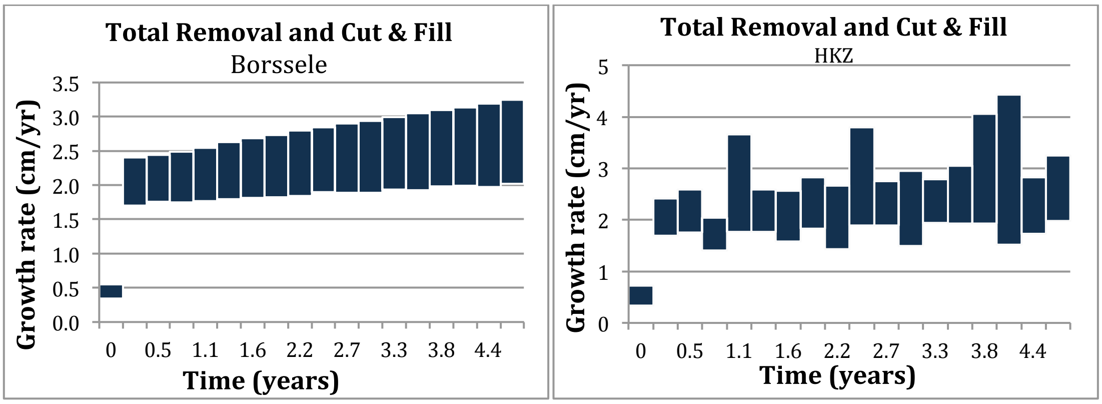

FIGURE 38A TOTAL REMOVAL AND CUT & FILL GROWTH RATE RANGES INCLUDING THE RESULTS OF THE BEHAVIOR STUDY

The growth rates of the full Peak Removal are significantly higher than the growth rates of Total Removal and Cut & Fill. This result complies with the initial assumption that the Peak Removal strategy results in higher growth rates than the previously discussed strategies. It can be seen that the trend of growth rates through time is slightly negative. Figure 36 shows that when the sand wave initially starts growing after the peak is cut off, the left side of the peak starts growing faster than the right side. This left side of the peak is the highest point of the crest, therefore this point is followed through time to determine the wave height and growth rate. However, the figure also shows that the right side of the peak starts growing more as time passes and a more rounded crest is formed. Therefore, the length of the part of the sand wave that is cut off (approximately 80 m in the case of HKZ) may affect the growth curve of sand waves where this dredging strategy is applied. It is explained previously that the sharp edge of the Peak Removal strategy causes extremely high sediment transport rates for the initial time steps and that is the cause of the shape of the peak development. Furthermore, the initial growth of that small perturbation may be the reason for the second range of growth rates in Figure 37B that is greater than the other growth rates.

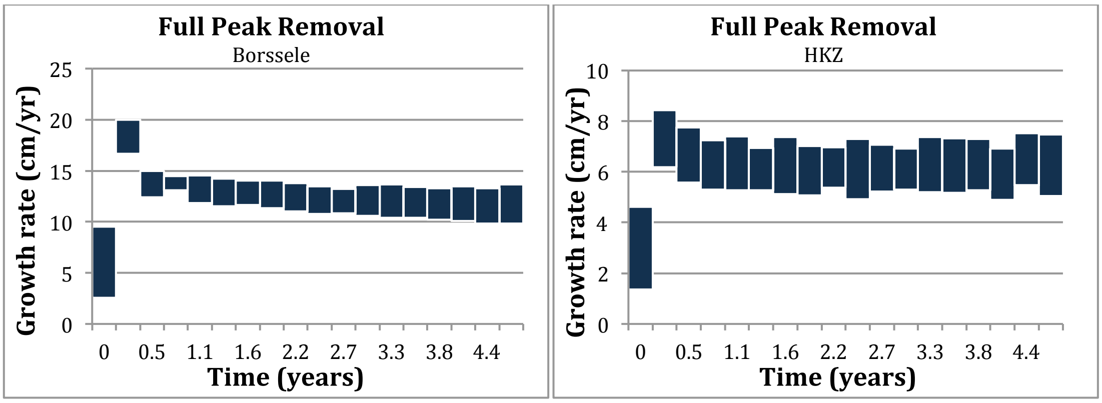

FIGURE 38B FULL PEAK REMOVAL GROWTH RATE RANGES INCLUDING THE RESULTS OF THE BEHAVIOR STUDY

The growth rates of the different peak removal strategies (and Cut & Fill for Borssele -10m) are shown in Figure 38C and D. It can be seen that in contradiction to the full Peak Removal, the 2/3 Peak Removal, and 1/3 Peak Removal do generally result in increasing growth rates. Furthermore, the growth rates of 1/3 Peak Removal are the highest of the Peak Removal strategies and full Peak Removal results in the lowest growth rates. It has to be noted that for full Peak Removal in Figure 38C, the mean values of the growth rates are plotted, merely to provide comparison with the other two Peak Removal strategies. For detailed growth rates of full Peak Removal refer to Figure 38B (left).

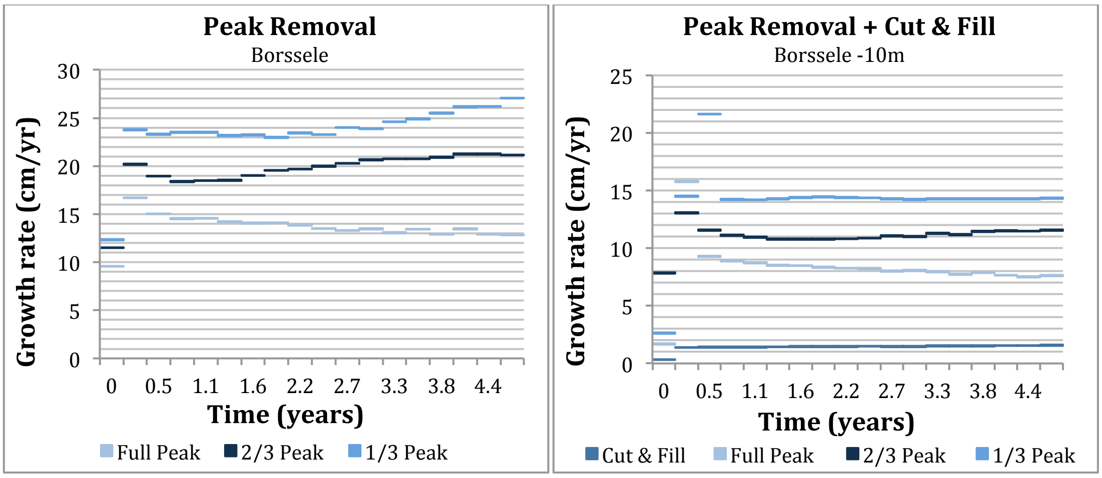

FIGURE 38C (LEFT) PEAK REMOVAL GROWTH RATES FOR BORSSELE

FIGURE 38D (RIGHT) PEAK REMOVAL + CUT & FILL GROWTH RATES FOR BORSSELE -10M

Growth curves:

The wave height curves/ growth curves and the growth rates of the three locations are shown in Figure 39. The resulting wave heights directly after dredging, and 5 years after dredging are plotted on the growth curve. Directly underneath, the growth rate for the location is plotted. The growth rates are directly related to the growth curve and it links the growth rate to a corresponding wave height at a specific point in time for the base case (solid black line). The same method is used to plot the results of the growth rates for the dredging strategies onto the base growth rate curve. It can be seen that for example the initial and final wave height of the Cut & Fill/ Total Removal strategy at Borssele occur on the base growth curve after approximately 2.7 *and* 8.3 *years* respectively. Therefore, the growth rates that are found for those dredging strategies are plotted on the base growth rates graph between 2.7 *and* 8.3 *years*.

Initial growth rates that are found for each dredging strategy are not taken into consideration here because they are significantly lower than the general trend, as well as extreme growth rate values that are found. The reason is that this gives a clearer idea of the general trend of the growth rates. The average growth rates for each dredging strategy are plotted on the curve in order to visualize the general trend rather than including extreme values. Furthermore, the wiggles that are visible in the growth rates are explained previously by the timing between the tide and the frequency that the model writes the output.

Figure 39A shows the wave heights and growth rates for Borssele, plotted on the base curves. It can be seen that the placement of the wave heights on the growth curve indicates that the 1/3 Peak removal has the highest growth rates whereas the Cut & Fill/ Total Removal shows the lowest growth rates. For 2/3 Peak Removal, and 1/3 Peak Removal, the upper limit of the growth rates seems to coincide with the base situation. However, the lower limits of 2/3, and 1/3 Peak removal do not fall on the base curve. Furthermore, full Peak Removal shows an opposite trend compared to the base growth rates, however a possible reason for this is explained previously regarding the small perturbation on the edge of the peak cut off.

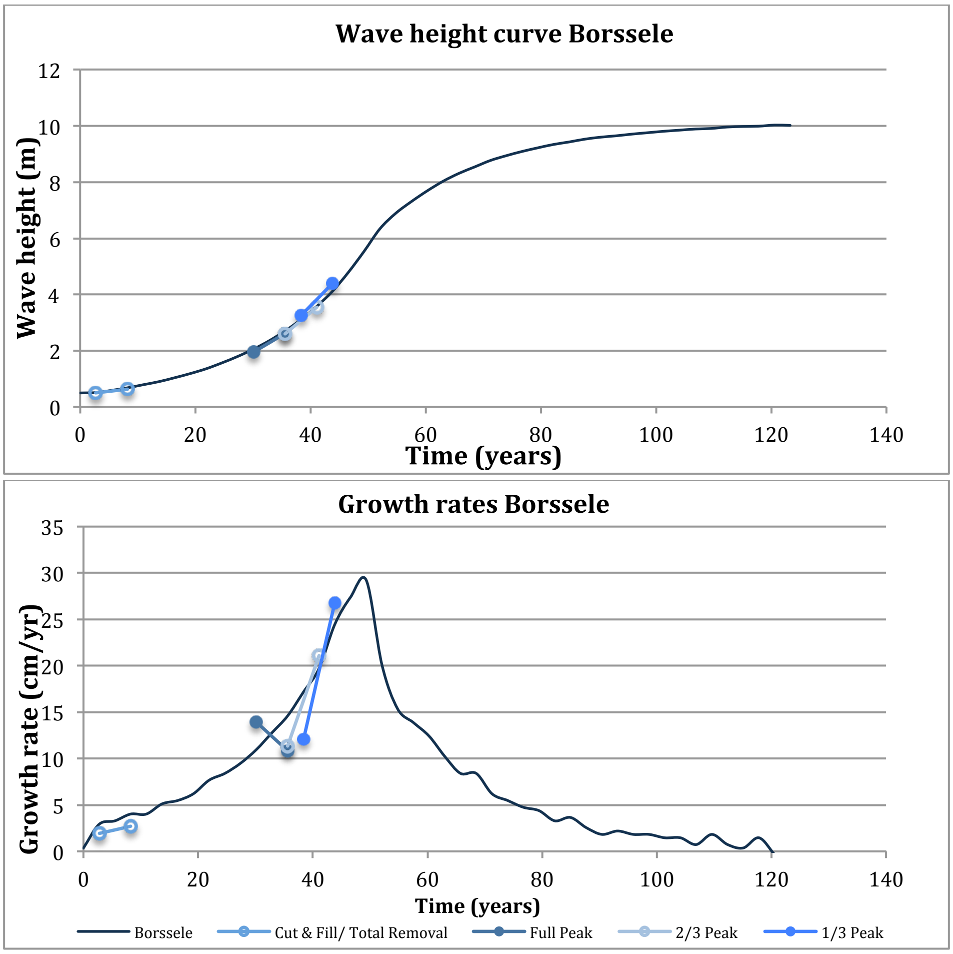

FIGURE 39A TOP: GROWTH CURVE AT BORSSELE RELATED TO THE BASE INPUT PARAMETERS AND NO DREDGING STRATEGIES ARE APPLIED. WAVE HEIGHT RESULTS FOR THE DREDGING STRATEGIES ARE PLOTTED ON THIS BASE CURVE. BOTTOM: GROWTH RATES OF THE DREDGING STRATEGIES COMPARED TO THE GENERAL GROWTH RATES AT BORSSELE

Figure 39B shows the growth curve, and the growth rates for Borssele -10m. It can be seen that full Peak Removal shows a negative trend whereas the base growth rate curve shows a positive trend at that point in time. Furthermore, the results of 1/3 Peak Removal may imply that the growth rates are approaching their maximum values, however the base curve shows growth rates up to 24 cm/yr.

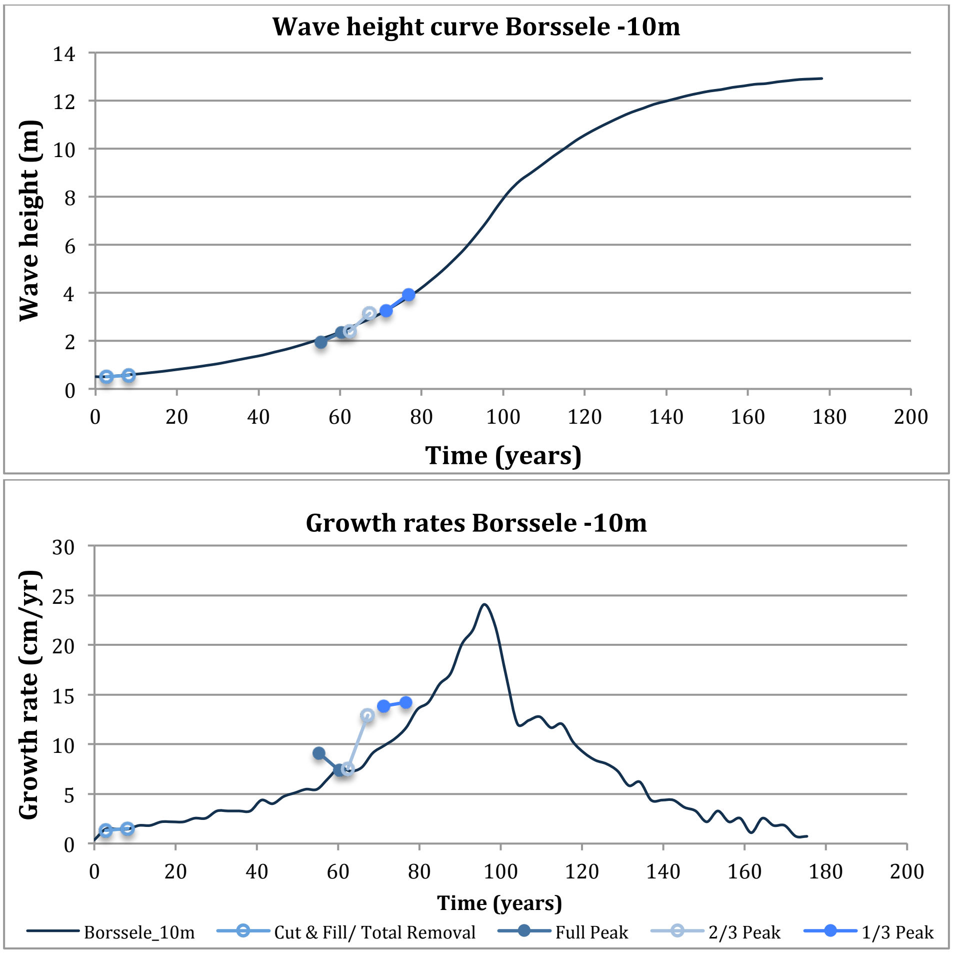

FIGURE 39B WAVE HEIGHT CURVE AT HOLLANDSE KUST ZUID RELATED TO THE BASE INPUT PARAMETERS AND NO DREDGING STRATEGIES ARE APPLIED.

At Hollandse Kust Zuid only two dredging strategies are applied and the results are plotted on the base growth curve and growth rate curve shown in Figure 39C.

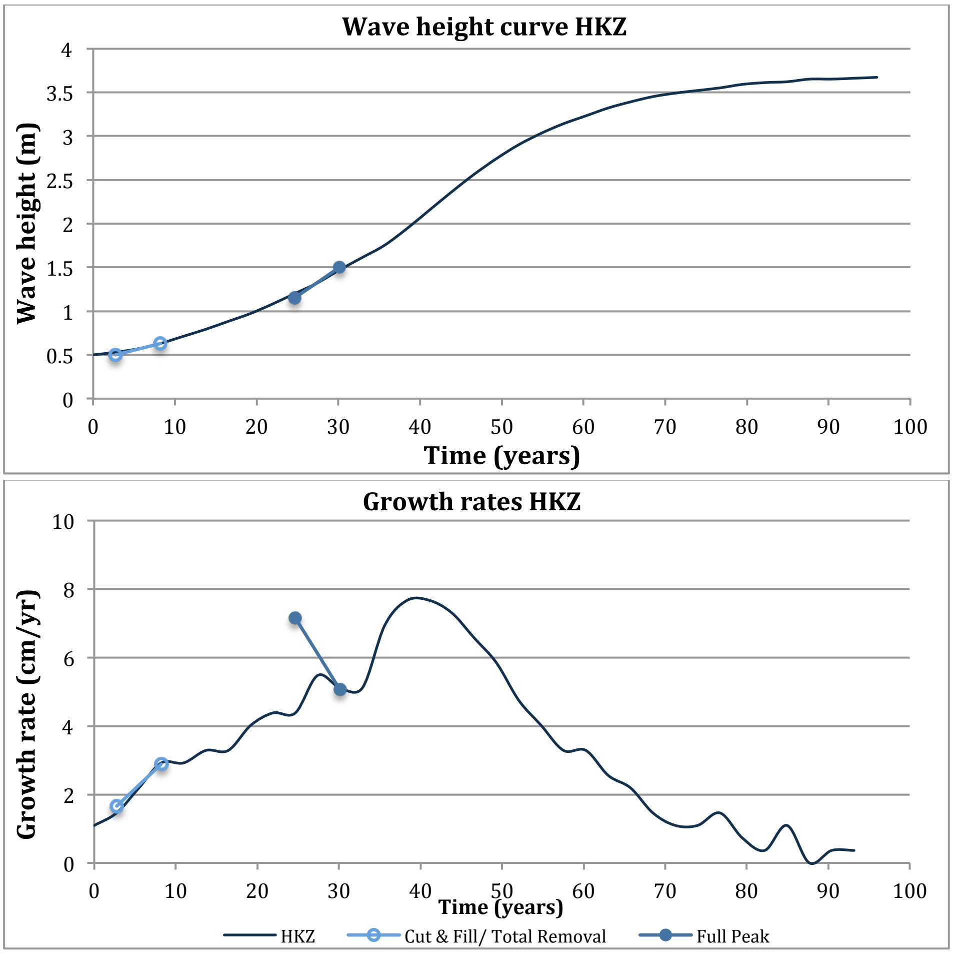

FIGURE 39C WAVE HEIGHT CURVE AT HOLLANDSE KUST ZUID RELATED TO THE BASE INPUT PARAMETERS AND NO DREDGING STRATEGIES ARE APPLIED.

The comparison of the results of the dredging strategies, with the general growth curve indicate that the resulting wave height after cutting off a peak, in combination with the general growth curve and growth rates of that area, can give a general idea of the growth rates of the dredged sand wave. However, the growth rate trends do not always agree, especially full Peak Removal showed controversial results.

Furthermore, the times that it takes for sand waves to reach their equilibrium height at Borssele, Borssele -10m, and Hollandse Kust Zuid are approximately 120 *years*, 180 *years*, and 95 *years* respectively. From these three locations, Borssele showed to have the highest sediment transport rates, followed by Borssele -10m and Hollandse Kust Zuid had the lowest sediment transport rates. Moreover, the growth curve of Hollandse Kust Zuid shows that it takes 95 *years* to reach a wave height of 3.7 *m* at that location whereas at Borssele and Borssele -10m it takes approximately 41 *years* and 75 *years* to reach that wave height respectively. Therefore it shows that the even though sand waves at Hollandse Kust Zuid reach their equilibrium height sooner than sand waves at Borssele, the growth rates at Borssele are higher. This corresponds to literature where it is found that higher bed load transport results in greater growth rates. Furthermore, the equilibrium wave heights for Borssele, Borssele -10m and Hollandse Kust Zuid prove that sand waves grow higher with a greater sediment grain size. Moreover, as can be seen by the resulting wave heights of Borssele and Borssele -10m, wave heights reach greater heights at a greater depths.

Table 22 through Table 26 in the Appendix show the wave heights and corresponding growth rates for the different dredging strategies at the three locations and for the different input parameter sets. Furthermore, after a dredging strategy is applied, the growth rate of only the crests could be of interest for specific projects (i.e. projects that require a minimum depth), therefore the wave heights and growth rates of the crests are presented there for the three different locations and different parameter sets as well.

7.5.2 SYNTHESIS FROM RESULTS TO CABLE ROUTING EXAMPLE

The example in this research for the application of this research in the design of dredging strategies is cable routing. It is found that it is important to know the requirements for the dredging strategy, in order to determine which strategy is best to use. In the case of determining the non-mobile seabed reference level, the strategy of Cut & Fill may be the better option because it resulted in one of the lowest growth rates. The resulting bathymetry between the Cut & Fill, and total sand wave Removal may be similar because both strategies flatten the seabed, however the total Removal strategy will result in a lower mean seabed level. For both strategies the seabed will find a new equilibrium where crests will grow higher and troughs will grow deeper. The greatest difference is the volume of dredged sediment, where less sediment has to be dredged for the Cut & Fill strategy, which could result in lower costs.

However, if there the requirement for design is a required minimum depth, the total Removal strategy may be a better solution because it lowers the mean seabed level and therefore it may take longer for the sand waves to grow to wave heights that reach the minimum depth.

8. DISCUSSION

In this section, the method and its influence on the results is discussed, as well as other remarkable results from this research.

8.1 DATA ANALYSIS

The grid size that is used is 5 by 5 m whereas the field data had a resolution of approximately 1 by 1 m. This decision emphasizes the grid points that are used whereas the grid points that are left out do not have an impact on the results. The Butterworth filters filtered out smaller bed forms than 50 m, however the greater grid size may have also filtered out some bed forms already.

In order to determine the orientation of the transects, a 2D-Fourier analysis would have provided more insight in the migration direction of the sand waves in the field. Therefore the orientation of the transects could have been selected more accurately to follow the sand wave development.

The decrease in wave heights of the undredged transect could be explained by the growth rates of the dredged transect. The interaction between the dredged and undredged transects can be the reason of this behavior.

Furthermore, the information about the study site stated that sand extractions have occurred after the closure of the sand extraction site between 2008 and 2009 and once more in 2010. These sand extractions had a relatively small volume, therefore it is assumed in the analysis of the results that these sand extractions had no effect on the results. However, the exact locations of these extractions are unclear, and therefore could have affected the results. An example could be the negative wave height trend of the undredged and parallel transects towards the end of the measurements. However as explained earlier, lateral interactions between dredged and undredged areas can be the reason for this behavior as well.

8.2 SENSITIVITY OF THE FASTEST GROWING MODE TO MODEL INPUT

The setup of the model that is used is similar to the set-up in *Van Gerwen* (2016), suspended load is included, as well as an asymmetrical tide. It is assumed that this setup suits the North Sea conditions as it is validated with data from the North Sea (Van Gerwen, 2016).

The effect of each input parameter can be determined by this sensitivity analysis, however it has to be noted that the ranges that are used for each parameter are not equal to each other. Therefore the relative impact of the parameter gives a better understanding of which parameter has a greater impact on the wavelength of the fastest growing mode. *Van Santen et al.* (2011) stated that greater sediment grain sizes result in greater wavelengths. Furthermore, *Borsje et al.* (2014) showed that a smaller sediment grain size causes the other input parameters to have a greater impact on the wavelengths, whereas greater sediment grain sizes limit those impacts. The results of the sensitivity analysis agreed with the statement by *Borsje et al.* (2014), however it disagreed with the statement by *Van Santen et al.* (2011). As the sediment grain size is decreased, the wavelength increased and vice versa. Furthermore, the effect of decreasing the sediment grain size was a lot greater than the effect of increasing the grain size. The effect of the tidal current velocity amplitude can be explained by the bed shear stress formula:

$$\tau_b = \rho_w g \frac{U^2}{C^2}$$

Where:
τ_b = bed shear stress
ρ_w = density of water
g = gravity
C = Chézy coefficient
U = depth average velocity

It can be seen that a small change in tidal current velocity amplitude causes big changes in bed shear stress, which is one of the mechanisms of the bed load transport. This complies with Németh et al. (2002) who showed that the bed shear stress is the dominant factor in linear sand wave dynamics. Therefore it can be assumed that an increased bed load transport results in greater lengths of the sand waves.
Blondeaux and Vittori (2012) showed that the wavelengths increase with an increase in water depth, which agrees with the results found in this study. The effect of the water depth on the fastest growing mode can be explained by the depth averaged water velocity, which shows that if the same current has to flow through a more shallow area, the depth average flow velocity has to increase. This links back to the bed shear stress formula stated above, where the increase of depth the average velocity results in an increase in bed shear stress. It can be concluded that the results from the sensitivity analysis generally agree with literature on the behavior of the wavelength of the fastest growing mode with respect to the input parameters. The exception is the grain size diameter.

The combination of the sediment transport formulas, and the model results show that the tidal constituent and the water depth are the most influential parameters. Furthermore, the effect of the sediment grain size should be considered when analyzing results of the fastest growing modes. It is important for engineering applications to carefully determine these parameters when this model is used for modeling in a specific location.

8.3 ASSESSMENT OF DIFFERENT INITIAL BEDS IN THE MODEL

The original bed that simulated a dredged situation with the greatest depth (Case I) has the largest equilibrium wave height, and it also has the greatest depth, this complies with literature where it is stated that sand waves reach greater heights at greater depths (Németh et al., 2007).

The comparison between the dredged and undredged situations (Case II and Case IV) shows that it is important to decide whether to model a dredged or undredged situation, even though in the end the resulting bed development may be similar, it can save simulation time.

The time scale of the regeneration of sand waves after dredging complies with literature and takes decades. However the regeneration time depends on the environment and the depth at the location where the sand waves develop.

The adjusted parameter sets that are used for Case VII and Case VIII (that use the idealized initial transects) are found by trial and error. Possible different combinations of parameters and corresponding wavelength of the fastest growing mode could be found and showed different results. Furthermore, the idealized transect that is implemented in the model consists of more than one wavelength, therefore the adjusted parameter set cannot represent all wavelengths present in the domain and an error is still made.

8.4 COMPARISON OF MODEL RESULTS AND FIELD DATA

It can be assumed that there are processes that are not included in the model, like the interaction between a dredged area and an undredged area, or storm events that occurred during the period of measurements in the field. These processes may explain some of the behavior of the sand waves in the field data that cannot be explained by the model as it is used here.

From the results of the growth curves for the different initial beds and the field data, it is argued that the original initial bed is the closest approximation to the field data. However, this case uses the 'old' parameter set whereas the new parameter set for the idealized beds showed to be more representative of the cross section. Therefore it should be questioned whether the original initial bed should also use that adjusted parameter set instead of the initial one. The investigation of the study site showed that there are ranges of input parameters present in the area, therefore it can be tough to determine which parameter set is best. In this case, both the initial parameter set, and the adjusted parameter set consisted of parameters with values that can be found in the area. This shows that the selection of parameters that is used can be crucial in evaluating a specific location with this numerical model.

The last noteworthy results were the underestimated migration rates, however this could be due to the tidal asymmetry that has a value that is too low for this location. However, previous research has shown that increasing the tidal asymmetry results in lower wave heights in the model (Van Gerwen, 2016).

8.5 DREDGING STRATEGIES AND MODEL PREDICTIONS

The tidal current velocity amplitude was hard to find, and from the sensitivity analysis of the fastest growing mode it showed that this parameter can have a great effect on the outcome. The combination of parameters used for Hollandse Kust Zuid resulted in wavelengths for the fastest growing modes that did not agree with the values found in the field. However, for Borssele these values did agree with the field data. Therefore, this may show the importance of the value and the combination of the input in the model for the three parameters (depth, grain size diameter, and tidal constituent). In this case, the values that are found for the fastest growing modes are still used for the behavior study. The equilibrium wave height for Borssele did not comply with the values of wave heights from the field data, which shows that the model overestimated the wave height or the sand waves in the field had not reached their equilibrium height. The range of wave heights that is found in the field at the Borssele location is 1.9 m through 5.9 m, whereas the model predicted an equilibrium height of 10 m. The difference between the model and the field data can be caused by the combination of input parameters (depth, sediment grain size, and tidal constituent) and for examples storm events that affected the sand wave height of the sand waves in the area.

The model has shown that the migration rates are still uncertain; therefore the migration rates are not analyzed for the dredging strategies. Furthermore, it has to be noted that for the dredging strategy where the complete sand wave is removed, the same fastest growing mode is used as for Cut & Fill, and Peak Removal. The reason for this is that the change in depth is not significant, and it is assumed that this does not change the system enough in order to a new wavelength of the fastest growing mode for these cases.

The initial beds that represent the Peak Removal strategies are implemented with sharp edges where the Peak has been removed. In reality this edge is not as sharp and therefore the shape of the evolution of the sand wave after dredging may look different than modeled in this research.

The data analysis that is performed in this research indicated that there is interaction between dredged and undredged parts of a sand extraction site. The application of the different dredging strategies on sand waves in the model does not take into account lateral interactions (i.e. trenching). Therefore it has to be noted that the results of the dredging strategies are strictly valid for a transect that is assumed to not be affected by its surrounding areas.

9. CONCLUSIONS, LIMITATIONS AND RECOMMENDATIONS

The conclusions that are drawn in previous chapters are combined in this section. Furthermore, the limitations of this research are discussed, and recommendations for further research or improvements are mentioned.

9.1 CONCLUSIONS

Research question 1:

What are the most influencing processes of a numerical model in order to predict the regeneration of tidal sand waves after dredging?

The answer to this research question is investigated by comparing the results from a numerical model with field data, therefore three sub-questions are formed and stated below. Chapter 2 provides the information on the study site, and Chapter 3 presents the data analysis that is performed and the results. These two chapters form the base to answer research question 1.a. Research question 1.b is answered by two different chapters, Chapter 4 that describes the numerical model, and a sensitivity analysis on the environmental input parameters. Moreover, Chapter 5 elaborates on the long-term simulations for the seabed development, and discusses the results from different initial beds that are used as input in the model. The last sub-question 1.c. is answered by combining the model results and the field data, which relates to Chapter 6.

a. *What are the environmental conditions (flow velocity amplitudes, water depths, and grain sizes) and the dynamics from the sand wave field (wavelength, wave height, growth rate and migration rate) of the study site in the North Sea?*

The environmental conditions and dynamics for the study site are determined by using literature and data analysis of the available field data. The water depth is found from the data analysis and ranged from 6.8 m to 22.8 m. Furthermore, the tidal constituent and grain size diameter are defined as $U_{S2} = 0.65\ m/s$ and $D_{50} = 0.30\ mm$ respectively. Tidal asymmetry is taken into account in order to simulate sand wave migration and is implemented in the model with a value of 0.05 m/s for the asymmetric flow velocity.

The wavelengths of the sand waves that are found in the field range from 75 m up to 327 m. The wave heights of the dredged transect showed a positive trend with a minimum wave height of 23 cm in March 2004, and a maximum wave height of 2.3 m in March 2013. Furthermore, the wave heights of the undredged transect showed less variation and varied from 1.8 m in March 2006 to 3.0 m in March 2014. These values comply with the values for wavelengths and wave heights for sand waves in the North Sea that are found in literature. Moreover, the growth curve of the dredged transect can be recognized in the initial stages of the general sand wave growth curve, whereas the undredged transect seems to have reached its equilibrium height.

The migration rates of the sand waves on the dredged and undredged transect ranged from 9.8 m/yr to 17.8 m/yr.

b. *What are the dynamics (wavelength, wave height, migration rate, and regeneration time) of the sand wave field when modeled in Delft3D, and what are the most influencing parameter settings?*

The results of the sensitivity analysis showed that the tidal current velocity amplitude relatively had the greatest effect on the wavelength of the fastest growing mode. It showed that an increase in velocity resulted in longer wavelengths, and a decrease in velocity caused shorter wavelengths. Similar behavior is seen for the water depth; the effect of this parameter on the wavelength is slightly smaller, however it showed a positive correlation between the water depth resulted and wavelengths. An interesting result came from the variation of the sediment grain size. Increasing the grain size showed smaller wavelengths, and decreasing the grain size results in larger wavelengths. Furthermore, a larger sediment grain size limits the effect of varying the depth and tidal current velocity amplitude.

The wavelengths of the fastest growing modes are found from the input parameters and are used in the model for different cases. The 'dredged' cases I and VII use wavelengths of 178 m and 257 m respectively. Whereas the 'undredged cases IV and VIII use wavelengths of 155 m for Case IV and 233 m for Case VIII. The regeneration time of sand waves (to reach 90% in height) is found for the 'dredged' cases and is approximately 45 years for Case I and 35 years for Case II (same input parameters as Case IV, different initial wave height). For Case I and IV the equilibrium heights of the sand waves are found and are 5.1 m and 4.2 m respectively. The wave heights after 11 $years$ are found as well in order to compare them to the wave heights of the field data. Case I, IV, VII and VIII recorded wave heights of 1.57 m, 4.11 m, 0.38 through 0.97 m and 2.86 through 3.83 m respectively. Furthermore, migration rates of these four cases ranged from 2.8 m/yr to 4.6 m/yr for crests and troughs and crests generally migrated faster than troughs.

c. *How do the wavelengths, wave heights, migration rates, and growth rates from the model (RQ1.b) compare to the field data from the study site (RQ1.a)?*

It is found that the wavelengths of the fastest growing modes fell within the range of wavelengths that were found in the field. Furthermore, the wave heights may be overestimated by the model and extreme weather events may limit the sand wave height in the field, this resulted in higher wave heights in the model than in the study site.

The comparison of the different initial beds in the model with the results of the field data showed that the original and schematized initial beds simulate the regeneration of sand waves well. However the different sets of input parameters emphasized the importance of accurate input data to represent the study area. Several different wavelengths are represented on the idealized initial bed, however the combination of input parameters can only represent the wavelength of the fastest growing mode. Therefore a fundamental error is made and this questions the validity of the results of the model with this implemented initial bed.

Moreover, the migration rates of the model are significantly lower than the migration rates in the field for all cases. Looking into adding another tidal constituent, could possibly improve this result. Adding another tidal constituent, or studying the tidal velocities more in depth may lower the wave heights, and increase the migration rates of the model.

There are still processes that could explain some behavior in the field that are not included in the model like lateral interaction between dredged and udredged areas or storm events.

Research question 2:

What insights does the model give towards the prediction of regeneration of tidal sand waves?

This research question focuses on the synthesis between the model results and engineering practices, and this part of the research is also split up into three sub-questions. However, all these questions are answered in Chapter 6, where the dredged transect, and a dredged model simulation are compared to each other. Furthermore, Chapter 7 describes different dredging strategies that are applied at specific locations in order to determine the growth rates for each dredging strategy.

a. *What insights does the model provide on the prediction of sand wave characteristics (wavelengths, wave height and migration rates) and about the time scale of the regeneration of tidal sand waves after dredging?*

This research has shown that a variety of input parameters can result in multiple parameter sets that can satisfy the environmental conditions and sand wave characteristics of a specific area. Furthermore, the original small sine function showed to be the most appropriate in the modeling of regeneration of tidal sand waves.

Different dredging strategies are applied at different locations to compare their growth curve and growth rates to a 'base' growth curve and corresponding growth rates, in order to find out whether the resulting wave height after dredging behaves similar to a growing sand wave with that wave height. The results showed that an estimation of the growth rates can be made for Peak Removal and Cut & Fill, 2/3 Peak Removal and 1/3 Peak Removal when they are plotted on the base growth curve of that location. Full Peak Removal showed contradicting results due to the behavior of the flattened area that forms a small perturbation that grows before the complete length of the peak starts developing again.

The time scale of regeneration to a specific height depends on the environmental and initial conditions of the location and dredging strategy. The Total Removal and Cut & Fill strategies resulted in the lowest growth rates, followed by full Peak Removal, 2/3 Peak Removal and 1/3 Peak Removal had the highest growth rates.

Previous parts of this research have shown that the model cannot yet simulate the migration rates of the sand waves accurately enough for this to be taken into account for the application of dredging strategies.

b. *What insights does the model provide about the usability for the design of offshore infrastructure in the North Sea?*

The model can provide insight into the growth rate of the resulting sand wave for the dredging strategies that are implemented in this research. The growth rates of the sand waves for different dredging strategies can be estimated by looking at the base growth rates. Lateral interactions are not implemented in the model and the sand wave development after the dredging strategy is applied is modeled for 5 years, therefore the time span of the results is limited to that period.

Furthermore, the growth rate of the crests and troughs can be tracked separately if this provides more information for a given situation than the sand wave growth.

9.2 LIMITATIONS AND RECOMMENDATIONS

9.2.1 *LIMITATIONS*

Troughout this research, different assumptions and simplifications are made. For the interpretation of the results it is important to be aware of these limitations.

Sensitivity of the orientation and location of the transects

The orientations and locations of the transects for this study are chosen by trial and error, however a 2D-fourier analysis could have given more insight in the migration direction of the sand wave field and resulted in different locations and orientations for the transects. Furthermore, it is not studied how sensitive the data analysis results are to the orientation and location of the transects.

Sensitivity of the analyzed troughs and crests

In order to analyze the dynamics of the sand wave field from the data analysis, specific crests and troughs are selected. Some sand waves migrated out of the domain during the time of the measurements whereas other sand waves entered the domain. Therefore only a limited amount of sand waves on the transects could be analyzed. Later on in the research, the same crests and troughs of the sand waves are analyzed for the model simulations. It is assumed that the analyzed crests and troughs are representative of the transect, however results showed that the behavior is different for each crest and trough.

Idealized transect

The idealized transect consists of several wavelength, however the forcing of the system corresponds to only one wavelength. Therefore, the use of an idealized transect contains a fundamental error and limits the usability of this initial bed.

Numerical modeling and implementation of dredging strategies

The field data showed that in reality there are lateral interactions between neighboring sections of a sand wave field. However, the numerical model is set up as a 2DV-model, and no lateral interactions are taken into account. Furthermore, the initial beds that are implemented in the model are schematized or idealized and assumed that they represent the actual bathymetry. Ideally, the dredged bed is simulated with a random initial bed as studied by *Choy* (2015), however this would result in extra computation time.

Other input parameters like the sediment grain size, water depth, and tidal current velocity amplitude are assumed to have a set value, however in reality these values can vary for the area of interest.

The fastest growing mode is not recalculated for the total removal dredging strategy that is used, the same wavelength is used as for the other dredging strategies in a parameter set. It is assumed that this still gives valid results because the depth difference is not more than 2 $meters$, and the model has proven to be able to handle wavelengths that are slightly different than the wavelength of the fastest growing mode as input parameter.

The simulations for the dredging strategies are only performed to cover 5 years, because this was determined the timespan of interest. However, the result is that the growth rates of the sand waves after dredging only represent the growth rates during those years. The growth curves of long-term calculations have shown, as well as literature, that this is not a linear trend and therefore this should be taken into account when considering the timescale of the regeneration of tidal sand waves after dredging.

Large computational effort

The long-term simulations of the model sometimes took up to 4 $days$, therefore a selection of cases had to be made and not all parameter sets or dredging strategies are analyzed.

Accurate available data on input parameters for the North Sea

For the locations in the North Sea, the input parameters (water depth, sediment grain size, and tidal current velocity amplitude) had to be determined. The water depth, and sediment grain size could be found in reports, however the value of the tidal constituent in a specific area was harder to find. Therefore, the value of this parameter that is used may not be very accurate.

The time span can be extended

The data that is provided consisted of 30 measurements spread out over 14 years total. However in order to compare long term bed development with field data, a data set that covers a longer period of time (not necessarily with more measurements in a year) could be valuable.

9.2.2 RECOMMENDATIONS

In this section, recommendations for further research are presented. The recommendations may provide validation to ensure the outcomes from this research, expand the knowledge in the field of tidal sand waves, or explore the possibilities of practical applications of this model.

Validation of the model with accurate input parameters

The results from the behavior study with the different initial beds showed that different combinations of parameters, that are all representative of a specific study site, can give significantly different results for the sand wave characteristics (i.e. growth curve). Therefore, it is recommended to model the regeneration tidal sand waves for a specific location with the most accurate input parameters that can be obtained in order to mimimize uncertainties caused by a range of input parameters.

Study the migration in this model

One of the conclusions in this research was that it may be beneficial to add another tidal component to improve the prediction of the migration of sand waves. Furthermore, it has been found that there is a relation between the asymmetric tide and the equilibrium wave height in this model, therefore this research may improve the overall behavior of the sand waves in the model.

Study non-mobile seabed reference level

As mentioned before, the non-mobile seabed reference level is one of the fundamental guidelines for the placing and routing of cables through a sand wave field. The current study focuses on the regeneration time of sand waves and the crest growth, however for this research the migration rates and the trough levels would be the focus.

Interaction between structures and sand waves after dredging

The design life of a cable placed in a sand wave field is approximately 30 years, and the regeneration timescale of sand waves is decades. It would be interesting to study the combination of the design life of a structure in comparison with the regeneration time scale of sand waves.

10. WORKS CITED

Bellec, V. K., Van Lancker, V., Degrendele, K., Roche, M., & Le Bot, S. (2010). Geo-environmental characterization of the Kwinte Bank. *Journal of Coastal Research , 51*, 63-76.

Besio, G., Blondeaux, P., Van Lancker, V., Verfaillie, E., & Vittori, G. (2008b). Sand wave characteristics: Theoretical predictions versus field data. *River, Coastal and Estuarine Morphodynamics: RCEM 2007* , 985-992.

Borsje, B. W., Kranenburg, W. M., Roos, P. C., Matthieu, J., & Hulscher, S. J. M. H. (2014). The role of suspended load transport in the occurence of tidal sand waves. *Journal of Geophysical Research: Earth Surface , 119(4)*, 701-716.

Borsje, B. W., Roos, P., Kranenburg, W., & Hulscher, S. J. M. H. (2013). Modeling tidal sand wave formation in a numerical shallow water model: The role of turbulence formation. *Continental Shelf Research , 60*, 17-27.

Brière, C., Roos, P. C., Garel, E., & Hulscher, S. J. M. H. (2010). Modelling the morphodynamics of the Kwinte Bank, subject to sand extraction. *Journal of Coastal Research , 51*, 117-126.

Cherlet, J., Besio, G., Blondeaux, P., van Lancker, V., Verfaillie, E., & Vittori, G. (2007). Modeling sand wave characteristics on the Belgian Continental Shelf and in the Calais-Dover Strait. *Journal of Geophysical Research , 112* (C06002).

Choy, D. Y. (2015). *Numerical modelling of the growth of offshore sand waves.* Master thesis, TU Delft, National University of Singapore.

Damen, J. M., van Dijk, T. A. G. P., & Hulscher, S. J. M. H. (Submitted). Spatially varyin environmental properties controlling observed sand wave morphology. *JGR-Earth Surface* .

Degrendele, K., Roche, M., de Mol, L., Schotte, P., & Vandenreyken, H. (2014). *Synthesis of the monitoring of the aggregate extraction on the Belgian Continental shelf from 2011 till 2014.* Blankenberge: FOD Economie.

Degrendele, K., Roche, M., Schotte, P., Van Lancker, V., Bellec, V. K., & Bonne, W. (2010). Morphological evolution of the Kwinte Bank central depression before and after the cessation of aggregate extraction. *Journal of Coastal Research , 51*, 77-86.

Deltares. (2016). *Hollandse Kust (Zuid) Wind Farm Zone Certification Report Morphodymics.* Netherlands Enterprise Agency.

Garel, E. (2010). Tidally-averaged currents and bedload transport over the Kwinte Bank, Southern North Sea. *Journal of Coastal Research , 51*, 87-94.

Hasselaar, R., Raaijmakers, T., Riezebos, H. J., Van Dijk, T. A. G. P., Borsje, B. W., & Vermaas, T. (2015). *Morphodynamics of Borssele Wind Farm Zone WFS-I and WFS-II - final report.* Deltares.

Hulscher, S. J. M. H. (1996). Tidal-induced large-scale regular bed form patterns in a three-dimensional shallow water model. *Journal of Geophysical Research , 101* (C9), 20, 727-20, 744.

Knaapen, M. A. F., & Hulscher, S. J. M. H.(2002). Regeneration of sand waves after dredging. *Coastal Engineering , 46*, 277-289.

Morelissen, R., Hulscher, S. J. M. H., Knaapen, M. A. F., Németh, A. A., & Bijker, R. (2003). Mathematical modelling of sand wave migration and the interaction with pipelines. *Coastal Engineering , 48*, 197-209.

Németh, A. A., Hulscher, S. J. M. H., & de Vriend, H. J. (2002). Modelling sand wave migration in shallow shelf seas. *Continental Shelf Research , 22*, 2795-2806.

Németh, A. A., Hulscher, S. J. M. H., & Van Damme, R. M. (2007). Modelling offshore sand wave evolution. *Continental Shelf Research , 27*, 713-728.

Roche, M., de Backer, A., & Van den Eynde, D. (2016). How sustainable is the Belgian sand extraction? Monitoring results and perspectives. FPS Economie.

Roche, M., Degrendele, K., de Mol, L., Schotte, P., Vandenreyken, H., van den Branden, R., et al. (2011). *Synthesis of the monitoring of the impact from the aggregate extraction on the Belgian Continental Shelf.* Bredene: FOD Economie.

Roos, P. C., & Hulscher, S. J. M. H. (2003). Large-scale seabed dynamics in offshore morphology: Modeling human intervention. *Reviews of Geophysics , 41(2)* (2), 1010.

Ruddick, K., & Lacroix, G. (2006). *Hydronamics and meteorology of the Belgian Coastal Zone.* Université libre de Bruxelles, Université D'Europe.

Tonnon, P., van Rijn, L., & Walstra, D. (2007). The morphodynamic modelling of tidal sand waves on the shoreface. *Coastal Engineering , 54*, 279-296.

Van den Eynde, D., Giardino, A., Portilla, J., Fettweis, M., Francken, F., & Monbaliu, J. (2010). Modelling the effects of sand extraction, on sediment transport due to tides, on the Kwinte Bank. *Journal of Coastal Research , 51*, 101-116.

Van Gerwen, W. (2016). *Modelling the equilibrium height of offshore sand waves.* University of Twente.

Van Santen, R. B. (2009). *Tidal sand waves in the North Sea, data analysis and modeling.* Msc thesis (unpublished), University of Utrecht.

Van Santen, R. B., De Swart, H. E., & Van Dijk, T. A. G. P. (2011). Sensitivity of tidal sand wavelength to environmental parameters: A combined data analysis and modelling approach. *Continental Shelf Research , 31*, 966-978.

Velema, J. (2010). *On the tidal dynamics of the North Sea: An idealised modelling study on the role of bottom friction, the Dover Strait and tidal resonance in the North Sea.* Master thesis, University of Twente, Enschede.

Verboven, I. (2017a). *Re-generation of tidal sand waves after dredging: literature review.*

Verfaillie, E., van Meirvenne, M., & van Lancker, V. (2006). Multivariate geostatistics for the predictive modelling of the surficial sand distribution in shelf seas. *Continental Shelf Research , 26*, 2454-2468.

A. APPENDIX

A.1 STUDY AREA

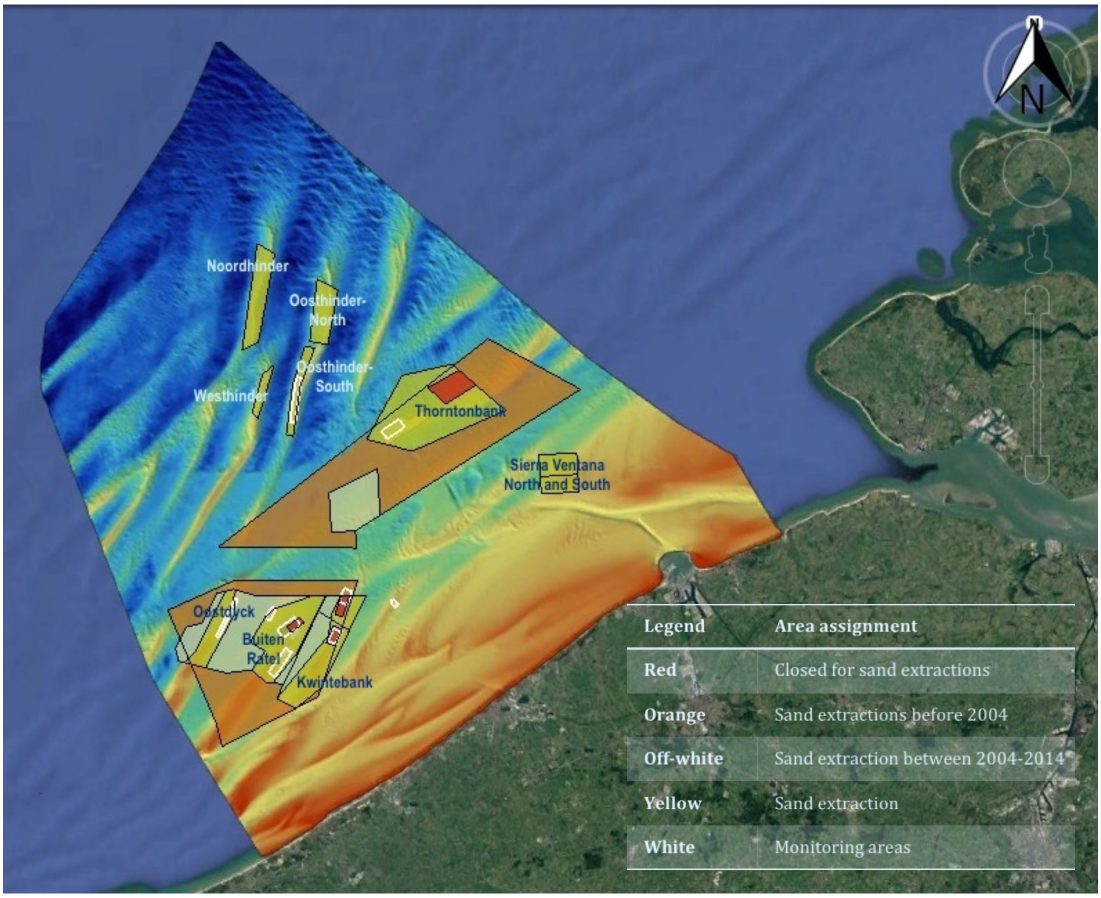

FIGURE 40 LOCATIONS SAND EXTRACTIONS IN THE BELGIAN CONTINENTAL SHELF, (GOOGLE EARTH, AND DIENST CONTINENTAL PLAT & VLAAMSE HYDROGRAFIE).

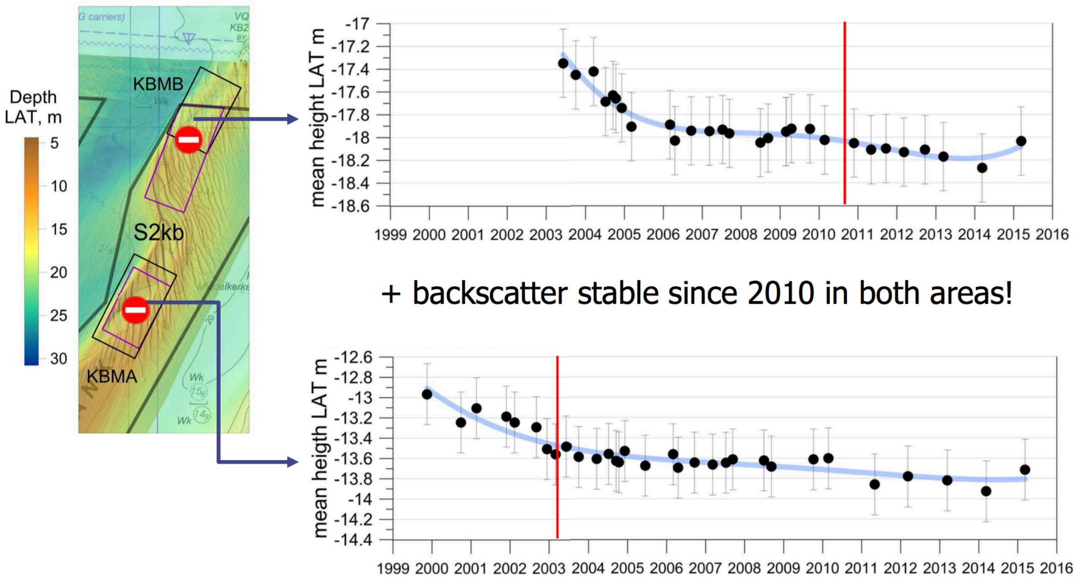

FIGURE 41 MEAN DEPTH TRENDS AT KBMA AND KBMB ROCHE ET AL., PRESENTATION 2016

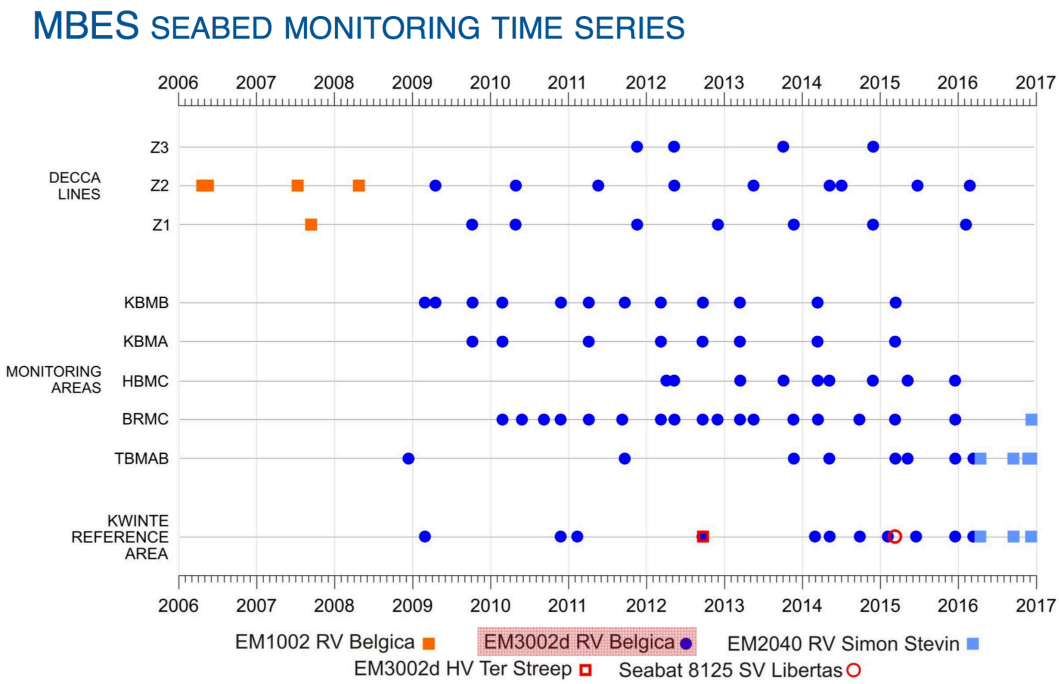

FIGURE 42 SEABED MONITORING TIME SERIES (ROCHE ET AL., 2016)

CAMPAIGN	SURVEY	MULTI-	CORRECTIONS (M)		CAMPAIGN	SURVEY	MULTI-BEAM	CORRECTIONS (M)
2001-04	KBMA0023	EM1002	-0.35		2003-06	KBMB0306	EM1002	-0.35
2001-04	KBMA0104	EM1002	-0.35		2003-15	KBMB0315	EM1002	-0.35
2001-31	KBMA0131	EM1002	-0.35		2003-24	KBMB0324	EM1002	-0.35
2002-03	KBMA0203	EM1002	-0.35		2004-06	KBMB0406	EM1002	-0.35
2002-19	KBMA0219	EM1002	-0.35		2004-15	KBMB0415	EM1002	-0.35
2002-29	KBMA0229	EM1002	-0.35		2004-20	KBMB0420	EM1002	-0.35
2003-06	KBMA0306	EM1002	-0.35		2004-23	KBMB0423	EM1002	-0.35
2003-15	KBMA0315	EM1002	-0.35		2004-29	KBMB0429	EM1002	-0.35
2003-24	KBMA0324	EM1002	-0.35		2005-04	KBMB0504	EM1002	-0.35
2004-06	KBMA0406	EM1002	-0.35		2005-14	KBMB0514	EM1002	-0.25
2004-15	KBMA0415	EM1002	-0.35		2006-04	KBMB0604	EM1002	-0.25
2004-20	KBMA0420	EM1002	-0.35		2006-08	KBMB0608	EM1002	-0.25
2004-23	KBMA0423	EM1002	-0.35		2006-19	KBMB0619	EM1002	-0.25
2004-29	KBMA0429	EM1002	-0.35		2007-06	KBMB0706	EM1002	-0.25
2005-04	KBMA0504	EM1002	-0.35		2007-16	KBMB0716	EM1002	-0.25
2005-14	KBMA0514	EM1002	-0.25		2007-19	KBMB0719	EM1002	-0.25
2006-04	KBMA0604	EM1002	-0.25		2008-16	KBMB0816	EM1002	-0.25
2006-08	KBMA0608	EM1002	-0.25		2008-20	KBMB0820	EM1002	-0.25
2006-19	KBMA0619	EM1002	-0.25		2009-06	KBMB0906	EM3002	
2007-06	KBMA0706	EM1002	-0.25		2009-11	KBMB0911	EM3002	
2007-16	KBMA0716	EM1002	-0.25		2009-26	KBMB0926	EM3002	
2007-19	KBMA0719	EM1002	-0.25		2010-05	KBMB1005	EM3002	
2008-16	KBMA0816	EM1002	-0.25		2010-30	KBMB1030	EM3002	
2008-20	KBMA0820	EM1002	-0.25		2011-13	KBMB1113	EM3002	
2009-26	KBMA0926	EM3002			2011-25	KBMB1125	EM3002	
2010-05	KBMA1005	EM3002			2012-07	KBMB1207	EM3002	
2011-13	KBMA1113	EM3002			2012-24	KBMB1224	EM3002	
2012-07	KBMA1207	EM3002			2013-08	KBMB1308	EM3002	
2013-08	KBMA1308	EM3002			2014-06	KBMB1406	EM3002	
2014-06	KBMA1406	EM3002						

TABLE 17 MEASUREMENTS AND THEIR CORRESPONDING CORRECTIONS

A.2 Data Analysis

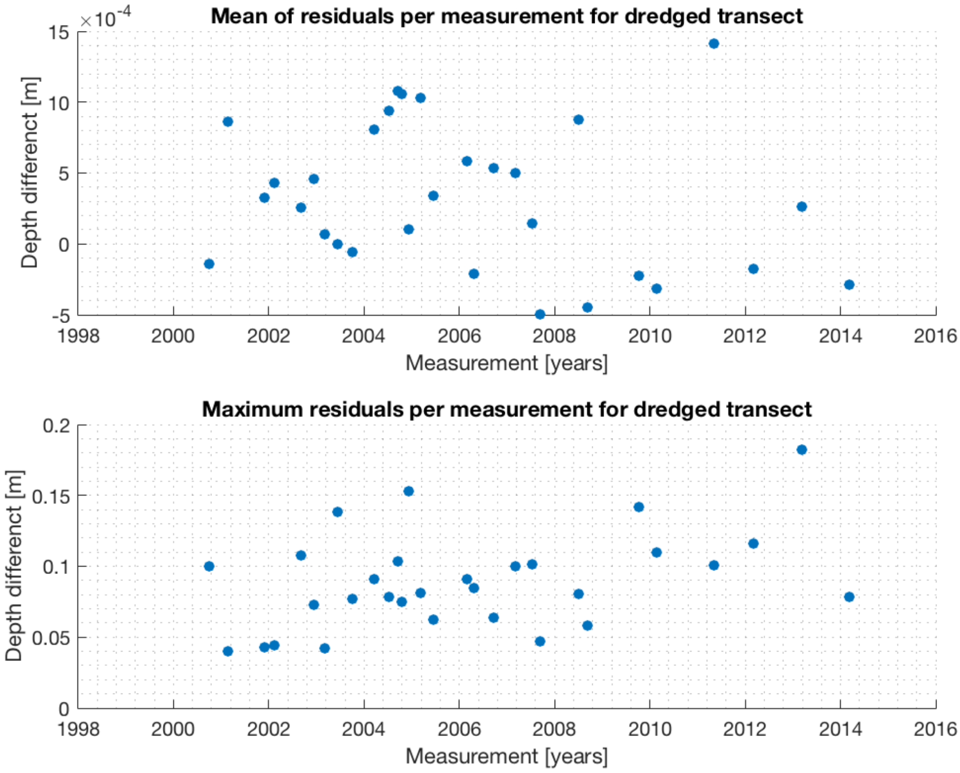

FIGURE 43 DIFFERENCES BETWEEN THE 1X1 M GRID AND THE 5X5 M GRID FOR THE DREDGED TRANSECT OF KBMA. IN FIGURE 43A, THE MEAN DIFFERENCE ALONG THE TRANSECT IS PLOTTED FOR EACH MEASUREMENT, WHEREAS IN FIGURE 43B, THE MAXIMUM DIFFERENCE THAT WAS FOUND ALONG THE TRANSECT IS PLOTTED FOR EACH MEASUREMENT.

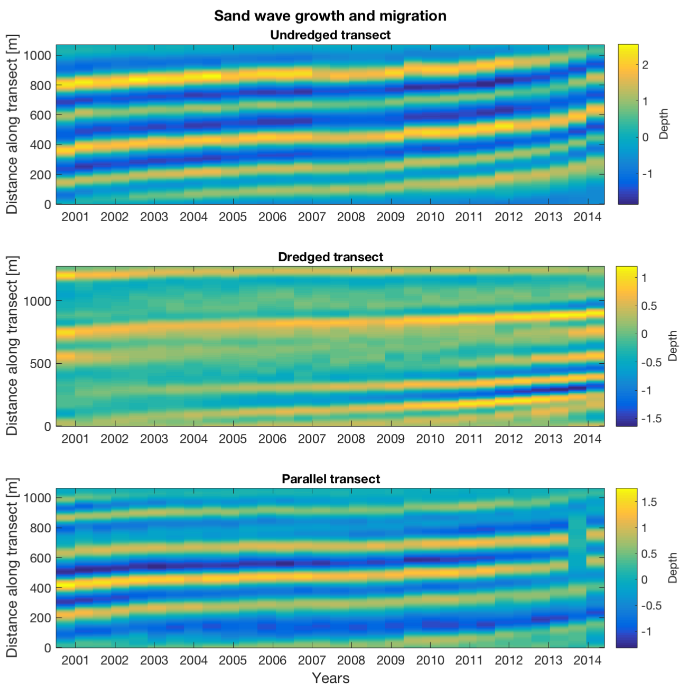

FIGURE 44 OVERVIEW OF THE DEPTH ALONG THE TRANSECTS

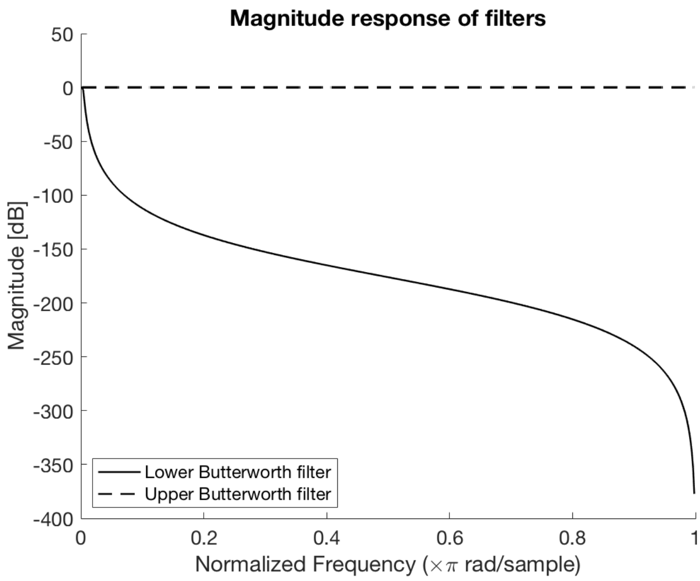

FIGURE 45 FOURIER ANALYSIS FOR THE DREDGED CROSS SECTION, WITH CUT-OFF FREQUENCY OF 100 HZ FOR THE LOW-PASS FILTER, AND 1000 HZ FOR THE HIGH-PASS FILTER

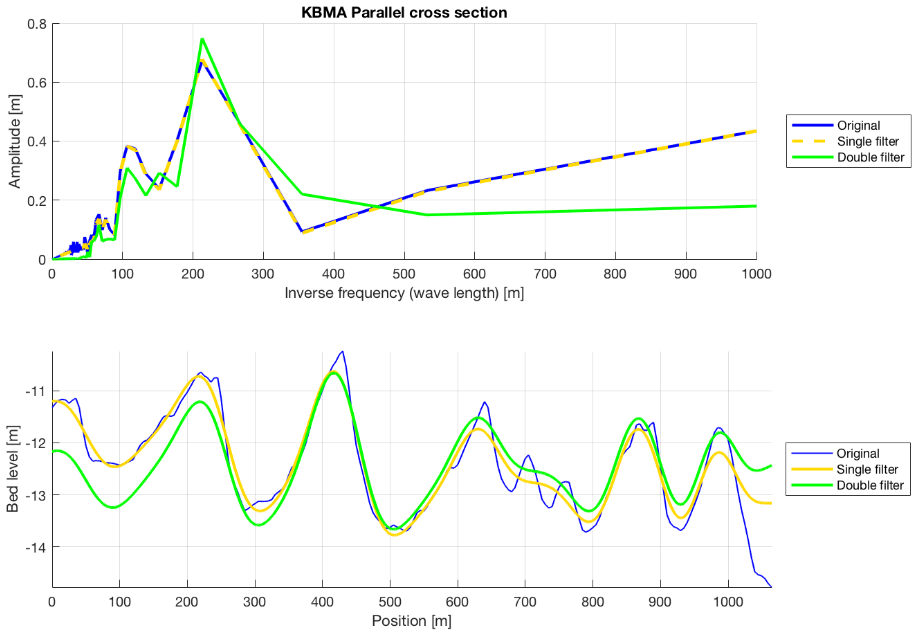

FIGURE 46 ADD FOURIER ANALYSIS FOR DIFFERENT FILTERS

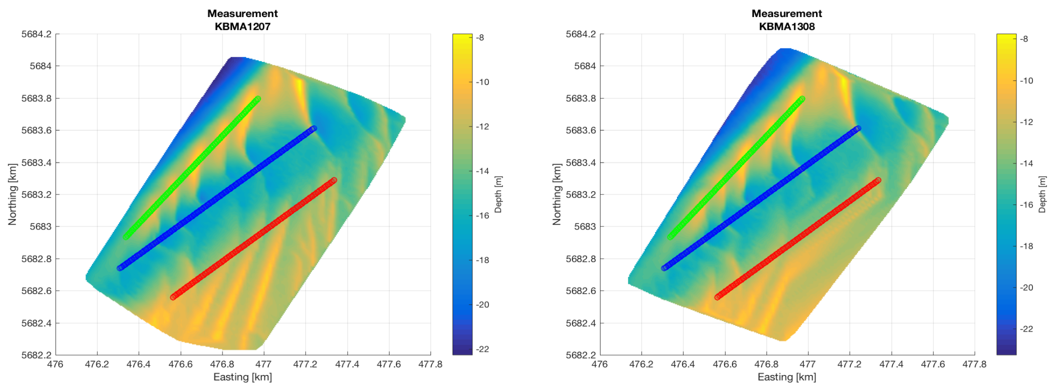

FIGURE 47 TWO MEASUREMENTS OF THE BATHYMETRY AT LOCATION A (MEASUREMENTS 28, 29) WHERE THE CHANGE IN BATHYMETRY AROUND THE PARALLEL TRANSECT IS SIGNIFICANTLY DIFFERENT FOR THE TWO MEASUREMENTS.

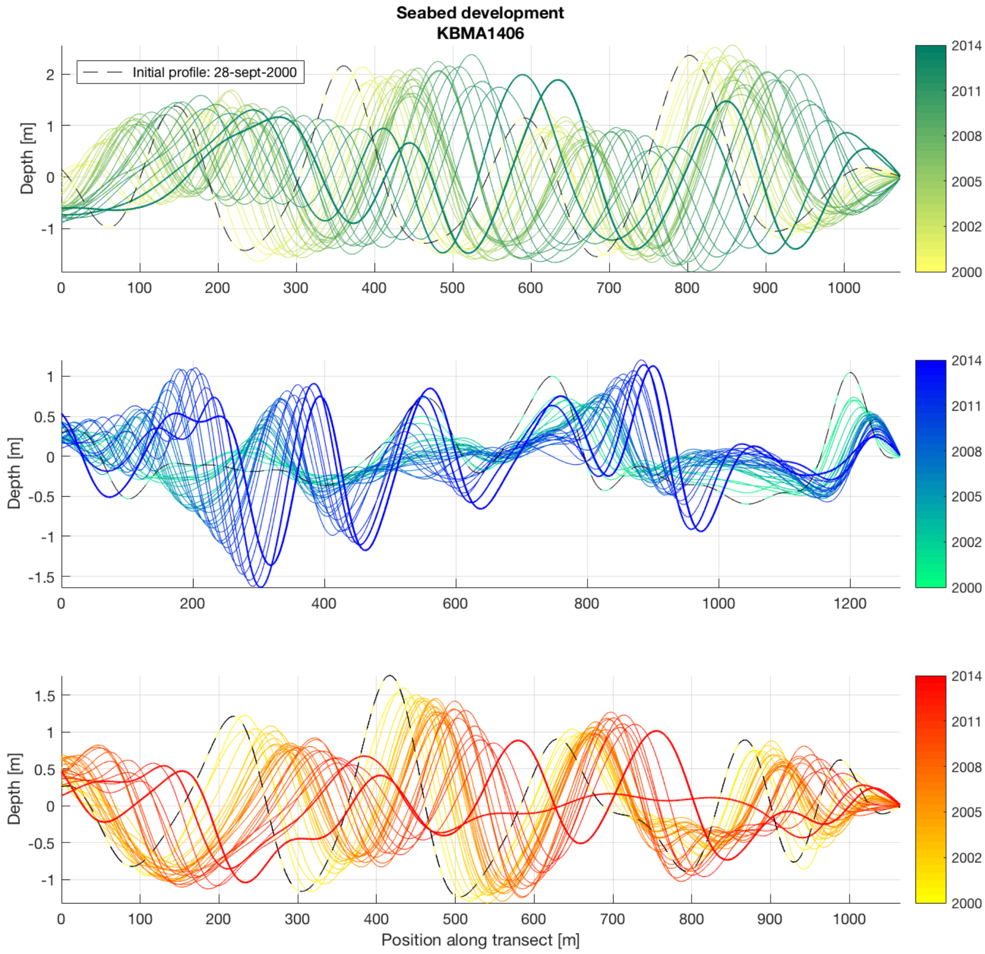

FIGURE 48 FULL BED DEVELOPMENT FROM 2001 THROUGH 2014

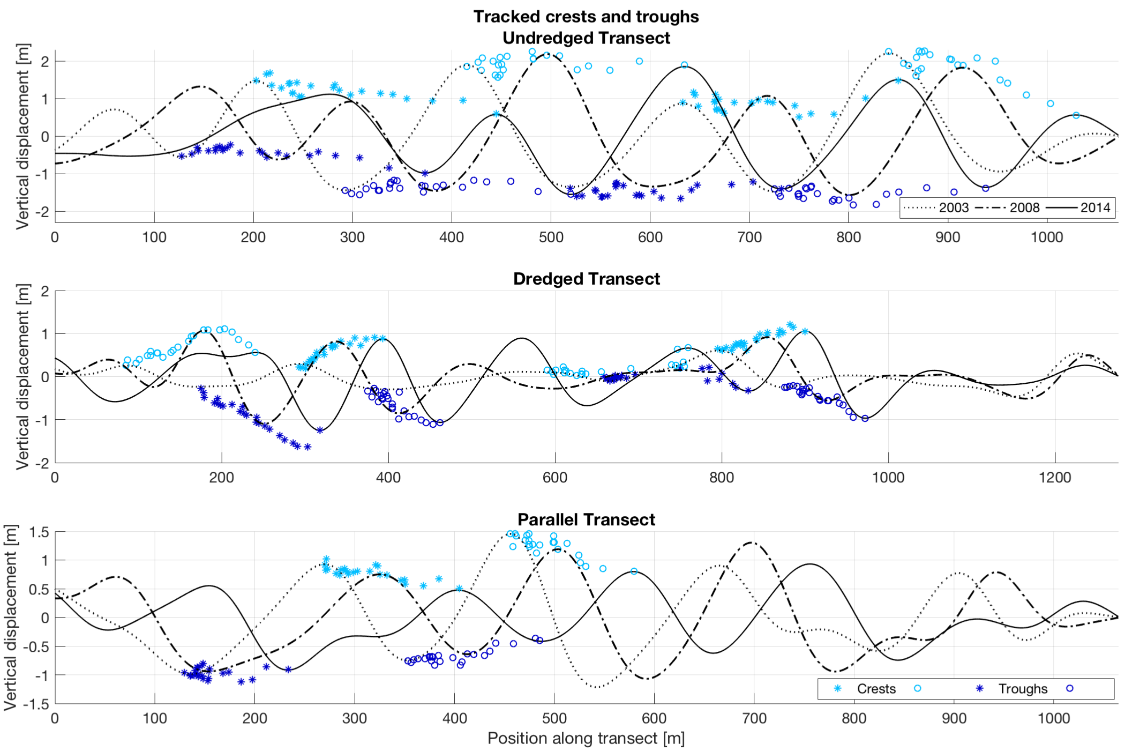

FIGURE 49 ALL TRACKED PEAKS AND TROUGHS

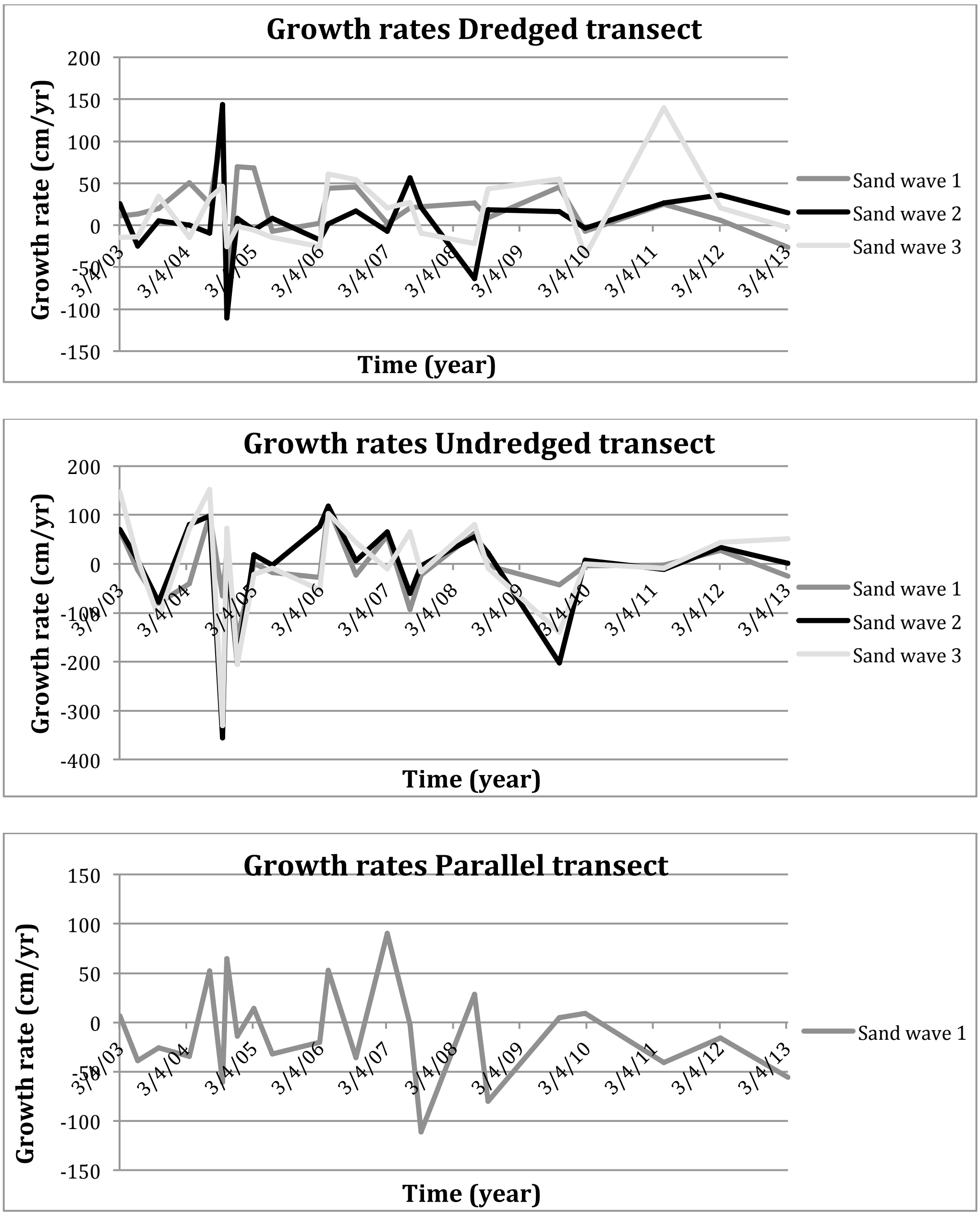

FIGURE 50 GROWTH RATES FOR EACH TIME MEASUREMENT. A: DREDGED TRANSECT

A.3 KBMB

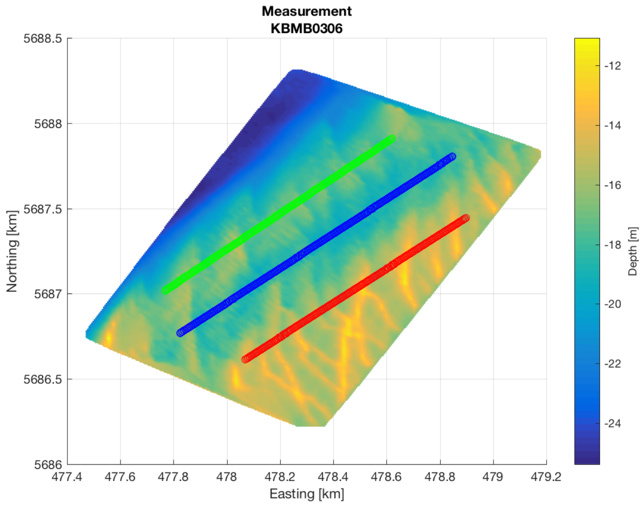

FIGURE 51 SEABED BATHYMETRY AT LOCATION B WITH THREE CHOSEN TRANSECTS (DREDGED: BLUE, UN-DREDGED: GREEN, PARALLEL: RED)

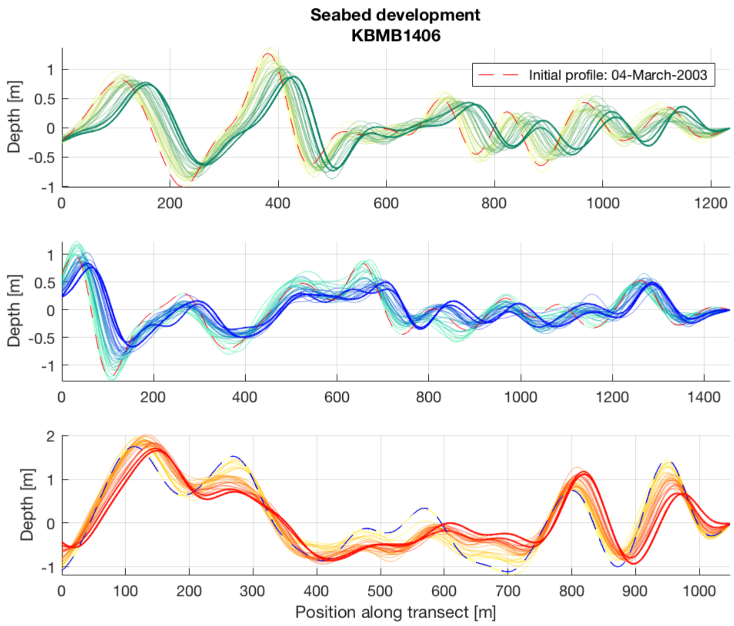

FIGURE 52 SEABED DEVELOPMENT ALONG TRANSECTS AT LOCATION B (DREDGED: BLUE, UN-DREDGED: GREEN, PARALLEL: RED)

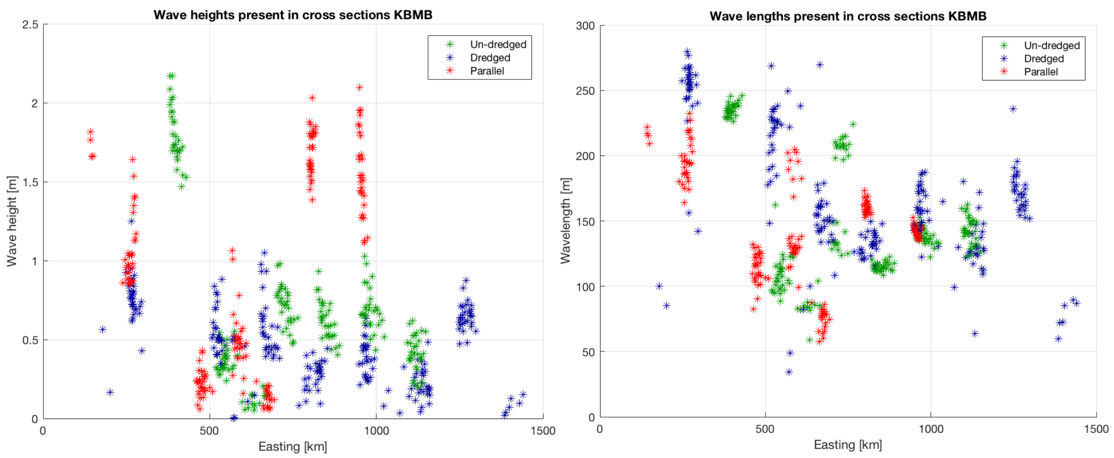

FIGURE 53A. WAVE HEIGHTS PRESENT IN TRANSECTS OF KBMB. FIGURE 53B. WAVE LENGTHS PRESENT IN TRANSECTS OF KBMB.

Wavelength	Range (m)
Un-dredged (green)	59.0 – 245.7
Dredged (blue)	34.4 – 279.8
Parallel (red)	57.4 – 232.3

TABLE 18A. WAVELENGTHS FOUND FOR CROSS SECTIONS OF KBMB

Wave height	Range (m)
Un-dredged (green)	0.05 – 2.17
Dredged (blue)	0.01 – 1.25
Parallel (red)	0.06 – 2.10

TABLE 18B. WAVE HEIGHTS FOUND FOR CROSS SECTIONS OF KBMA

A.4 Modeling in Delft3D

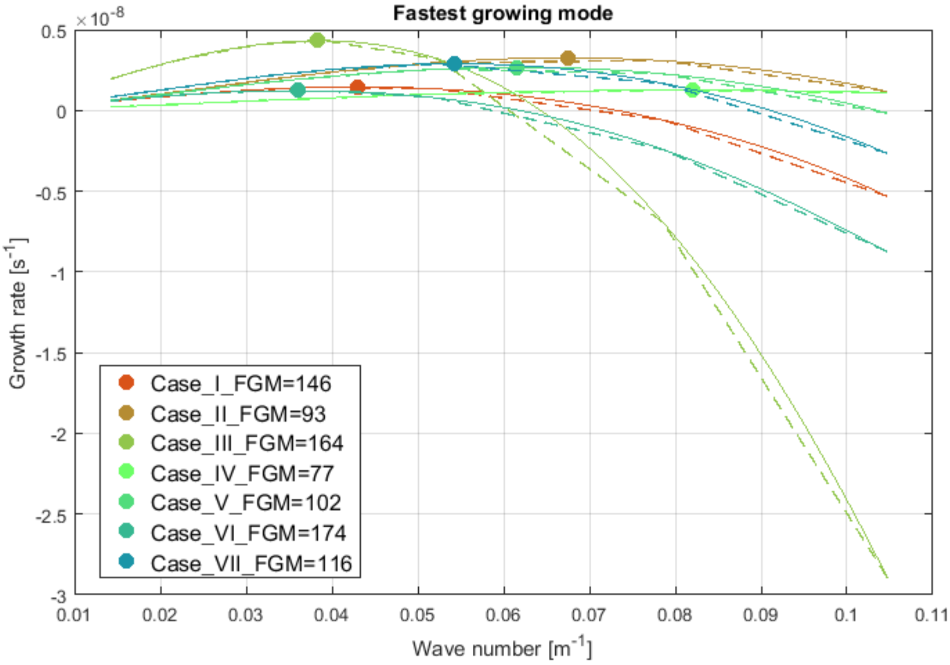

FIGURE 54 FASTEST GROWING MODES FOR ALL CASES IN THE SENSITIVITY ANALYSIS

Run	$H_0\ (m)$	D_{50} (mm)	U_{S2} (m/s)	L_{FGM} (m)
D1	16.5	0.35	0.75	201
D2	16.5	0.30	0.70	191
D3	16.5	0.25	0.65	190
D4	16.5	0.20	0.65	311
D5	16.5	0.20	0.55	175
D6	16.5	0.20	0.60	238
D7	16.5	0.20	0.63	305
D8	16.5	0.20	0.62	257

Run	$H_0\ (m)$	D_{50} (mm)	U_{S2} (m/s)	L_{FGM} (m)
U1	13.8	0.35	0.75	177
U2	13.8	0.30	0.70	177
U3	13.8	0.25	0.65	189

U4	13.8	0.20	0.65	265
U5	13.8	0.20	0.60	209
U6	13.8	0.20	0.62	214
U7	13.8	0.20	0.63	233

TABLE 19 PARAMETER SETS USED IN THE TRIAL AND ERROR METHOD TO FIND A PARAMETER SET TO FIT THE WAVELENGTHS PRESENT IN THE IDEALIZED CROSS SECTION (D: DREDGED AND U: UNDREDGED)

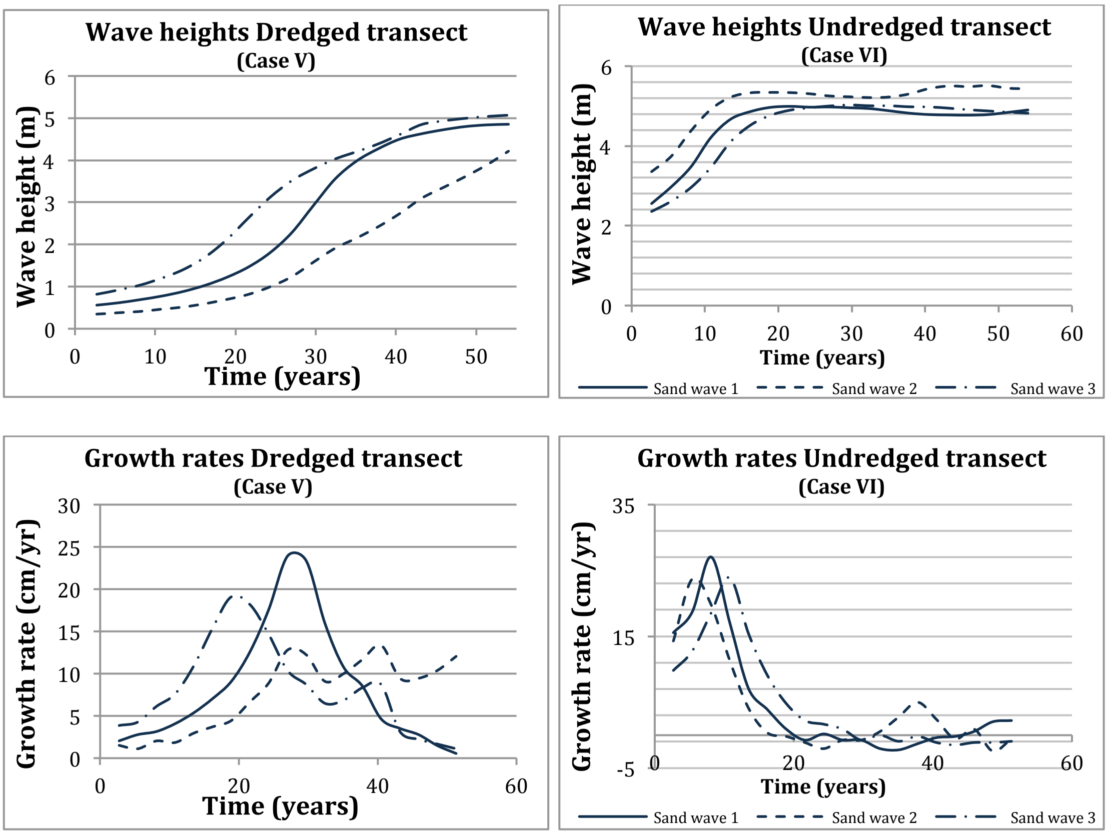

FIGURE 55 WAVE HEIGHT AND GROWTH RATE RESULTS FOR CASE V AND VI

Migration	Crest (m/yr)	Trough (m/yr)
Case V	3.8	2.6
Case VI	4.5	3.1

TABLE 20 MIGRATION RATES FOR CASE V AND VI

A.5 Dredging strategies

		DEPTH	SEDIMENT GRAIN SIZE	TIDAL CURRENT VELOCITY AMPLITUDE	
	Case	H_0 (m)	D_{50} (mm)	U_{S2} (m/s)	L_{FGM} (m)
HKZ	I	21.5	0.25	0.55	161
	II	21.5	0.25	0.55	
	III	22.65	0.25	0.55	
BORSSELE	IV	27.5	0.35	0.75	305
	V	27.5	0.35	0.75	
	VI	29.45	0.35	0.75	
	VII	27.5	0.35	0.75	
	VIII	27.5	0.35	0.75	
D_{50}	IX	21.5	0.30	0.55	139
	X	21.5	0.30	0.55	
	XI	22.65	0.30	0.55	
	XII	27.5	0.30	0.75	315
	XIII	27.5	0.30	0.75	
	XIV	29.45	0.30	0.75	
U_{S2}	XV	21.5	0.25	0.65	259
	XVI	21.5	0.25	0.65	
	XVII	22.65	0.25	0.65	
	XVIII	27.5	0.35	0.65	229
	XIX	27.5	0.35	0.65	
	XX	29.45	0.35	0.65	
BORSSELE 10 M	XXI	37.5	0.35	0.75	392
	XXII	37.5	0.35	0.75	
	XXIII	37.5	0.35	0.75	
	XXIV	37.5	0.35	0.75	

TABLE 21 WAVELENGTHS OF THE FASTEST GROWING MODES (FGM) FOR THE DIFFERENT PARAMETER SETS THAT ARE USED FOR THE LONG-TERM DREDGING STRATEGY SIMULATIONS

	Case	H_0 (m)	D_{50} (mm)	U_{S2} (m/s)	Strategy
HKZ	I	21.5	0.25	0.55	Peak Removal (full)
	II	21.5	0.25	0.55	Cut & Fill
	III	22.65	0.25	0.55	Removal
BORSSELE	IV	27.5	0.35	0.75	Peak Removal (full)
	V	27.5	0.35	0.75	Cut & Fill
	VI	29.45	0.35	0.75	Removal
	VII	27.5	0.35	0.75	Peak Removal (2/3)
	VIII	27.5	0.35	0.75	Peak Removal (1/3)
D_{50}	IX	21.5	0.30	0.55	Peak Removal (full)
	X	21.5	0.30	0.55	Cut & Fill
	XI	22.65	0.30	0.55	Removal
	XII	27.5	0.30	0.75	Peak Removal (full)
	XIII	27.5	0.30	0.75	Cut & Fill
	XIV	29.45	0.30	0.75	Removal
U_{S2}	XV	21.5	0.25	0.65	Peak Removal (full)
	XVI	21.5	0.25	0.65	Cut & Fill
	XVII	22.65	0.25	0.65	Removal
	XVIII	27.5	0.35	0.65	Peak Removal (full)
	XIX	27.5	0.35	0.65	Cut & Fill
	XX	29.45	0.35	0.65	Removal
BORSSELE 10 M	XXI	37.5	0.35	0.75	Cut & Fill
	XXII	37.5	0.35	0.75	Peak Removal (full)
	XXIII	37.5	0.35	0.75	Peak Removal (2/3)
	XXIV	37.5	0.35	0.75	Peak Removal (1/3)

TABLE 22 PARAMETER SET FOR EACH DREDGING STRATEGY

Wave heights (m):

Time (yr)	Case I	Case II	Case III	Case IV	Case V	Case VI
	Full peak	Cut & Fill	Removal	Full peak	Cut & Fill	Removal
0	1.15	0.50	0.50	1.95	0.50	0.50
0.3	1.16	0.50	0.50	1.98	0.50	0.50
0.5	1.18	0.51	0.51	2.02	0.51	0.51
0.8	1.19	0.51	0.51	2.06	0.51	0.51
1.1	1.21	0.52	0.52	2.10	0.52	0.52
1.4	1.22	0.52	0.52	2.14	0.53	0.53
1.6	1.24	0.53	0.53	2.18	0.54	0.53
1.9	1.25	0.53	0.53	2.22	0.54	0.54
2.2	1.26	0.54	0.54	2.26	0.55	0.55
2.5	1.28	0.55	0.54	2.29	0.56	0.55
2.7	1.29	0.55	0.55	2.33	0.57	0.56
3.0	1.31	0.56	0.55	2.37	0.57	0.57
3.3	1.32	0.56	0.56	2.40	0.58	0.57
3.6	1.34	0.57	0.56	2.44	0.59	0.58
3.8	1.35	0.57	0.57	2.48	0.60	0.59
4.1	1.36	0.58	0.57	2.51	0.61	0.60
4.4	1.38	0.59	0.58	2.55	0.62	0.60
4.6	1.39	0.59	0.59	2.58	0.62	0.61
4.9	1.41	0.60	0.59	2.62	0.63	0.62

Time (yr)	Case VII	Case VIII	Case IX	Case X	Case XI	Case XII
	2/3 peak	1/3 peak	Full peak	Cut & Fill	Removal	Full peak
0	2.60	3.25	1.15	0.50	0.50	1.95
0.3	2.63	3.28	1.16	0.50	0.50	1.96
0.5	2.69	3.35	1.19	0.51	0.51	2.01
0.8	2.74	3.41	1.21	0.52	0.51	2.04
1.1	2.79	3.47	1.23	0.52	0.52	2.08

1.4	2.84	3.54	1.25	0.53	0.53	2.11
1.6	2.89	3.60	1.27	0.54	0.53	2.14
1.9	2.94	3.66	1.29	0.54	0.54	2.17
2.2	2.99	3.72	1.31	0.55	0.55	2.21
2.5	3.05	3.79	1.32	0.56	0.55	2.24
2.7	3.10	3.85	1.34	0.56	0.56	2.26
3.0	3.15	3.92	1.36	0.57	0.57	2.29
3.3	3.21	3.98	1.38	0.58	0.57	2.32
3.6	3.27	4.05	1.40	0.59	0.58	2.35
3.8	3.32	4.11	1.42	0.60	0.59	2.38
4.1	3.38	4.18	1.44	0.60	0.60	2.41
4.4	3.44	4.25	1.46	0.62	0.60	2.44
4.6	3.49	4.33	1.48	0.62	0.61	2.46
4.9	3.55	4.40	1.50	0.63	0.62	2.49

Time (yr)	**CaseXIII**	**Case XIV**	**Case XV**	**Case XVI**	**Case XVII**	**Case XVIII**
	Cut & Fill	Removal	Full peak	Cut & Fill	Removal	Full peak
0	0.50	0.50	1.15	0.50	0.50	1.95
0.3	0.50	0.50	1.15	0.50	0.50	1.96
0.5	0.51	0.51	1.17	0.51	0.51	2.01
0.8	0.51	0.51	1.19	0.51	0.51	2.05
1.1	0.52	0.52	1.20	0.52	0.52	2.09
1.4	0.52	0.52	1.21	0.52	0.52	2.12
1.6	0.53	0.53	1.23	0.53	0.52	2.16
1.9	0.53	0.53	1.24	0.53	0.53	2.19
2.2	0.54	0.54	1.26	0.54	0.53	2.23
2.5	0.55	0.54	1.27	0.54	0.54	2.27
2.7	0.55	0.55	1.29	0.55	0.55	2.30
3.0	0.56	0.56	1.30	0.55	0.55	2.34
3.3	0.56	0.56	1.32	0.56	0.56	2.38
3.6	0.57	0.57	1.33	0.57	0.56	2.41
3.8	0.58	0.57	1.35	0.57	0.57	2.45
4.1	0.58	0.58	1.36	0.58	0.57	2.49
4.4	0.59	0.58	1.38	0.58	0.58	2.52
4.6	0.60	0.59	1.39	0.59	0.58	2.56
4.9	0.60	0.59	1.40	0.59	0.59	2.60

Time (yr)	**CaseXIX**	**Case XX**	**Case XXI**	**Case XXII**	**Case XXIII**	**Case XIV**
	Cut & Fill	Removal	Cut & Fill	Full peak	2/3 peak	1/3 peak
0	0.50	0.50	0.50	1.95	2.60	3.25
0.3	0.50	0.50	0.50	1.95	2.62	3.26
0.5	0.51	0.51	0.50	2.00	2.66	3.30
0.8	0.51	0.51	0.51	2.02	2.69	3.35
1.1	0.52	0.52	0.51	2.05	2.72	3.39
1.4	0.53	0.52	0.52	2.07	2.75	3.43
1.6	0.53	0.53	0.52	2.09	2.77	3.47
1.9	0.54	0.53	0.52	2.11	2.80	3.51
2.2	0.54	0.54	0.53	2.14	2.83	3.54
2.5	0.55	0.55	0.53	2.16	2.86	3.58
2.7	0.56	0.55	0.53	2.18	2.89	3.62
3.0	0.56	0.56	0.54	2.20	2.92	3.66
3.3	0.57	0.56	0.54	2.22	2.95	3.70

3.6	0.58	0.57	0.55	2.25	2.98	3.73
3.8	0.59	0.58	0.55	2.27	3.01	3.77
4.1	0.59	0.58	0.55	2.29	3.04	3.81
4.4	0.60	0.59	0.56	2.31	3.07	3.85
4.6	0.61	0.60	0.56	2.33	3.10	3.89
4.9	0.61	0.60	0.57	2.35	3.13	3.93

TABLE 23 WAVE HEIGHTS (M) FOR THE DIFFERENT DREDGING CASES

Crest heights (m):

Time (yr)	Case I	Case II	Case III	Case IV	Case V	Case VI
	Full peak	Cut & Fill	Removal	Full peak	Cut & Fill	Removal
0	0.00	0.25	0.25	0.00	0.25	0.25
0.3	0.01	0.25	0.25	0.02	0.25	0.25
0.5	0.02	0.25	0.25	0.04	0.25	0.25
0.8	0.03	0.25	0.25	0.06	0.25	0.25
1.1	0.03	0.26	0.26	0.07	0.26	0.26
1.4	0.04	0.26	0.26	0.09	0.26	0.26
1.6	0.05	0.26	0.26	0.10	0.26	0.26
1.9	0.06	0.26	0.26	0.12	0.27	0.27
2.2	0.06	0.27	0.27	0.13	0.27	0.27
2.5	0.07	0.27	0.27	0.14	0.27	0.27
2.7	0.08	0.27	0.27	0.16	0.28	0.28
3.0	0.08	0.27	0.27	0.17	0.28	0.28
3.3	0.09	0.28	0.27	0.18	0.29	0.28
3.6	0.10	0.28	0.28	0.19	0.29	0.29
3.8	0.10	0.28	0.28	0.21	0.29	0.29
4.1	0.11	0.29	0.28	0.22	0.30	0.30
4.4	0.12	0.29	0.29	0.23	0.30	0.30
4.6	0.12	0.29	0.29	0.24	0.31	0.30
4.9	0.13	0.29	0.29	0.26	0.31	0.31

Time (yr)	Case VII	Case VIII	Case IX	Case X	Case XI	Case XII
	2/3 peak	1/3 peak	Full peak	Cut & Fill	Removal	Full peak
0	0.65	1.30	0.00	0.25	0.25	0.00
0.3	0.67	1.32	0.01	0.25	0.25	0.00
0.5	0.70	1.36	0.02	0.25	0.25	0.03
0.8	0.72	1.39	0.03	0.26	0.26	0.05
1.1	0.74	1.42	0.04	0.26	0.26	0.06
1.4	0.76	1.45	0.05	0.26	0.26	0.08
1.6	0.78	1.48	0.06	0.27	0.26	0.09
1.9	0.80	1.50	0.07	0.27	0.27	0.10
2.2	0.82	1.53	0.08	0.27	0.27	0.11
2.5	0.84	1.55	0.09	0.28	0.27	0.12
2.7	0.86	1.58	0.10	0.28	0.28	0.14
3.0	0.88	1.60	0.10	0.28	0.28	0.15
3.3	0.90	1.63	0.11	0.29	0.28	0.16
3.6	0.92	1.65	0.12	0.29	0.29	0.17
3.8	0.94	1.67	0.13	0.29	0.29	0.18
4.1	0.96	1.70	0.14	0.30	0.29	0.19
4.4	0.98	1.72	0.14	0.30	0.30	0.20
4.6	1.00	1.74	0.15	0.31	0.30	0.21
4.9	1.02	1.77	0.16	0.31	0.30	0.23

Time (yr)	CaseXIII	Case XIV	Case XV	Case XVI	Case XVII	Case XVIII

	Cut & Fill	Removal	Full peak	Cut & Fill	Removal	Full peak
0	0.25	0.25	0.00	0.25	0.25	0.00
0.3	0.25	0.25	0.00	0.25	0.25	0.00
0.5	0.25	0.25	0.01	0.25	0.25	0.04
0.8	0.25	0.25	0.01	0.25	0.25	0.05
1.1	0.26	0.26	0.02	0.26	0.25	0.07
1.4	0.26	0.26	0.02	0.26	0.26	0.08
1.6	0.26	0.26	0.02	0.26	0.26	0.09
1.9	0.26	0.26	0.03	0.26	0.26	0.10
2.2	0.27	0.27	0.03	0.26	0.26	0.12
2.5	0.27	0.27	0.04	0.27	0.27	0.13
2.7	0.27	0.27	0.04	0.27	0.27	0.14
3.0	0.28	0.28	0.04	0.27	0.27	0.15
3.3	0.28	0.28	0.05	0.27	0.27	0.16
3.6	0.28	0.28	0.05	0.28	0.28	0.17
3.8	0.29	0.29	0.05	0.28	0.28	0.18
4.1	0.29	0.29	0.06	0.28	0.28	0.19
4.4	0.29	0.29	0.06	0.29	0.28	0.21
4.6	0.29	0.29	0.06	0.29	0.28	0.22
4.9	0.30	0.30	0.07	0.29	0.29	0.23

Time (yr)	CaseXIX	Case XX	Case XXI	Case XXII	Case XXIII	Case XIV
	Cut & Fill	Removal	Cut & Fill	Full peak	2/3 peak	1/3 peak
0	0.25	0.25	0.25	0.00	0.65	1.30
0.3	0.25	0.25	0.25	0.00	0.66	1.30
0.5	0.25	0.25	0.25	0.03	0.68	1.32
0.8	0.25	0.25	0.25	0.04	0.70	1.36
1.1	0.26	0.26	0.25	0.05	0.71	1.38
1.4	0.26	0.26	0.25	0.06	0.72	1.40
1.6	0.26	0.26	0.26	0.07	0.74	1.42
1.9	0.27	0.26	0.26	0.08	0.75	1.44
2.2	0.27	0.27	0.26	0.09	0.76	1.46
2.5	0.27	0.27	0.26	0.09	0.77	1.48
2.7	0.27	0.27	0.26	0.10	0.78	1.50
3.0	0.28	0.27	0.27	0.11	0.79	1.51
3.3	0.28	0.28	0.27	0.12	0.81	1.53
3.6	0.28	0.28	0.27	0.13	0.82	1.55
3.8	0.29	0.28	0.27	0.13	0.83	1.57
4.1	0.29	0.28	0.27	0.14	0.84	1.58
4.4	0.29	0.29	0.28	0.15	0.85	1.60
4.6	0.29	0.29	0.28	0.16	0.86	1.61
4.9	0.30	0.29	0.28	0.16	0.87	1.63

TABLE 24 CREST HEIGHTS (M) FOR THE DIFFERENT DREDGING CASES

Growth rates (cm/yr):

Time (yr)	Case I	Case II	Case III	Case IV	Case V	Case VI
	Full peak	Cut & Fill	Removal	Full peak	Cut & Fill	Removal
0	2.78	0.46	0.47	9.52	0.55	0.51
0.3	7.12	1.94	1.73	16.63	2.41	2.22
0.5	5.89	1.91	1.88	14.97	2.44	2.26
0.8	5.44	2.04	1.79	14.47	2.49	2.30
1.1	5.28	2.00	1.88	14.50	2.54	2.33
1.4	5.26	1.85	1.77	14.19	2.62	2.34
1.6	5.12	2.13	2.01	14.02	2.68	2.43
1.9	5.06	2.09	1.92	14.05	2.73	2.42

2.2	5.47	2.09	1.94	13.80	2.79	2.46
2.5	4.91	2.16	1.96	13.46	2.84	2.52
2.7	5.27	2.14	1.98	13.23	2.89	2.54
3.0	5.28	2.14	1.88	13.41	2.94	2.56
3.3	5.18	2.19	2.16	13.03	2.99	2.63
3.6	5.16	2.22	2.04	13.40	3.05	2.66
3.8	5.45	2.23	1.93	12.86	3.09	2.66
4.1	4.90	2.28	2.22	13.40	3.13	2.74
4.4	5.64	2.28	2.16	12.86	3.19	2.77
4.6	5.05	2.24	1.98	12.79	3.24	2.78

Time (yr)	**Case VII**	**Case VIII**	**Case IX**	**Case X**	**Case XI**	**Case XII**
	2/3 peak	1/3 peak	Full peak	Cut & Fill	Removal	Full peak
0	11.34	12.08	4.62	0.72	0.67	2.57
0.3	20.04	23.51	8.43	2.41	2.25	19.09
0.5	18.81	23.06	7.75	2.59	2.41	12.37
0.8	18.24	23.27	7.24	1.57	1.40	13.13
1.1	18.35	23.26	7.40	3.66	3.48	11.84
1.4	18.37	22.92	6.95	2.58	2.45	11.51
1.6	18.87	22.97	7.37	1.58	2.56	11.64
1.9	19.40	22.74	7.01	2.83	2.48	11.33
2.2	19.54	23.18	6.97	2.66	1.44	11.02
2.5	19.82	23.01	7.28	2.88	3.80	10.77
2.7	20.13	23.74	7.06	2.75	2.71	10.85
3.0	20.49	23.63	6.92	2.95	1.49	10.59
3.3	20.60	24.36	7.37	2.78	2.64	10.42
3.6	20.60	24.65	7.32	3.05	2.80	10.37
3.8	20.76	25.25	7.29	2.91	4.06	10.19
4.1	21.09	25.93	6.92	4.43	1.52	10.07
4.4	21.09	25.96	7.51	1.74	2.82	9.83
4.6	20.98	26.83	7.47	3.24	2.89	9.84

Time (yr)	**CaseXIII**	**Case XIV**	**Case XV**	**Case XVI**	**Case XVII**	**Case XVIII**
	Cut & Fill	Removal	Full peak	Cut & Fill	Removal	Full peak
0	0.41	0.40	1.36	0.35	0.34	3.24
0.3	1.96	1.87	6.19	1.84	1.70	19.96
0.5	1.98	1.95	5.56	1.87	1.75	13.87
0.8	2.01	1.96	5.30	1.92	1.75	13.09
1.1	2.03	1.98	5.37	1.92	1.77	12.93
1.4	2.04	2.01	5.27	1.92	1.80	13.23
1.6	2.08	2.00	5.44	1.93	1.81	13.09
1.9	2.13	1.99	5.26	1.99	1.83	13.26
2.2	2.16	2.00	5.37	2.02	1.84	13.16
2.5	2.17	2.00	5.43	2.02	1.89	13.46
2.7	2.24	2.01	5.22	2.00	1.89	13.13
3.0	2.26	2.02	5.43	2.10	1.89	13.57
3.3	2.28	2.03	5.25	2.06	1.94	13.66
3.6	2.35	2.03	5.44	2.12	1.92	13.40
3.8	2.38	2.04	5.26	2.16	1.98	13.29
4.1	2.42	2.07	5.20	2.16	1.99	13.48
4.4	2.45	2.08	5.47	2.16	1.98	13.26
4.6	2.49	2.09	5.30	2.21	2.02	13.65

Time (yr)	CaseXIX	Case XX	Case XXI	Case XXII	Case XXIII	Case XIV
	Cut & Fill	Removal	Cut & Fill	Full peak	2/3 peak	1/3 peak
0	0.52	0.46	0.28	1.53	7.52	2.37
0.3	2.14	1.93	1.33	15.43	12.93	14.24
0.5	2.23	2.00	1.37	9.12	11.34	21.29
0.8	2.24	2.06	1.37	8.75	10.88	13.89
1.1	2.29	2.05	1.36	8.60	10.68	13.85
1.4	2.31	2.05	1.39	8.34	10.56	13.93
1.6	2.34	2.12	1.41	8.34	10.55	14.03
1.9	2.32	2.09	1.40	8.19	10.54	14.09
2.2	2.42	2.19	1.41	8.11	10.56	14.04
2.5	2.44	2.13	1.45	8.11	10.63	14.02
2.7	2.38	2.23	1.44	7.86	10.82	13.95
3.0	2.55	2.22	1.44	7.93	10.76	13.88
3.3	2.51	2.20	1.47	7.82	11.04	13.93
3.6	2.51	2.33	1.48	7.57	10.92	13.92
3.8	2.63	2.25	1.48	7.73	11.19	13.95
4.1	2.57	2.36	1.50	7.51	11.28	13.95
4.4	2.65	2.36	1.51	7.36	11.24	13.95
4.6	2.70	2.33	1.52	7.47	11.33	13.97

TABLE 25 GROWTH RATES IN CM/YR FOR THE DIFFERENT DREDGING CASES

Crest growth rates (cm/yr):

Time (yr)	Case I	Case II	Case III	Case IV	Case V	Case VI
	Full peak	Cut & Fill	Removal	Full peak	Cut & Fill	Removal
0	2.2	0	0	6.6	-0.7	-0.7
0.3	3.9	0.8	0.7	8.0	1.1	1.1
0.5	3.4	0.8	0.8	6.4	1.2	1.1
0.8	2.9	0.9	0.8	5.7	1.2	1.1
1.1	2.8	0.9	0.8	5.4	1.2	1.2
1.4	2.7	0.8	0.8	5.1	1.2	1.2
1.6	2.6	0.9	0.8	5.0	1.3	1.2
1.9	2.5	0.9	0.9	4.9	1.3	1.2
2.2	2.5	0.9	0.9	4.8	1.3	1.3
2.5	2.5	1.0	0.9	4.7	1.3	1.3
2.7	2.5	1.0	0.8	4.7	1.3	1.3
3.0	2.4	1.0	0.9	4.7	1.4	1.3
3.3	2.4	1.0	0.9	4.7	1.4	1.4
3.6	2.5	1.0	1.0	4.6	1.4	1.4
3.8	2.4	1.0	0.9	4.7	1.4	1.4
4.1	2.4	1.0	0.9	4.7	1.5	1.4
4.4	2.3	1.0	0.9	4.8	1.5	1.4
4.6	2.4	1.0	1.0	4.8	1.5	1.4

Time (yr)	Case VII	Case VIII	Case IX	Case X	Case XI	Case XII
	2/3 peak	1/3 peak	Full peak	Cut & Fill	Removal	Full peak
0	7.76	8.11	2.84	0.10	0.07	-0.09
0.3	9.99	12.31	4.79	1.04	0.97	12.20
0.5	8.29	11.46	4.11	1.16	1.06	5.42
0.8	7.59	11.40	3.56	1.15	1.06	6.05
1.1	7.33	11.07	3.61	1.17	1.08	4.74
1.4	7.13	10.44	3.32	1.12	1.04	4.39
1.6	7.18	9.94	3.20	1.23	1.19	4.36
1.9	7.17	9.44	3.10	1.29	1.06	4.24
2.2	7.24	9.15	2.99	1.23	1.17	4.14
2.5	7.31	8.80	3.33	1.29	1.19	4.13

2.7	7.36	8.68	3.05	1.31	1.25	4.07
3.0	7.40	8.44	2.96	1.28	1.21	4.02
3.3	7.44	8.38	2.97	1.32	1.20	4.43
3.6	7.50	8.47	3.10	1.33	1.26	4.05
3.8	7.48	8.57	3.09	1.38	1.25	4.05
4.1	7.49	8.76	2.93	1.46	1.27	4.09
4.4	7.52	8.74	3.05	1.38	1.32	4.01
4.6	7.50	8.72	3.05	1.45	1.26	4.16

Time (yr)	**CaseXIII**	**Case XIV**	**Case XV**	**Case XVI**	**Case XVII**	**Case XVIII**
	Cut & Fill	Removal	Full peak	Cut & Fill	Removal	Full peak
0	-0.91	-0.90	-0.06	-0.47	-0.50	0.63
0.3	0.93	0.97	2.44	0.78	0.72	12.46
0.5	0.97	1.04	1.83	0.83	0.77	5.82
0.8	0.99	1.08	1.60	0.85	0.78	5.08
1.1	1.01	1.07	1.51	0.86	0.79	4.85
1.4	1.02	1.09	1.44	0.86	0.79	4.62
1.6	1.05	1.08	1.40	0.87	0.81	4.39
1.9	1.07	1.07	1.35	0.88	0.83	4.35
2.2	1.09	1.07	1.31	0.91	0.82	4.26
2.5	1.10	1.07	1.31	0.92	0.85	4.19
2.7	1.11	1.07	1.27	0.90	0.86	4.14
3.0	1.13	1.07	1.27	0.94	0.83	4.10
3.3	1.14	1.07	1.25	0.93	0.88	4.16
3.6	1.16	1.07	1.24	0.94	0.88	4.05
3.8	1.19	1.08	1.24	0.97	0.88	4.00
4.1	1.20	1.08	1.27	0.97	0.88	4.14
4.4	1.21	1.08	1.27	0.98	0.88	4.10
4.6	1.23	1.08	1.30	0.98	0.92	4.12

Time (yr)	**CaseXIX**	**Case XX**	**Case XXI**	**Case XXII**	**Case XXIII**	**Case XIV**
	Cut & Fill	Removal	Cut & Fill	Full peak	2/3 peak	1/3 peak
0	-0.21	-0.24	-0.82	-0.57	5.12	-0.26
0.3	0.88	0.78	0.62	10.62	7.04	7.66
0.5	0.94	0.85	0.65	4.40	5.51	14.77
0.8	0.94	0.86	0.65	3.88	4.90	7.23
1.1	1.00	0.87	0.65	3.58	4.67	7.17
1.4	0.98	0.86	0.67	3.40	4.45	7.13
1.6	1.01	0.91	0.68	3.26	4.33	7.15
1.9	0.99	0.91	0.68	3.11	4.25	7.05
2.2	1.06	0.93	0.68	3.07	4.17	6.93
2.5	1.05	0.91	0.70	2.96	4.16	6.78
2.7	1.03	0.97	0.70	2.90	4.14	6.60
3.0	1.10	0.95	0.70	2.88	4.14	6.42
3.3	1.09	0.95	0.70	2.87	4.16	6.32
3.6	1.08	1.00	0.72	2.83	4.18	6.17
3.8	1.14	0.97	0.72	2.79	4.19	6.05
4.1	1.12	1.01	0.72	2.77	4.35	5.93
4.4	1.21	1.08	1.27	0.98	0.88	4.10
4.6	1.23	1.08	1.30	0.98	0.92	4.12

TABLE 26 CREST GROWTH RATES IN CM/YR FOR THE DIFFERENT DREDGING CASES

A.6 Raw data

Vessel	Campaign	Survey	Area	Start time	End time	Multi-beam	Frequency	Positioning system
Belgica	2001-04	KBMA 0104	KBMA	21/02/01 18:07	21/02/01 23:50	em1002	100 kHz	Sercel NR103
Belgica	2001-31	KBMA 0131	KBMA	27/11/01 07:20	27/11/01 11:00	em1002	100 kHz	Sercel NR103
Belgica	2002-03	KBMA 0203	KBMA	12/02/2 22:2	13/02/02 01:40	em1002	100 kHz	Sercel NR103
Belgica	2002-19	KBMA 0219	KBMA	04/09/02 22:40	05/09/02 01:45	em1002	100 kHz	Sercel NR103
Belgica	2002-29	KBMA 0229	KBMA	12/12/02 04:08	12/12/02 08:10	em1002	100 kHz	Sercel NR103
Belgica	2003-06	KBMA 0306	KBMA	03/03/03 21:29	04/03/03 01:25	em1002	100 kHz	Sercel NR103
Belgica	2003-15	KBMA 0315	KBMA	10/06/03 23:21	11/06/03 03:05	em1002	100 kHz	Thales Acquarius
Belgica	2003-24	KBMA 0324	KBMA	01/10/03 19:25	02/10/03 01:10	em1002	100 kHz	Thales Acquarius
Belgica	2004-06	KBMA 0406	KBMA	18/03/04 20:21	19/03/04 00:25	em1002	100 kHz	Thales Acquarius
Belgica	2004-15	KBMA 0415	KBMA	09/07/04 03:10	09/07/04 06:30	em1002	100 kHz	Thales Acquarius
Belgica	2004-20	KBMA 0420	KBMA	15/09/04 21:41	17/09/04 02:05	em1002	100 kHz	Thales Acquarius
Belgica	2004-23	KBMA 0423	KBMA	12/10/04 00:19	12/10/04 23:40	em1002	100 kHz	Thales Acquarius
Belgica	2004-29	KBMA 0429	KBMA	07/12/04 07:08	07/12/04 10:20	em1002	100 kHz	Thales Acquarius
Belgica	2005-04	KBMA 0504	KBMA	08/03/05 19:33	09/03/05 00:55	em1002	100 kHz	Thales Acquarius
Belgica	2005-14	KBMA 0514	KBMA	15/06/05 03:26	16/06/05 05:20	em1002	100 kHz	Thales Acquarius
Belgica	2006-04	KBMA 0604	KBMA	03/03/06 00:05	03/03/06 04:21	em1002	100 kHz	Thales Acquarius
Belgica	2006-08	KBMA 0608	KBMA	19/04/06 01:39	20/04/06 04:10	em1002	100 kHz	Thales Acquarius
Belgica	2006-19	KBMA 0619	KBMA	19/09/06 19:26	19/09/06 23:20	em1002	100 kHz	Thales Acquarius
Belgica	2007-06	KBMA 0706	KBMA	08/03/07 23:53	09/03/07 04:43	em1002	100 kHz	Thales Acquarius
Belgica	2007-16	KBMA 0716	KBMA	10/07/07 23:58	11/07/07 19:39	em1002	100 kHz	Thales Acquarius
Belgica	2007-19	KBMA 0719	KBMA	11/09/07 21:10	12/09/07 02:45	em1002	100 kHz	Thales Acquarius
Belgica	2008-16	KBMA 0816	KBMA	30/06/08 21:12	01/07/08 01:16	em1002	100 kHz	Thales Acquarius

Belgica	2008-20	KBMA 0820	KBMA	09/09/08 20:58	10/09/08 01:18	em1002	100 kHz	Thales Acquarius
Belgica	2009-26	KBMA 0926	KBMA	07/10/09 02:15	07/10/09 04:23	em3002	300 kHz	Thales Acquarius
Belgica	2010-05	KBMA 1005	KBMA	24/02/10 21:14	25/02/10 00:07	em3002	300 kHz	Thales Acquarius
Belgica	2011-13	KBMA 1113	KBMA	04/05/2011 00:3	04/05/201103:4	em3002	300 kHz	Thales Acquarius
Belgica	2012-07	KBMA 1207	KBMA	07/03/12 21:51	08/03/1 00:4	em3002	300 kHz	Thales Acquarius
Belgica	2012-24	KBMA 1224	KBMA	18/09/12 23:35	19/09/12 01:10	em3002	300 kHz	Thales Acquarius
Belgica	2013-08	KBMA 1308	KBMA	13/03/13 01:40	13/03/13 05:20	em3002	300 kHz	Thales Acquarius
Belgica	2014-06	KBMA 1406	KBMA	11/03/14 18:28	11/03/14 22:11	em3002	300 kHz	Thales Acquarius
Belgica	2003-06	KBMB 0306	KBMB	03/03/03	04/03/03	em1002	100 kHz	Sercel NR103
Belgica	2003-15	KBMB 0315	KBMB	12/06/03	12/06/03	em1002	100 kHz	Thales Acquarius
Belgica	2003-24	KBMB 0324	KBMB	30/09/03	30/09/03	em1002	100 kHz	Thales Acquarius
Belgica	2004-06	KBMB 0406	KBMB	18/03/04	23/03/04	em1002	100 kHz	Thales Acquarius
Belgica	2004-15	KBMB 0415	KBMB	08/07/04	08/07/04	em1002	100 kHz	Thales Acquarius
Belgica	2004-20	KBMB 0420	KBMB	16/09/04	16/09/04	em1002	100 kHz	Thales Acquarius
Belgica	2004-23	KBMB 0423	KBMB	12/10/04	12/10/04	em1002	100 kHz	Thales Acquarius
Belgica	2004-29	KBMB 0429	KBMB	06/12/04	07/12/04	em1002	100 kHz	Thales Acquarius
Belgica	2005-04	KBMB 0504	KBMB	08/03/05	09/03/05	em1002	100 kHz	Thales Acquarius
Belgica	2005-14	KBMB 0514	KBMB	13/06/05	14/06/05	em1002	100 kHz	Thales Acquarius
Belgica	2006-04	KBMB 0604	KBMB	02/03/06 19:57	02/03/06 23:48	em1002	100 kHz	Thales Acquarius
Belgica	2006-08	KBMB 0608	KBMB	19/04/06	20/04/06	em1002	100 kHz	Thales Acquarius
Belgica	2006-19	KBMB 0619	KBMB	19/09/06 00:17	19/09/06 04:51	em1002	100 kHz	Thales Acquarius
Belgica	2007-06	KBMB 0706	KBMB	08/03/07 20:12	08/03/07 23:39	em1002	100 kHz	Thales Acquarius
Belgica	2007-16	KBMB 0716	KBMB	09/07/07 20:52	09/07/07 23:40	em1002	100 kHz	Thales Acquarius
Belgica	2007-19	KBMB 0719	KBMB	12/09/2007	12/09/2007	em1002	100 kHz	Thales Acquarius

Belgica	2008-16	KBMB 0816	KBMB	30/06/08 18:22	30/06/08 21:01	em1002	100 kHz	Thales Acquarius
Belgica	2008-20	KBMB 0820	KBMB	10/09/08 01:40	10/09/08 04:31	em1002	100 kHz	Thales Acquarius
Belgica	2009-06	KBMB 0906	KBMB	26/02/09 01:56	26/02/09 03:59	em3002	300 kHz	Thales Acquarius
Belgica	2009-11	KBMB 0911	KBMB	17/04/09 02:08	17/04/09 03:47	em3002	300 kHz	Thales Acquarius
Belgica	2009-26	KBMB 0926	KBMB	07/10/09 19:04	07/10/09 21:07	em3002	300 kHz	Thales Acquarius
Belgica	2010-05	KBMB 1005	KBMB	23/02/10 23:49	24/02/10 02:20	em3002	300 kHz	Thales Acquarius
Belgica	2010-30	KBMB 1030	KBMB	25/11/2010 20:2	25/11/201023:1	em3002	300 kHz	Thales Acquarius
Belgica	2011-13	KBMB 1113	KBMB	04/05/2011 06:5	04/05/211 09:4	em3002	300 kHz	Thales Acquarius
Belgica	2011-25	KBMB 1125	KBMB	20/09/11 23:15	21/09/11 02:00	em3002	300 kHz	Thales Acquarius
Belgica	2012-07	KBMB 1207	KBMB	07/03/12 18:44	07/03/12 21:40	em3002	300 kHz	Thales Acquarius
Belgica	2012-24	KBMB 1224	KBMB	21/09/12 00:40	21/09/12 02:40	em3002	300 kHz	Thales Acquarius
Belgica	2013-08	KBMB 1308	KBMB	12/03/13 21:12	13/03/13 01:30	em3002	300 kHz	Thales Acquarius
Belgica	2014-06	KBMB 1406	KBMB	11/03/14 22:19	12/03/14 02:22	em3002	300 kHz	Thales Acquarius

TABLE 27 RAW DATA PROVIDED BY KOEN DEGRENDELE OF THE FEDERAL PUBLIC SERVICE OF BELGIUM, AND VERA VAN LANCKER OF THE ROYAL BELGIAN INSTITUTE OF NATURAL SCIENCES